



LASER INTERFEROMETER GRAVITATIONAL WAVE OBSERVATORY

LIGO Laboratory / LIGO Scientific Collaboration

LIGO-T050014-00-D

Advanced LIGO

5 Jul 2005

Coupled Dynamics Analysis of the Seismic Isolation System (SEI) Stage 2 Structure and the Quadruple Suspension (SUS) Structure

Dennis Coyne

Distribution of this document:
LIGO Science Collaboration

This is an internal working note
of the LIGO Project.

California Institute of Technology
LIGO Project – MS 18-34
1200 E. California Blvd.
Pasadena, CA 91125
Phone (626) 395-2129
Fax (626) 304-9834
E-mail: info@ligo.caltech.edu

LIGO Hanford Observatory
P.O. Box 1970
Mail Stop S9-02
Richland WA 99352
Phone 509-372-8106
Fax 509-372-8137

Massachusetts Institute of Technology
LIGO Project – NW17-161
175 Albany St
Cambridge, MA 02139
Phone (617) 253-4824
Fax (617) 253-7014
E-mail: info@ligo.mit.edu

LIGO Livingston Observatory
P.O. Box 940
Livingston, LA 70754
Phone 225-686-3100
Fax 225-686-7189

<http://www.ligo.caltech.edu/>

1	<i>Introduction</i>	4
2	<i>Seismic Isolation System (SEI)</i>	4
2.1	SEI Stage2 Finite Element Model	7
2.2	SEI Stage 2 Modes (with point mass payload approximations)	9
3	<i>Beam & Rigid Body Model</i>	11
4	<i>Suspension Structure</i>	17
4.1	quadx33	17
4.2	quadx51	19
4.3	quady2	21
4.4	D040519-04	31
5	<i>Transfer functions</i>	36
5.1	Damping	36
5.2	D040519-04	36
5.3	Quady2	41
6	<i>Conclusions and Further Work</i>	41
7	<i>Appendix A: Beam and Rigid Body Mass Model</i>	43
8	<i>Appendix B: Matlab Script for Modal Transfer Functions</i>	44
9	<i>Appendix C: SUS D040519-04 Quad Structure Transfer functions</i>	45

List of Figures

<i>Figure 1: Overall BSC SEI system installation</i>	5
<i>Figure 2: BSC SEI System</i>	6
<i>Figure 3: BSC SEI System, elevation view indicating the location of the upper counter-balance mass</i>	6
<i>Figure 4: Sectional (view A-A from figure 3) of the BSC SEI system indicating the locations of the actuators and sensors</i>	7
<i>Figure 5: Stage 2 finite element model</i>	8
<i>Figure 6: Discrete Masses in the SEI Stage 2 finite element model</i>	8
<i>Figure 7: Stage2 first "global" elastic mode</i>	10
<i>Figure 8: Stage2 second "global" elastic mode</i>	10
<i>Figure 9: Payload Mode</i>	11
<i>Figure 10: Simple Beam and Rigid Mass Model</i>	12
<i>Figure 11: Beam and Rigid Body Model Result for Stage 2 and SUS Quad D040519-04</i>	13
<i>Figure 12: Finite Element Transfer Function for Modal Actuation on a coupled model of Stage 2 and SUS Quad D040519-04</i>	14
<i>Figure 13: Beam and Rigid Body Model Result for Horizontal Translation: Gain & Phase Changes versus Beam Mass (with varying damping factor)</i>	15
<i>Figure 14: Beam and Rigid Body Model Result for Rotation about a Horizontal Axis: Gain & Phase Changes versus Beam Mass (with varying damping factor)</i>	16

List of Tables

<i>Table 1: SEI Stage2 Mass Properties (inch, lbf, slinch units)</i>	9
<i>Table 2: Stage2 Modes</i>	10
<i>Table 3: Quadruple Suspension Structure Designs</i>	17

1 Introduction

The perturbation to the seismic isolation system (SEI) transfer functions due to the addition of the quadruple suspension (SUS) structure is calculated. The gain and phase variations must not destabilize the active seismic isolation system control or cause a significant increase in the control law complexity, with a concomitant decrease in robustness. The current planned upper unity gain frequency for the SEI system is about 60 Hz.

The stiffness requirements¹ of the seismic isolation inner stage structure are essentially that:

- the phase lag is less than 90 degrees below 150 Hz for the transfer function from each actuator (force) to each non-collocated sensor (displacement), and
- the phase lag is less than 90 degrees below 500 Hz for the transfer function from each actuator (force) to each collocated sensor (displacement)

The starting requirement for the SUS quad structure stiffness was a first resonance of greater than 150 Hz (for attachment to a perfectly stiff interface). The SUS group found that it was not possible to meet either this requirement, or the SEI structural stiffness requirements, within the mass and envelope allocations² for the quad structure. The current SUS working baseline³ goal is as follows:

- > 200 Hz first resonance for the upper quad SUS structure
- > 100 Hz lower quad SUS structure (the SUS design has a provision to un-couple the lower structure from the upper structure and then support the lower structure from the support tubes of the chamber)
- > 100 Hz combined upper and lower quad SUS structure

A more appropriate requirement⁴ for the coupled SEI/payload system might be no more than 90 degrees of phase lag under 100 Hz, for each modal transfer function (force actuation to sensed modal displacement response). The modal transfer functions for a coupled system (quadruple suspension and seismic isolation stage with optics table) are presented in this memo for a few different suspension structure designs.

2 Seismic Isolation System (SEI)

The SEI conceptual design⁵ consists of two stages that are mechanically sprung from one another and actively controlled in six degrees of freedom for each stage. The coupled rigid body modes for these stages have frequencies between 1.2 and 10 Hz. As a reasonable approximation, the inner stage is decoupled and inertially free above the highest rigid body frequency. Consequently in this

¹ D. Coyne, J. Giaime, L. Jones, B. Lantz, Design Requirements for the In-Vacuum Mechanical Elements of the Advanced LIGO Seismic Isolation System for the BSC Chamber, section C.8, LIGO-E03-179-A, 5/21/2004.

² D. Coyne, Seismic Isolation System (SEI) Payload Mass Properties, LIGO-E040136-00, 3/18/2004.

³ D. Coyne, Quad Interface Issues, LIGO-T050005-01, 1/20/2005.

⁴ J. Giaime, verbal communication Jan 2005; draft, not yet reviewed/approved requirement.

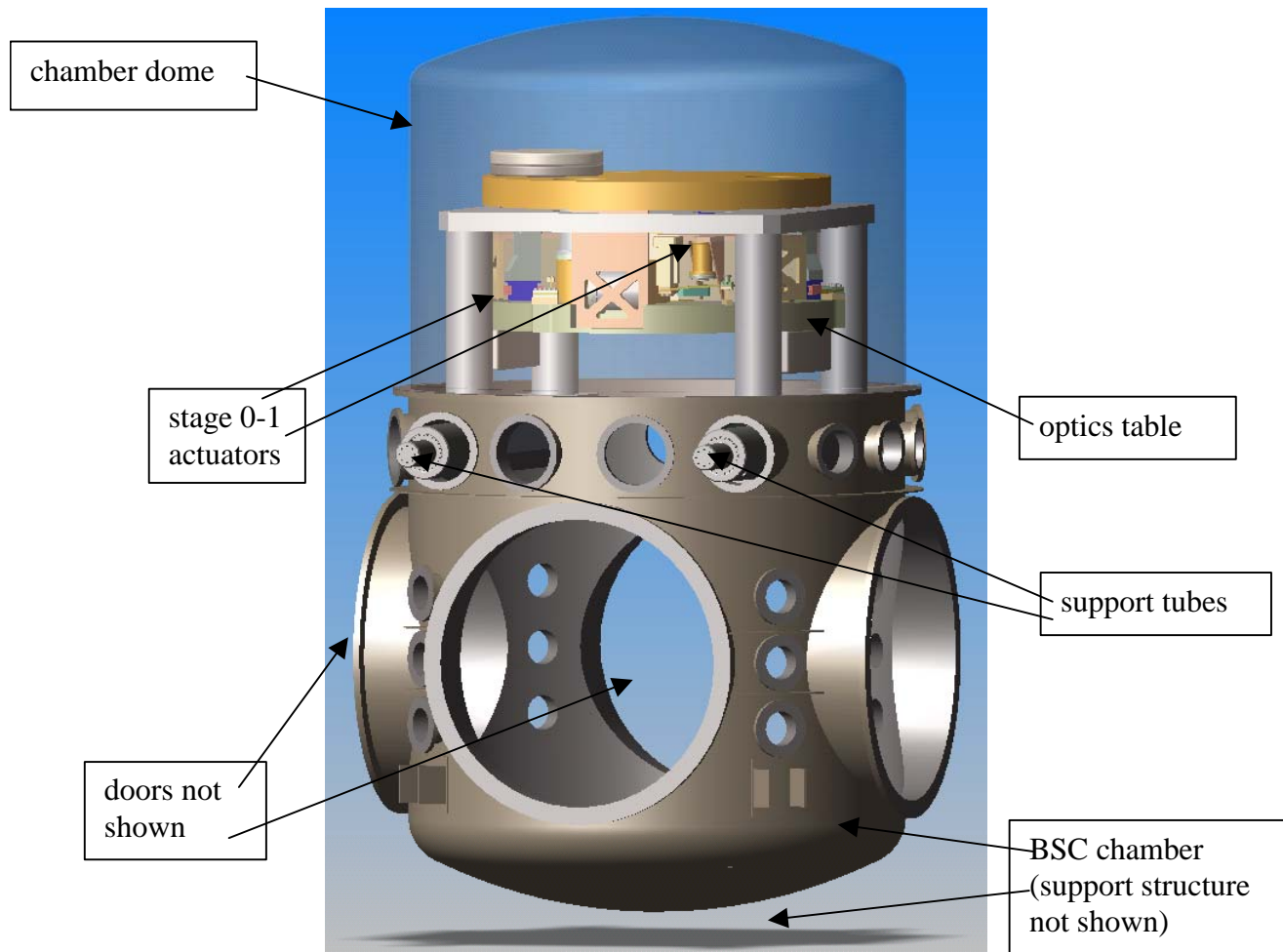
⁵ J. Giaime, B. Lantz, et. al., Advanced LIGO Seismic Isolation System Conceptual Design, LIGO-E010016-00, 1/20/2001

analysis only the inner stage (stage 2) is included with the quadruple suspension structure as a payload element.

The SEI/BSC structural/mechanical design was performed by ASI⁶, under contract to LIGO. The finite element model used in this analysis was delivered by ASI 3/2004. An update for the final design will likely be needed. (A new model, consistent with the final design, has been delivered by ASI.) The overall SEI assembly is depicted within the BSC chamber in Figure 1. An isometric view of the SEI/BSC system is shown in Figure 2. The inter-nested active stages, stages 1 and 2, are shown in the elevation view of Figure 3. The cross-section A-A of Figure 3 is given in Figure 4, which also shows the layout of the sensors and actuators. The layout consists of tri-fold symmetry; Actuators and sensors are located at three "corners" in each of the stages. Note that the sheer physical size of the sensors and actuators makes physical collocation difficult. The stiffness requirements stated above are designed to ensure that from a controls and dynamics perspective the actuators and sensors are collocated, i.e. that no flexible body modes add phase lag between the actuator and sensor.

Figure 1: Overall BSC SEI system installation

Note: This is an old rendering of the SEI design; see ASI Tech Memo No. 20009033-A for latest.



⁶ K. Smith, Post CDR Design Assessments of BSC Structure, Alliance Spacesystems Inc., Tech Memo No. 20009033-A, 15 oct 2004.

Note: This is an old rendering of the SEI design; see ASI Tech Memo No. 20009033-A for latest.

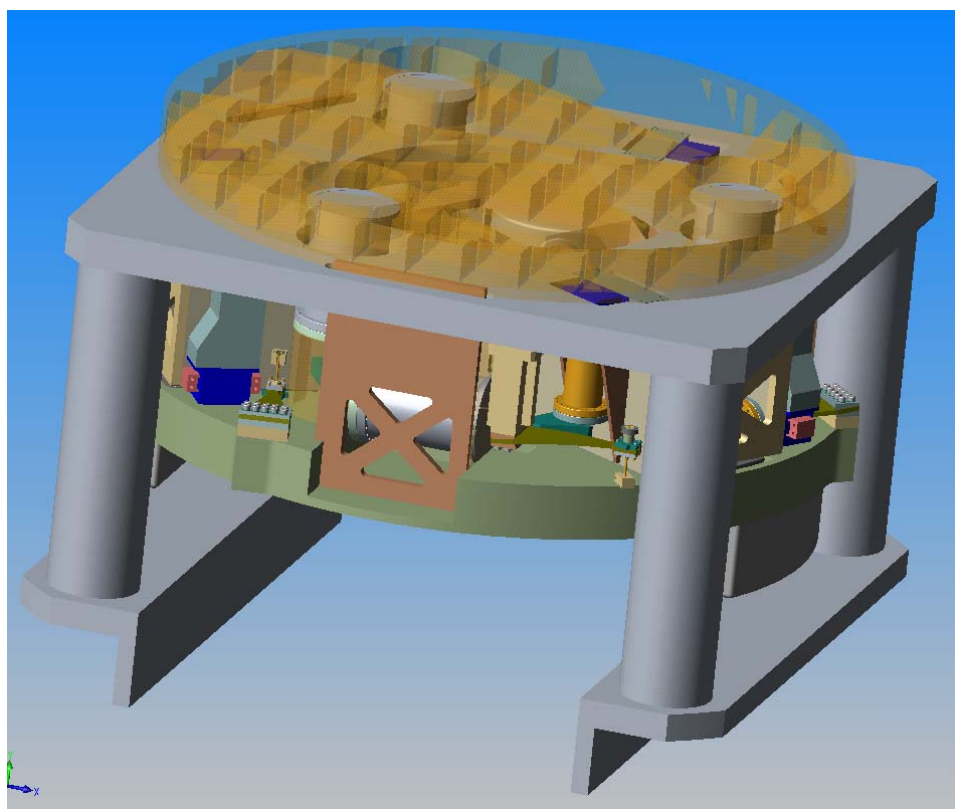


**Figure 3: BSC SEI System, elevation view
indicating the location of the upper counter-balance mass**

Note: This is an old rendering of the SEI design; see ASI Tech Memo No. 20009033-A for latest.

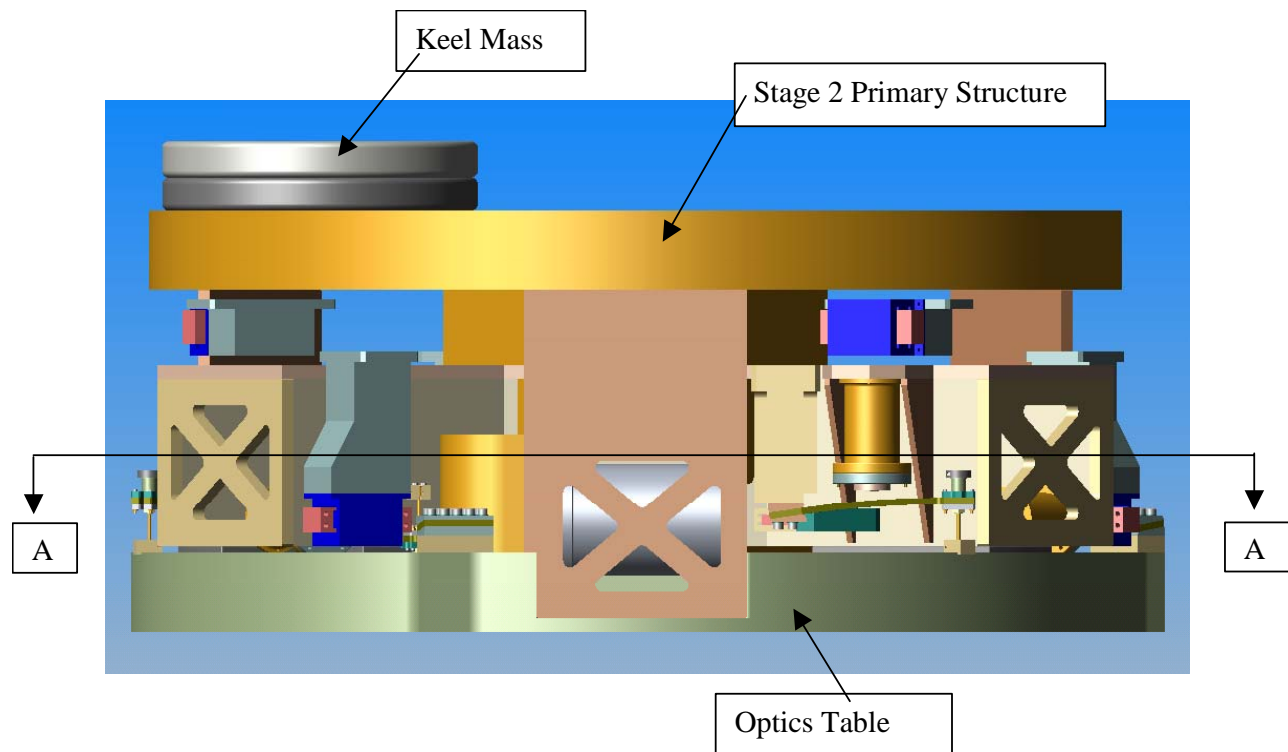
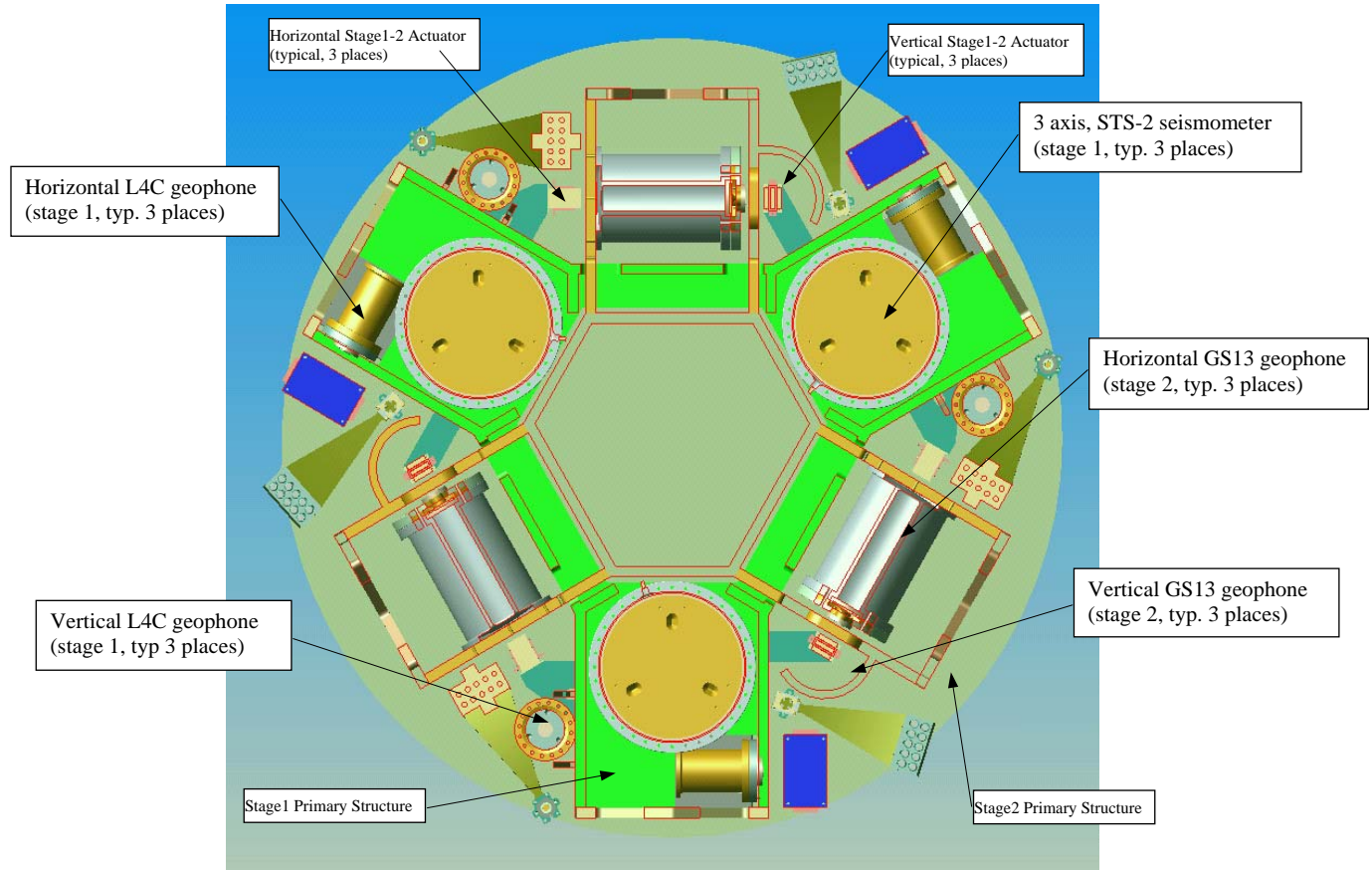


Figure 4: Sectional (view A-A from figure 3) of the BSC SEI system indicating the locations of the actuators and sensors

Note: This is an old rendering of the SEI design; see ASI Tech Memo No. 20009033-A for latest.



2.1 SEI Stage2 Finite Element Model

The Nastran finite element model of the inner (stage 2) structure, created by ASI, is shown in Figure 5 (rendered in I-DEAS). The locations of the discrete mass representations of the sensor and actuator subassemblies are depicted in Figure 6.

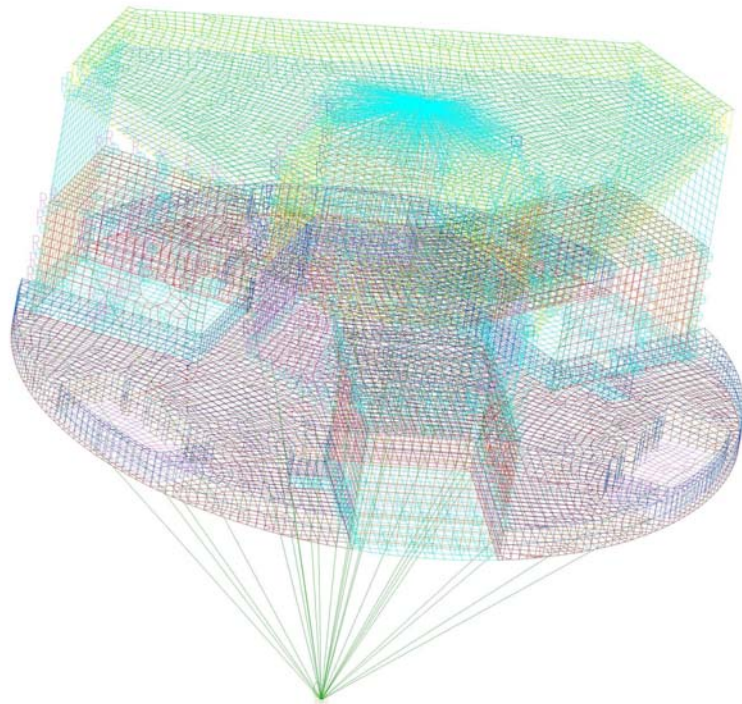
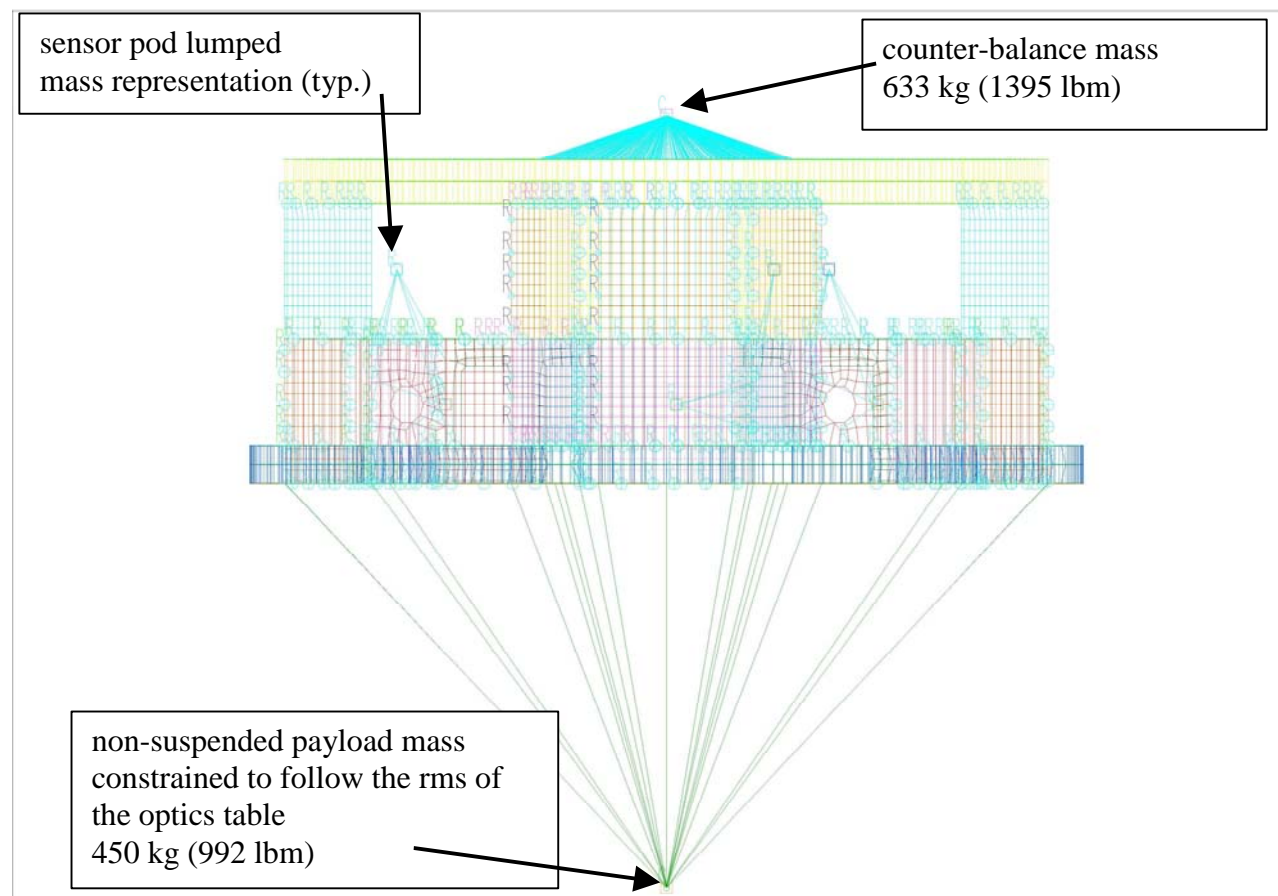


Figure 6: Discrete Masses in the SEI Stage 2 finite element model



The mass properties of Stage2 are given in the following Table. The total stage2 mass is 14.48 lbf-s²/inch (slinch) or 5591 lbm or 2536 kg. This stage mass is comprised of a payload mass of 450 kg, a "keel" ballast of 633 kg and a stage structure mass of 1454 kg.

Table 1: SEI Stage2 Mass Properties (inch, lbf, slinch units)

All elements will be used				
Volume : 4.586D+04				
Mass : 1.448D+01				
Center of gravity : 4.510D-07 2.931D-07 -8.610D+00				
Moments of Inertia about c.g.				
Ixx	Iyy	Izz	: 1.117D+04	1.117D+04 5.315D+03
Ixy	Iyz	Izx	: 1.704D-04	1.396D-03 -2.217D-04
Moments of Inertia about origin				
Ixx	Iyy	Izz	: 1.224D+04	1.224D+04 5.315D+03
Ixy	Iyz	Izx	: 1.704D-04	1.359D-03 -2.780D-04
Principal axes				
1	:	0.000	0.000	1.000
2	:	1.000	0.000	0.000
3	:	0.000	1.000	0.000
Principal Moments of Inertia				
I11	I22	I33	: 5.315D+03	1.117D+04 1.117D+04

In this finite element model, the payload mass is represented as a point mass at the estimated center of mass position. The "keel" mass is positioned to place the composite system center of mass in the plane of actuation and centered horizontally.

2.2 SEI Stage 2 Modes (with point mass payload approximations)

The frequencies of the first 11 modes of the unconstrained stage2 model described above (6 rigid body modes and 5 elastic modes) are given in the following table. The first 3 elastic modes involve motion of the three vertical (horizontal?) GS-13 seismometers on their local structure/attachment. The next two modes at 212 Hz and 214 Hz (depicted in figures 7 and 8) are large spatial scale ("global"), stage2 structure bending which includes the optics table.

In the revised design and finite element model, the first "global" elastic mode⁷ occurs at 174 Hz. In addition, a "payload lateral" mode of 153 Hz is predicted in the final ASI model. This mode is predicted for a discrete point mass representing the beamsplitter suspension mode at its expected center of mass and constrained to follow the rms of the optics table nodes within the suspension structure's planform envelope. This was predicted by ASI to be the lowest suspension structure coupled mode, where suspension structure are modeled as point masses at their center of mass positions and constrained to follow the patch of optics table within their envelope. Smaller payload elements with less definition, such as the pickoff mirror structures were represented as a single composite mass, constrained to follow the optics table. Early modeling by ASI indicated that lighter mass payload elements like the pickoff mirror structures (mass = ? kg) with small footprints (? m x ? m) and low centers of mass (? m from the optics table) could have "low" frequency coupled modes (93 Hz), especially if the footprint was on an unsupported span near the table edge, as depicted in Figure 9.

⁷ Table 1.3 of K. Smith, Post CDR Design Assessments of BSC Structure, Alliance Spacesystems Inc., Tech Memo No. 20009033-A, 15 oct 2004, lists the modal frequencies with a brief description.

Table 2: Stage2 Modes

Mode #	Frequency(Hz)	Modal Prop.			--Damping Factors--		
	Undamped	Mass	% X-Mass	% Y-Mass	% Z-Mass	% Viscous	% Hysteretic
*4	0.0000	8081.42	0.00	3.03	28.20	0.00	0.00
*5	0.0000	11830.4	2.65	18.92	3.20	0.00	0.00
*3	0.0000	21822.7	5.84	49.46	33.57	0.00	0.00
*2	0.0001	9757.53	5.04	15.15	34.95	0.00	0.00
*6	0.0001	5381.46	39.94	9.78	0.00	0.00	0.00
*1	0.0001	5188.23	46.54	3.66	0.07	0.00	0.00
*7	194.8470	23.0292	0.00	0.00	0.00	0.00	1.00
*8	203.3161	63.895	0.00	0.00	0.00	0.00	1.00
*9	204.2418	63.7459	0.00	0.00	0.00	0.00	1.00
*10	211.9377	123.26	0.00	0.00	0.00	0.00	1.00
*11	213.9923	178.736	0.00	0.00	0.00	0.00	1.00

*=Active

100.00

100.00

100.00

Figure 7: Stage2 first "global" elastic mode

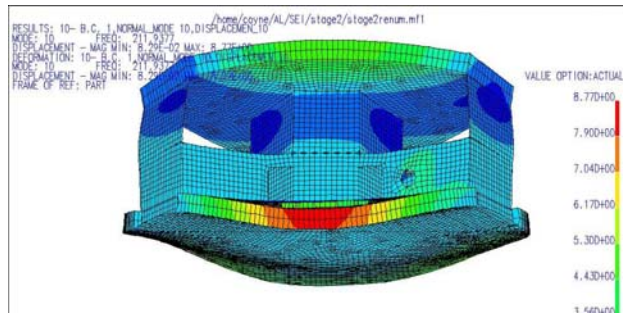


Figure 8: Stage2 second "global" elastic mode

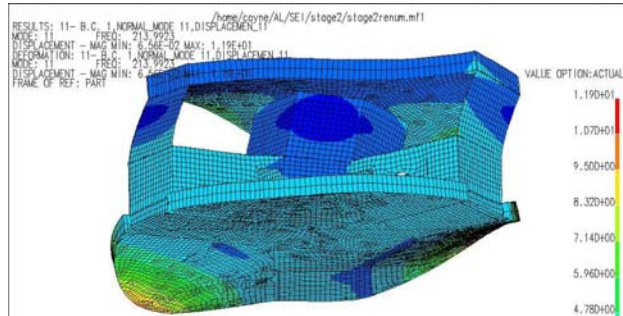
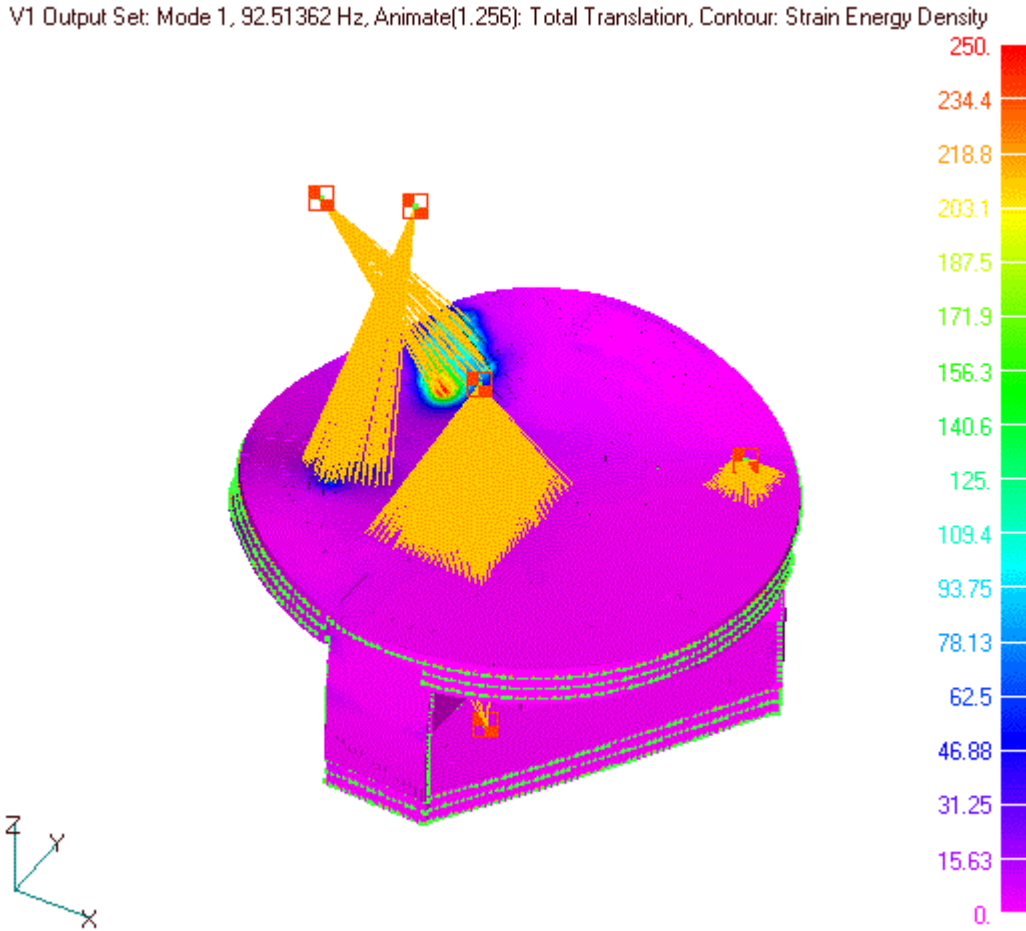
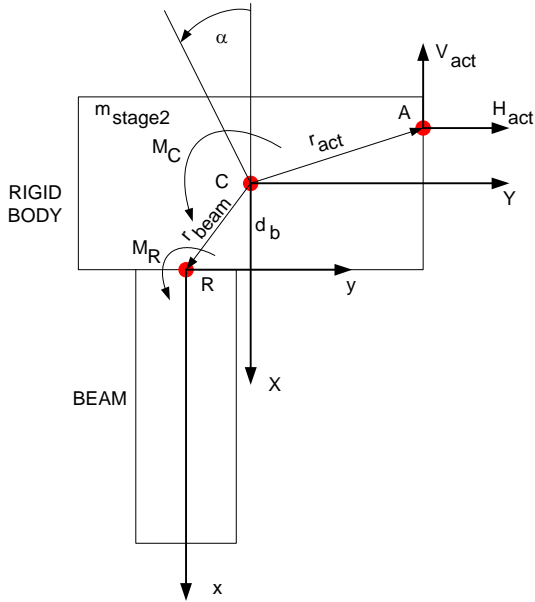


Figure 9: Payload Mode

3 Beam & Rigid Body Model

The suspension structures (and optics payloads in general) have been constrained to a minimum, or "shrink fit", envelope so as to allow flexibility in the use of the optics table (not block access, or unduly constrain the placement of other payloads). The overall length of the test mass quadruple pendulums sets the distance from the optics table to the laser beam line. This results in BSC chamber suspension caging structures of 2.0 m in length. The global elastic modes (i.e. not including local structure modes with very limited mass participation) of the suspension structure are typical of cantilevered beams. The lower part of the suspension structure tends to be smaller in cross-section and lower in lineal density than the upper structure, i.e. the suspension structure designs tend to be like tapered beams. Nonetheless a uniform beam is a reasonable first order approximation⁸. This suggests that a simple model of a beam connected to a rigid mass (Figure 10) might be a reasonable approximation to the low frequency coupled dynamics of a suspension structure and the stage2 structure, since (1) the first elastic mode of the suspension structure is likely about 100 Hz, (2) the first stage2 "global" structure elastic mode is ~174 Hz (including payload mass loading), and (3) the suspension structure footprint is large relative to the optics table (and so should not couple to local table/structure compliance).

⁸ D. Coyne, Frequency Analysis of the Quadruple Pendulum Structure, T030044-03.

Figure 10: Simple Beam and Rigid Mass Model

Using this simple model, one can predict (derivation is in Appendix A) the magnitude and phase perturbations to the rigid body transfer function for horizontal translation and rotation about a horizontal axis. An example is given in Figure 11 for the parameters the quad suspension structure design, D040519-04. The finite element response is given in Figure 12. There is qualitative and semi-quantitative agreement between this simple model and the detailed finite element model (discussed in a following section). The magnitude and phase perturbations are overestimated by the beam and rigid body model probably because the beam is assumed to be uniform whereas the suspension structure is tapered.

The beam/mass model predicts that the first and second bending modes each add a zero-pole pair (in that order), which reduces phase lag, when the root of the beam is coincident with, or near to, the center of mass of the rigid body (when $r_{\text{beam}} \sim 0$ and 'R' is coincident near 'C' in Figure 10). The transfer functions in Figures 11 and 12 are typical of the effect of a flexible appendage when the control is collocated. These modes do not destabilize the system since phase lag is decreased (between the added zero-pole pair). However these modes do reduce the integral of phase and therefore the average gain slope and available feedback decrease somewhat.⁹

When the beam root and center of mass are distant from each other (~ 5 times greater than the nominal distance of 7 inches) then the order of the pair reverses to pole-zero for the 2nd beam mode with rotation actuation (around a horizontal axis through 'C') and phase lag is increased.

The beam/mass model predicts that the magnitude and phase perturbations are independent of frequency and, for fixed rigid mass properties, depend only on the beam mass and modal damping factor. The beam/mass model predicted variation of magnitude and phase perturbations as a function of beam mass is given in Figures 13 and 14 for horizontal translation and rotation respectively. Also shown in these figures are the results from finite element analyses of two suspension structure designs that are somewhat close to and bounded by the beam/mass model prediction.

⁹ P. Enright, Classical Feedback Control with Matlab, Marcel Dekker, 2000, section 4.3.6.

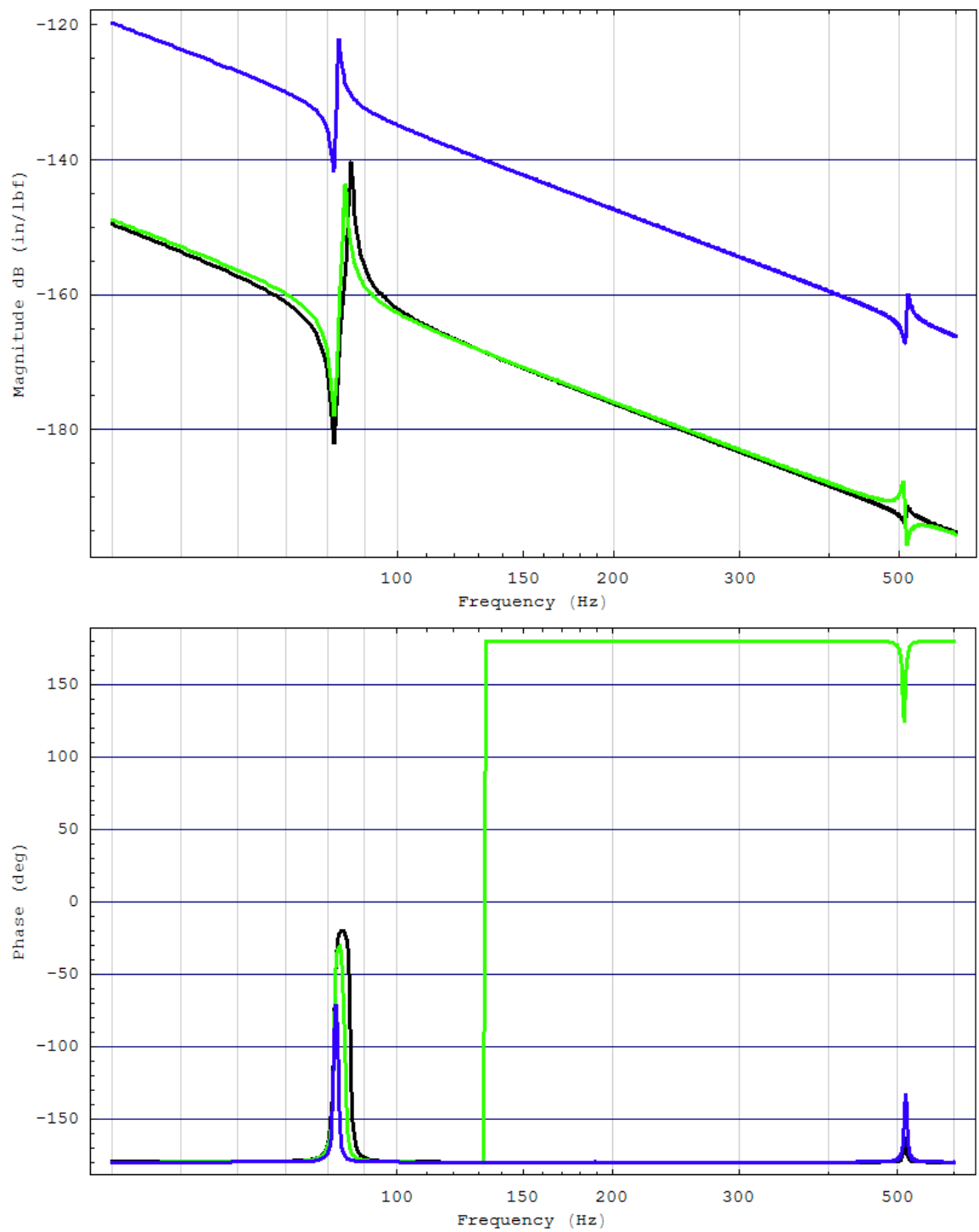
Figure 11: Beam and Rigid Body Model Result for Stage 2 and SUS Quad D040519-04

Figure 12: Finite Element Transfer Function for Modal Actuation on a coupled model of Stage 2 and SUS Quad D040519-04

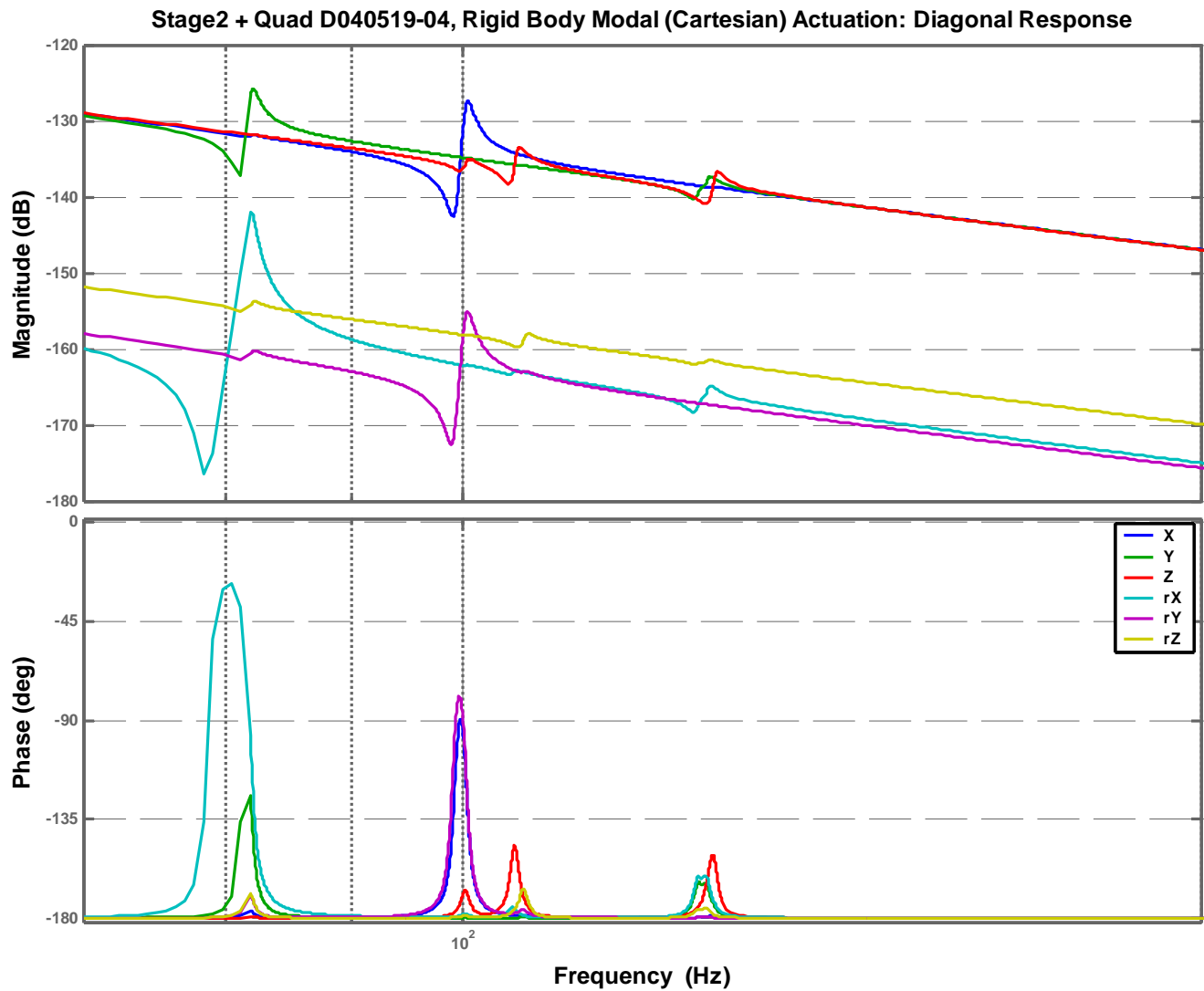


Figure 13: Beam and Rigid Body Model Result for Horizontal Translation: Gain & Phase Changes versus Beam Mass (with varying damping factor)

Points are FEA results for 2 suspension structure designs with a damping factor of 0.01

Curves are for damping factor varying from .5% to 8%. The bold black curve is for 1% damping.

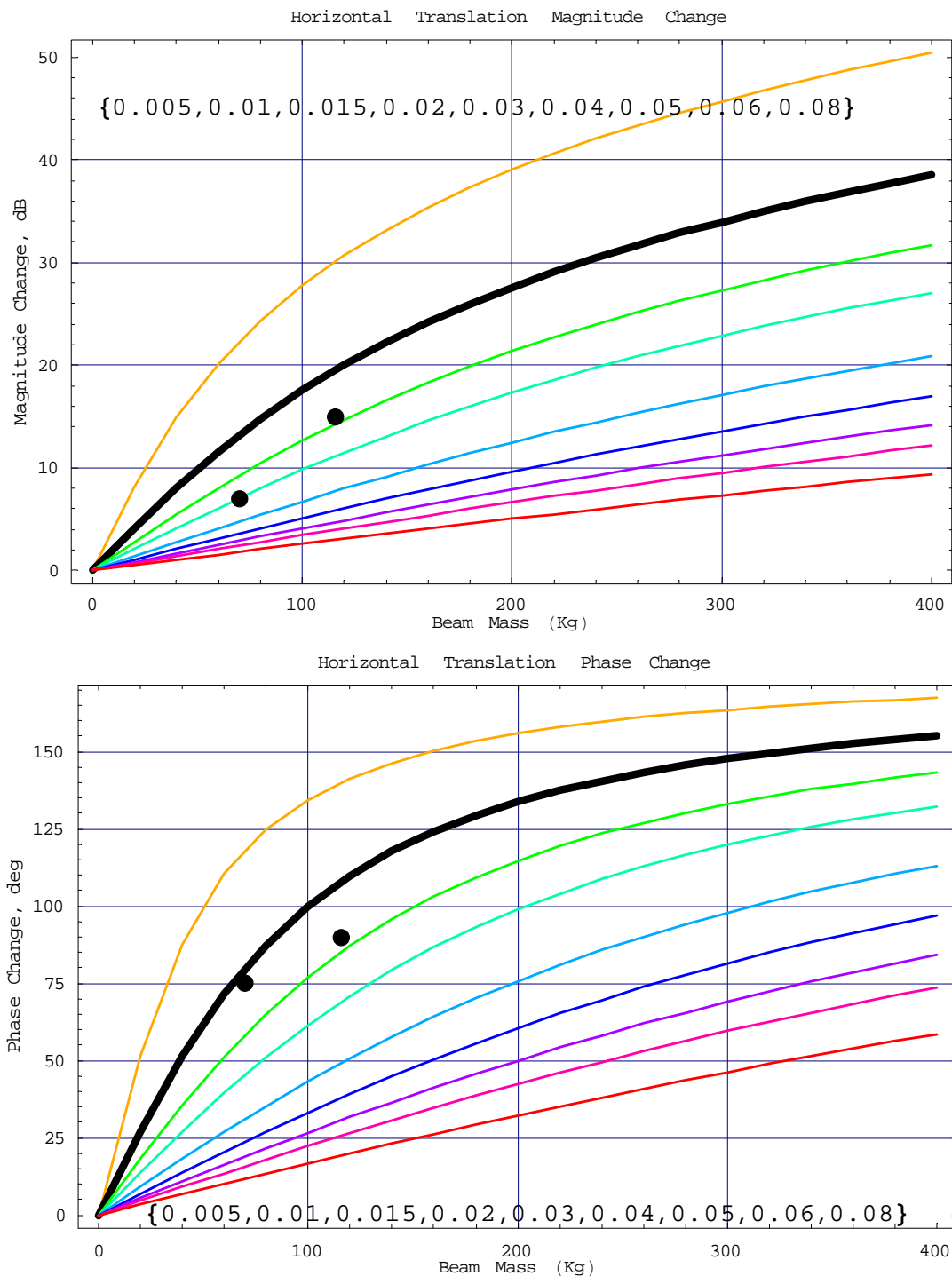
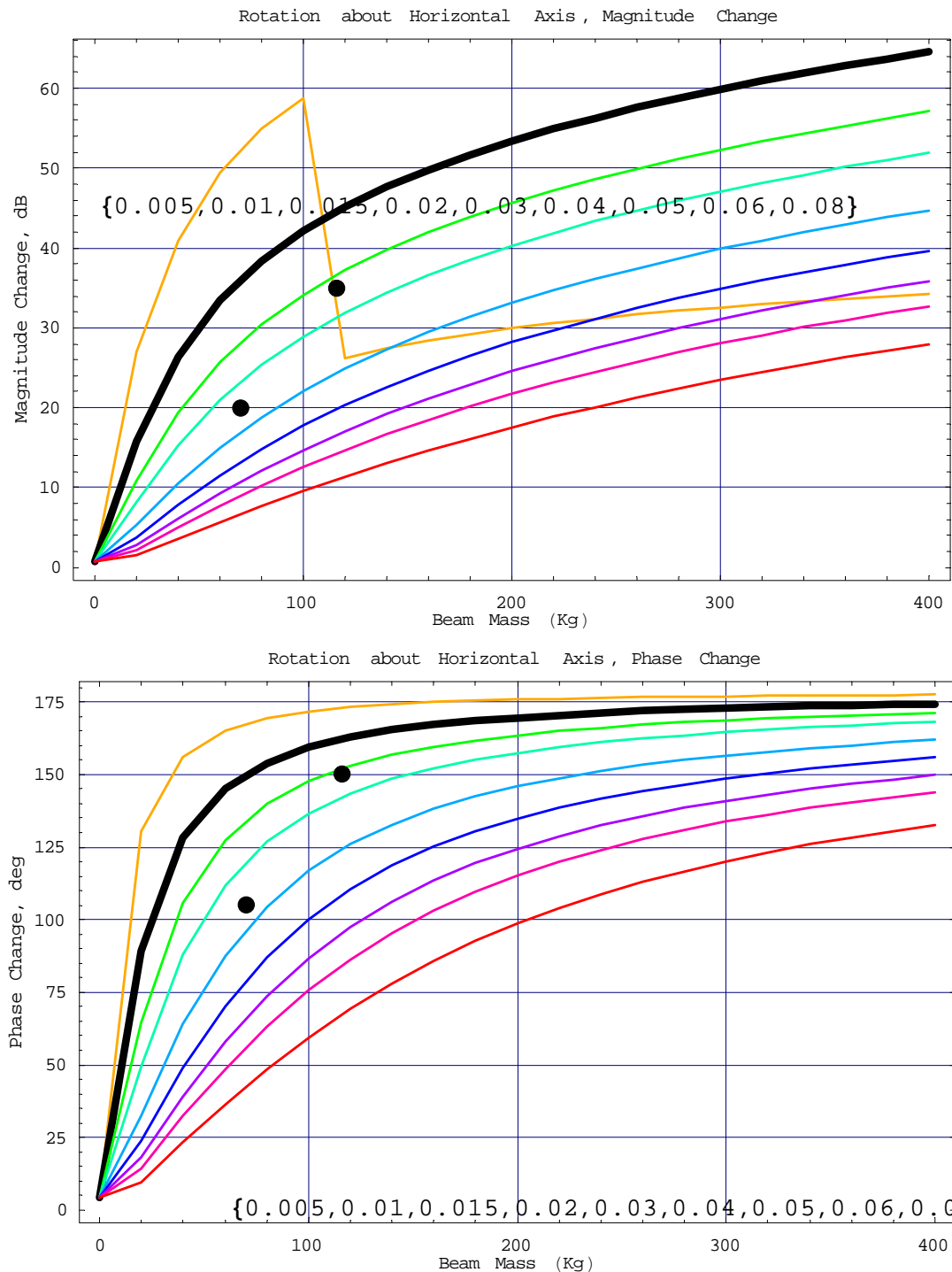


Figure 14: Beam and Rigid Body Model Result for Rotation about a Horizontal Axis: Gain & Phase Changes versus Beam Mass (with varying damping factor)

Points are FEA results for 2 suspension structure designs with a damping factor of 0.01

Curves are for damping factor varying from .5% to 8%. The bold black curve is for 1% damping.

The 0.5% damping curve is incorrect (numerical problem with FindMinimum)



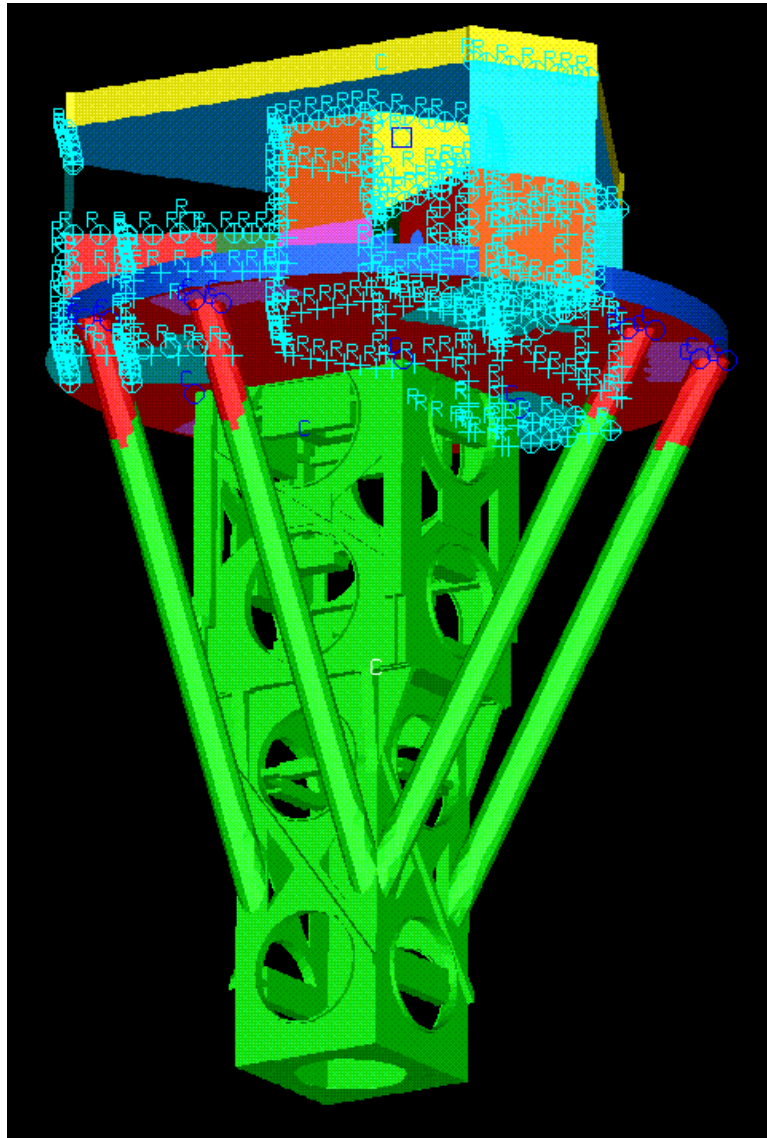
4 Suspension Structure

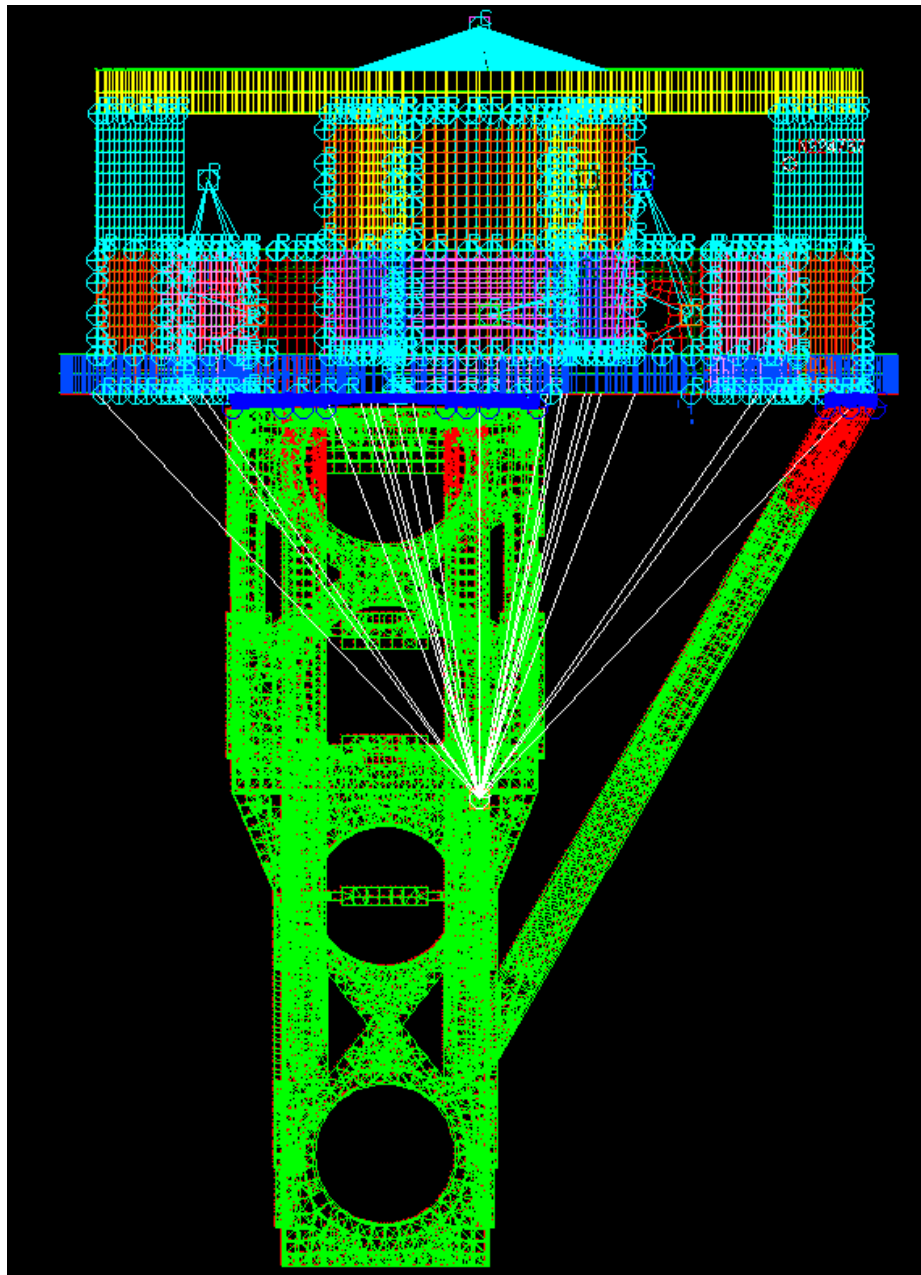
The quad suspension structure designs in the following table were considered.

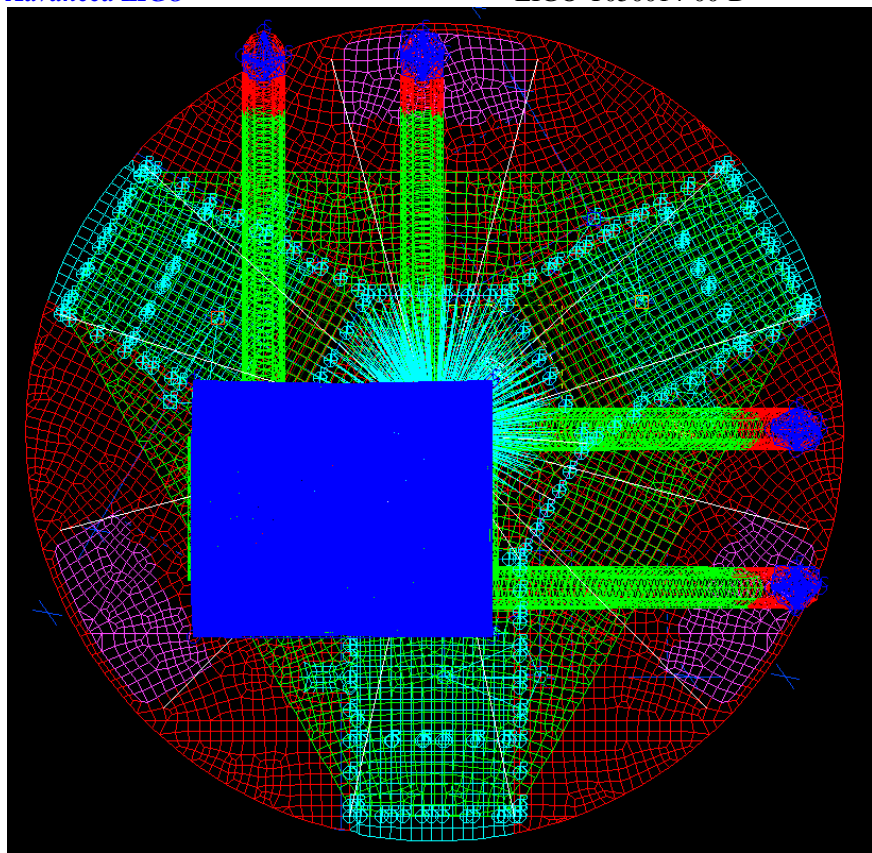
Table 3: Quadruple Suspension Structure Designs

Name	Description	Mass (kg)	Freq. (Hz)
quadx33	structure with outriggers, heavy, high frequency	214	147, 153, 163, 168, ...
quadx51	light, low frequency	84 total	77, 91, 150, 157, 189, ...
quady2	lighter still, lower half light weight and flexible	70 total (9 lower)	27, 86, 91, 93, 123, ...
D040519-04	medium mass, design used for quad SUS controls prototype	115 total 38 lower	86, 101, 102, 108, ...

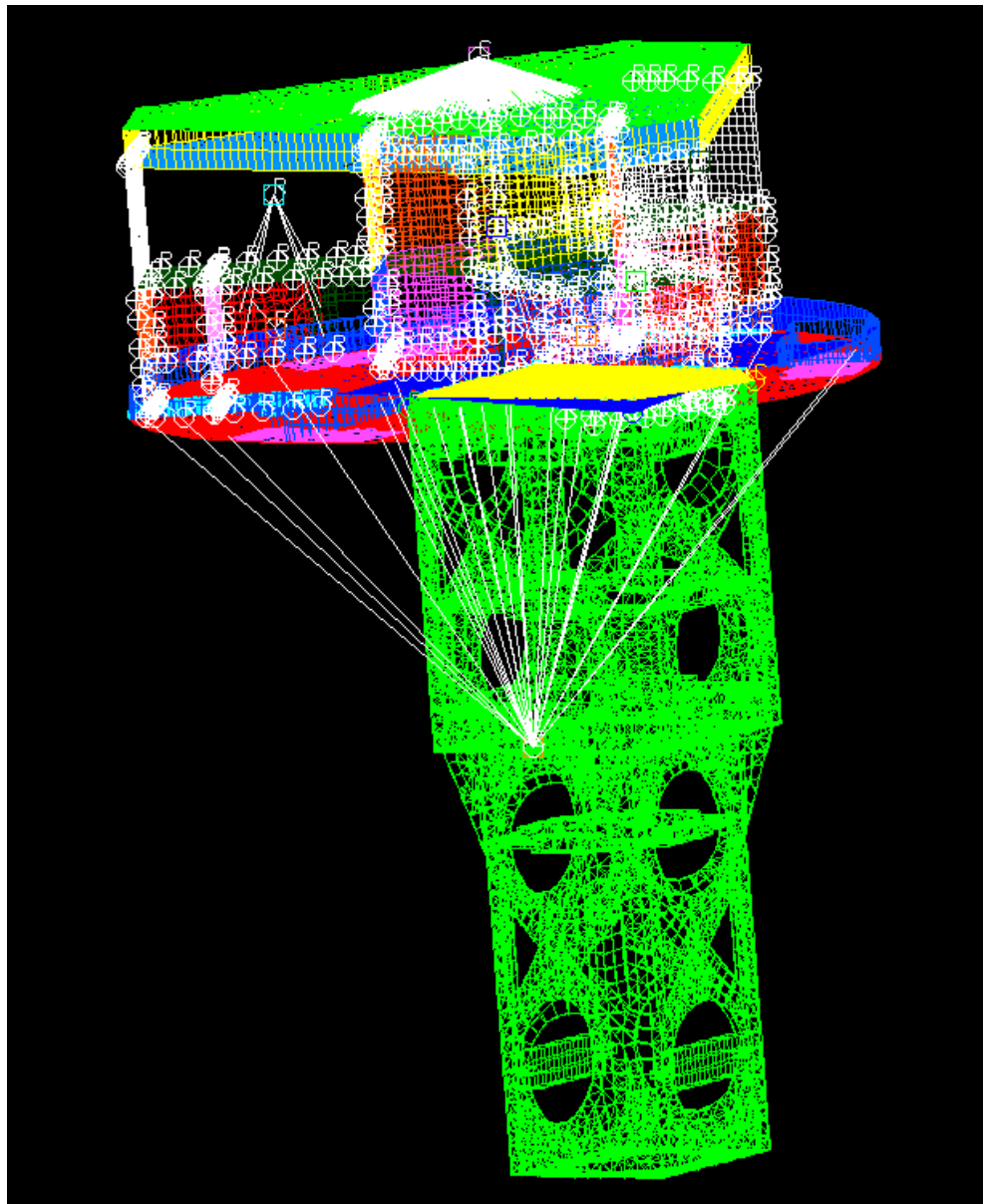
4.1 quadx33

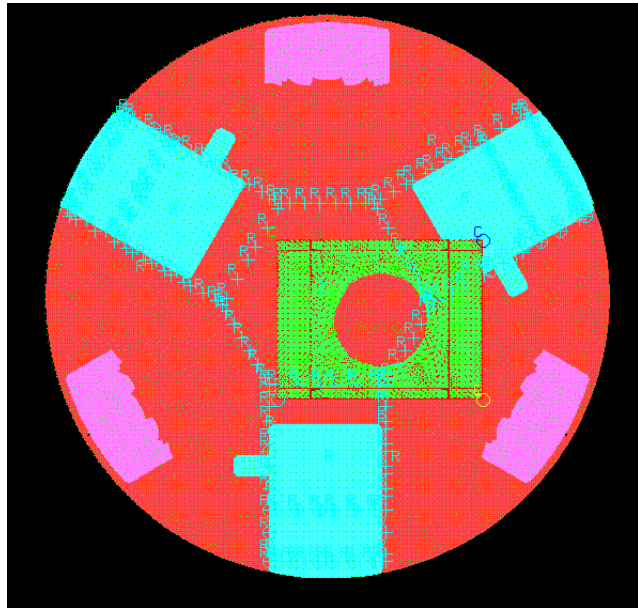




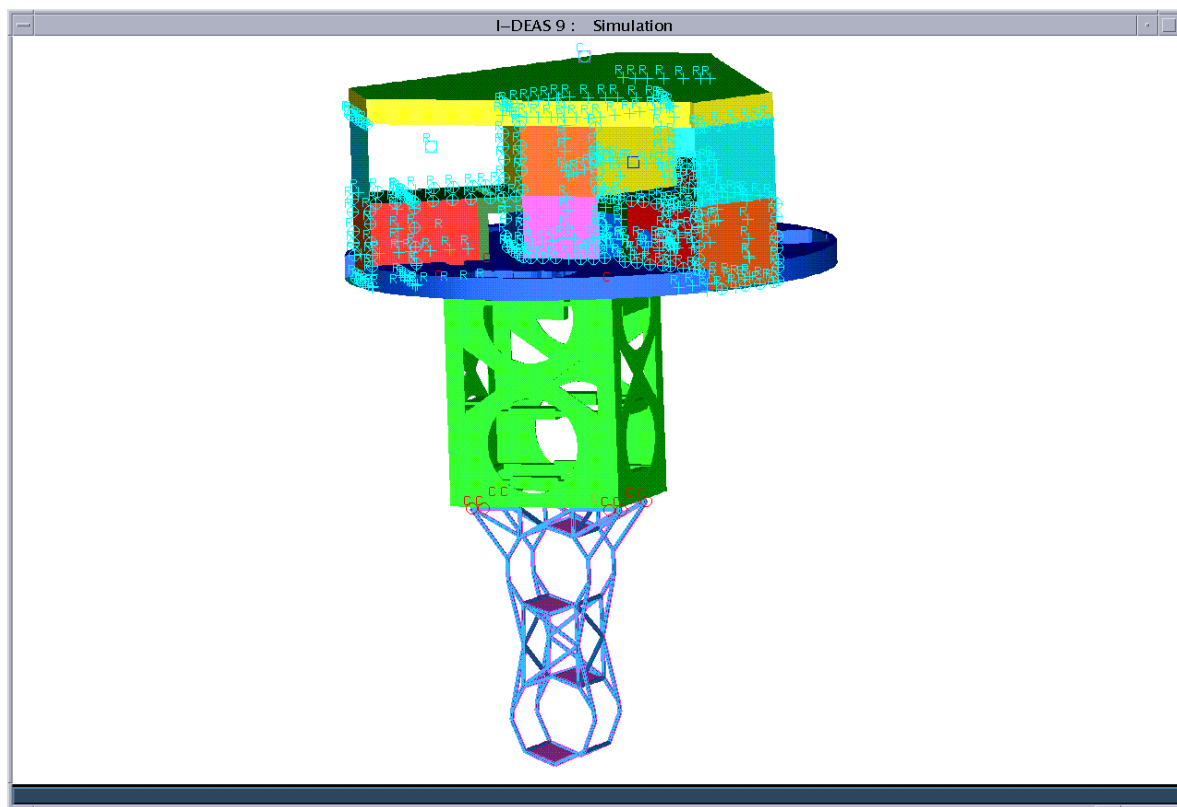


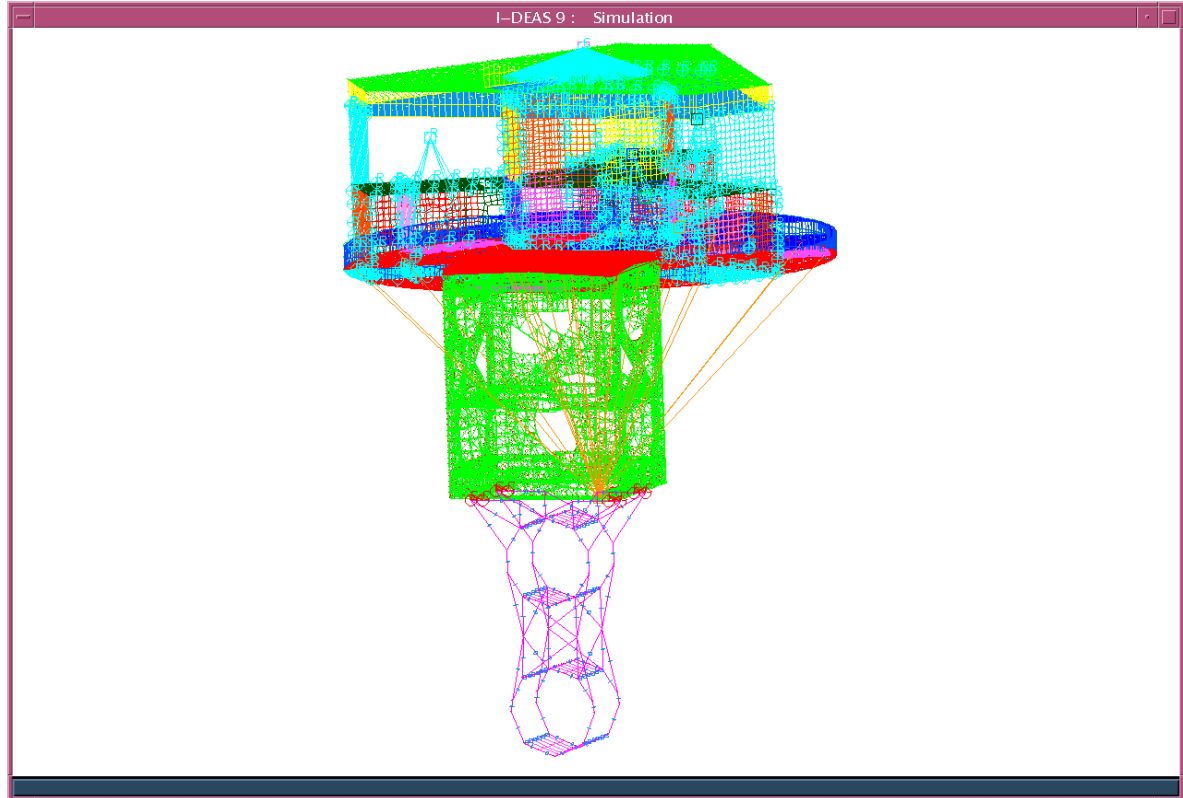
4.2 quadx51



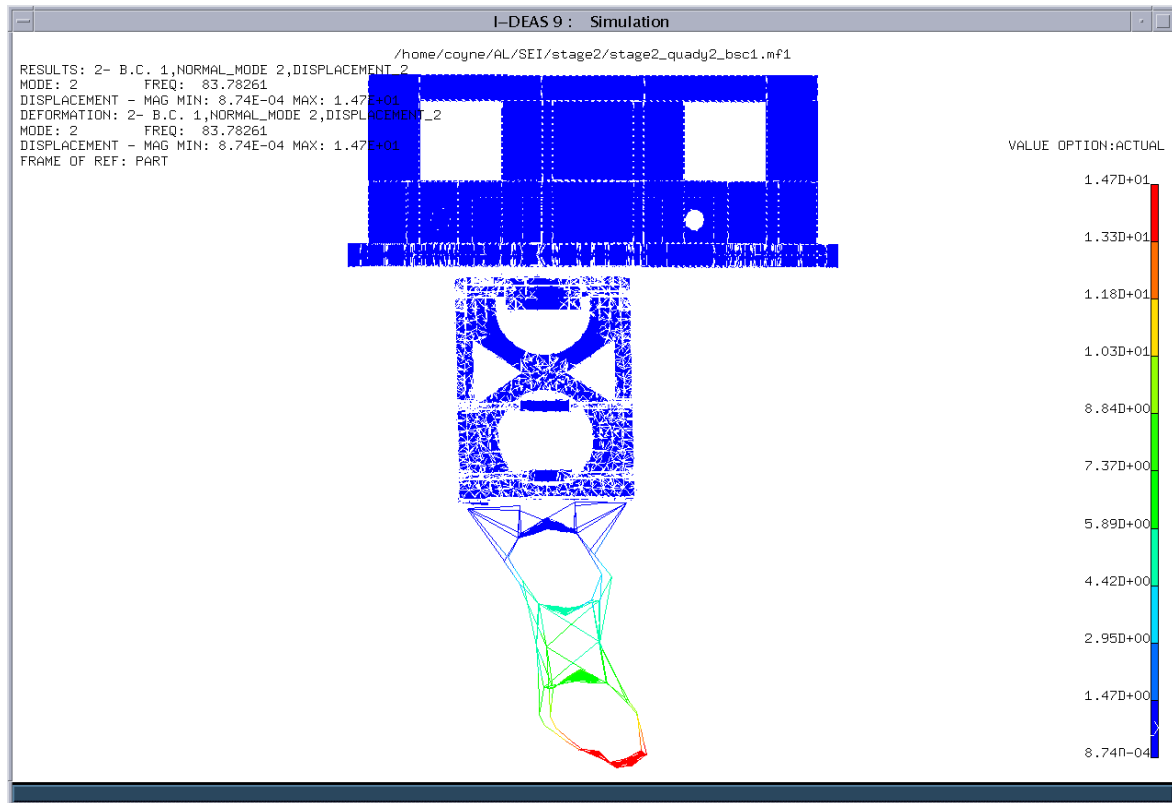
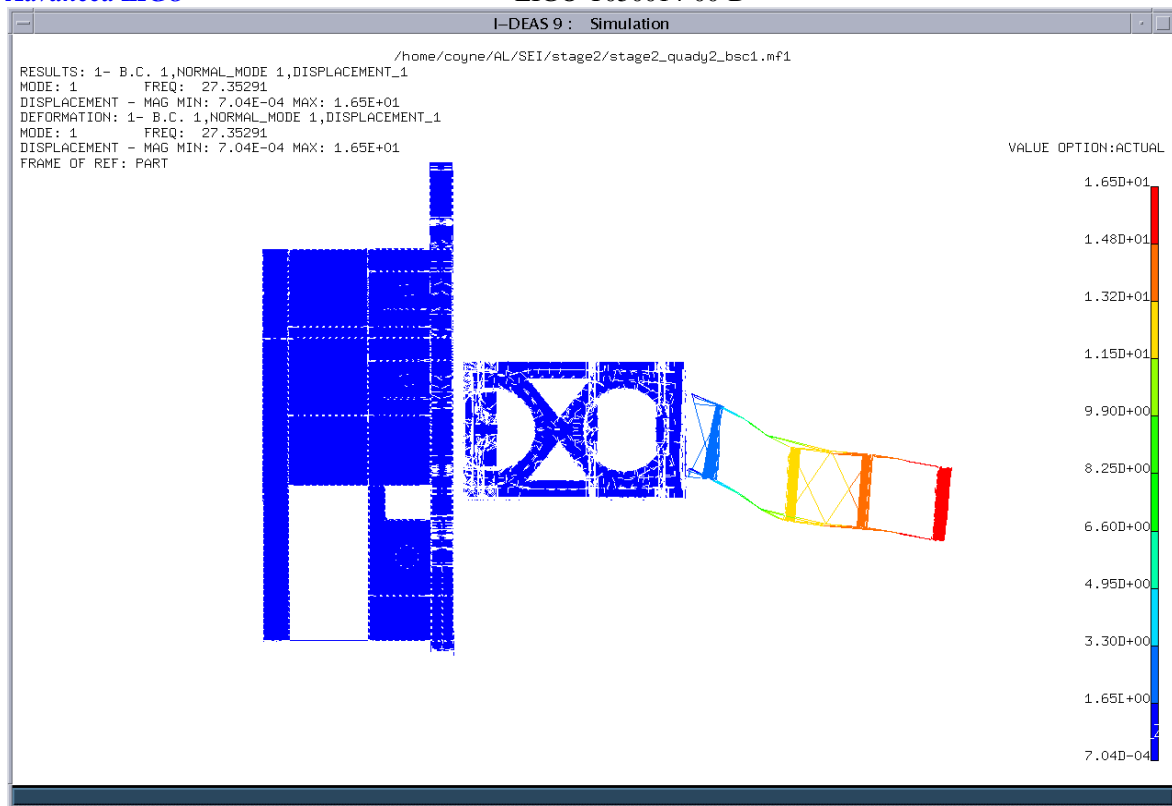


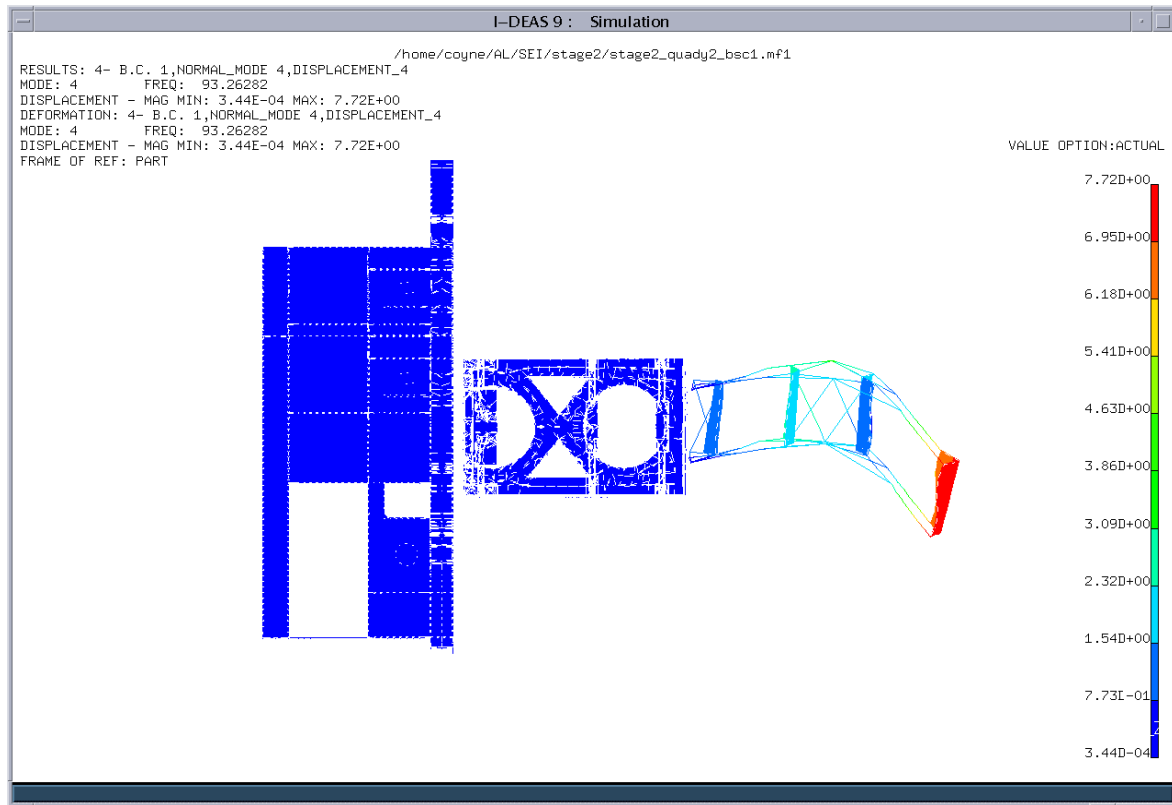
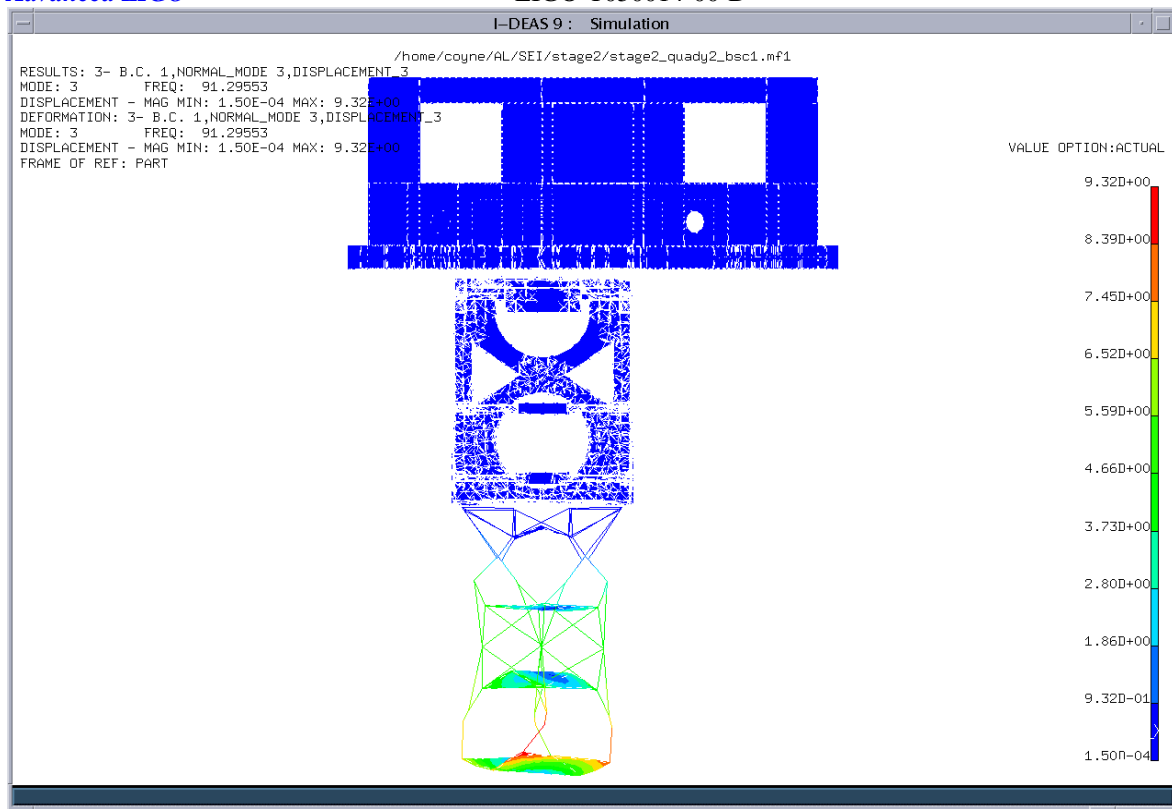
4.3 quady2

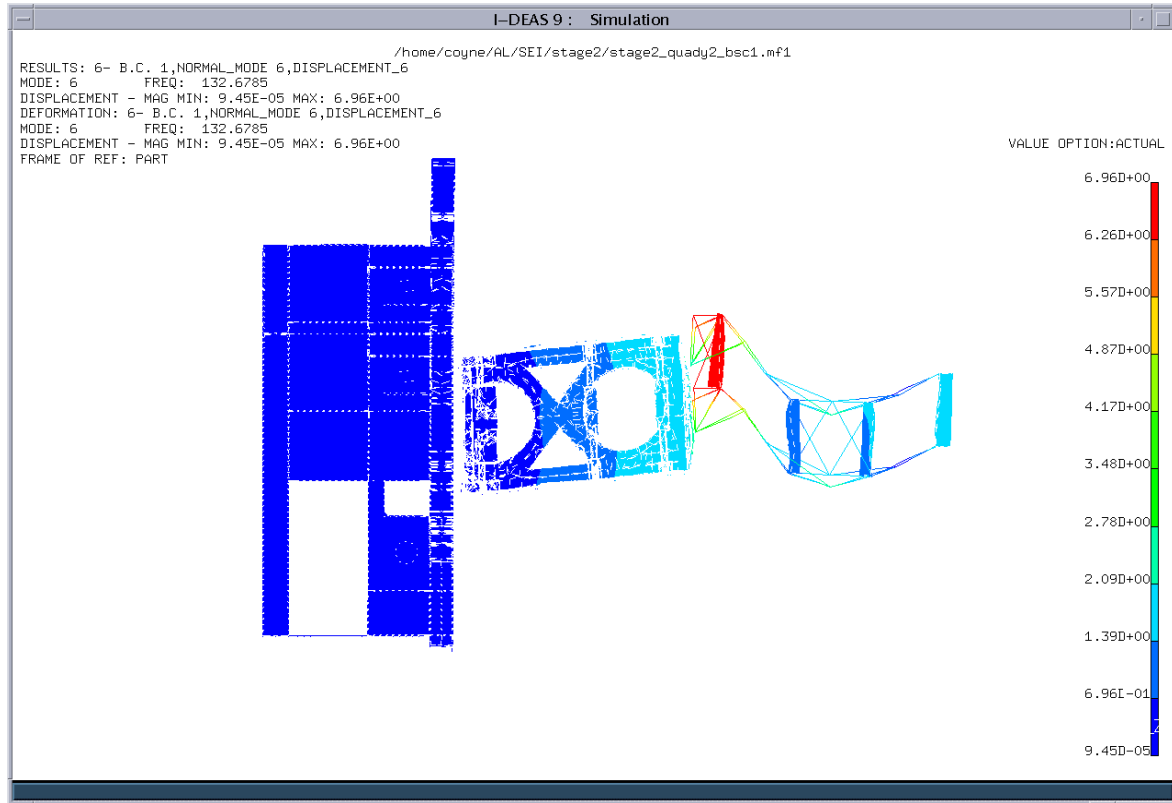
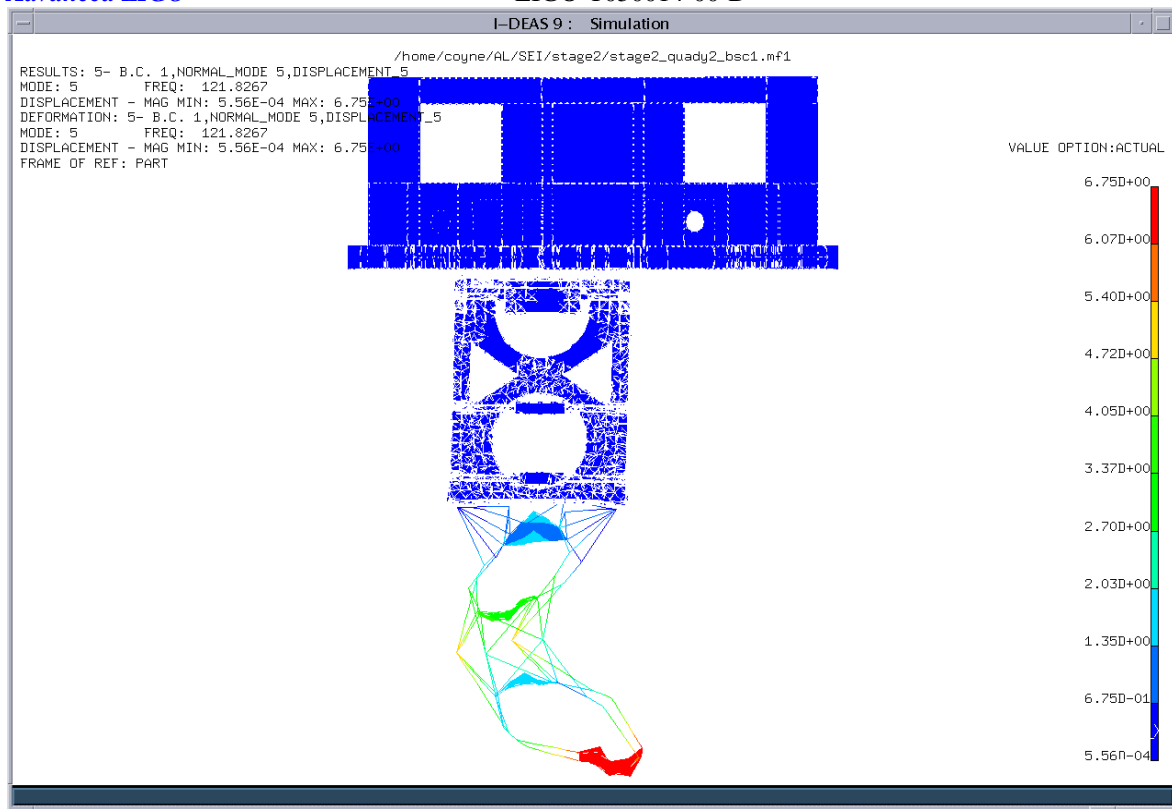


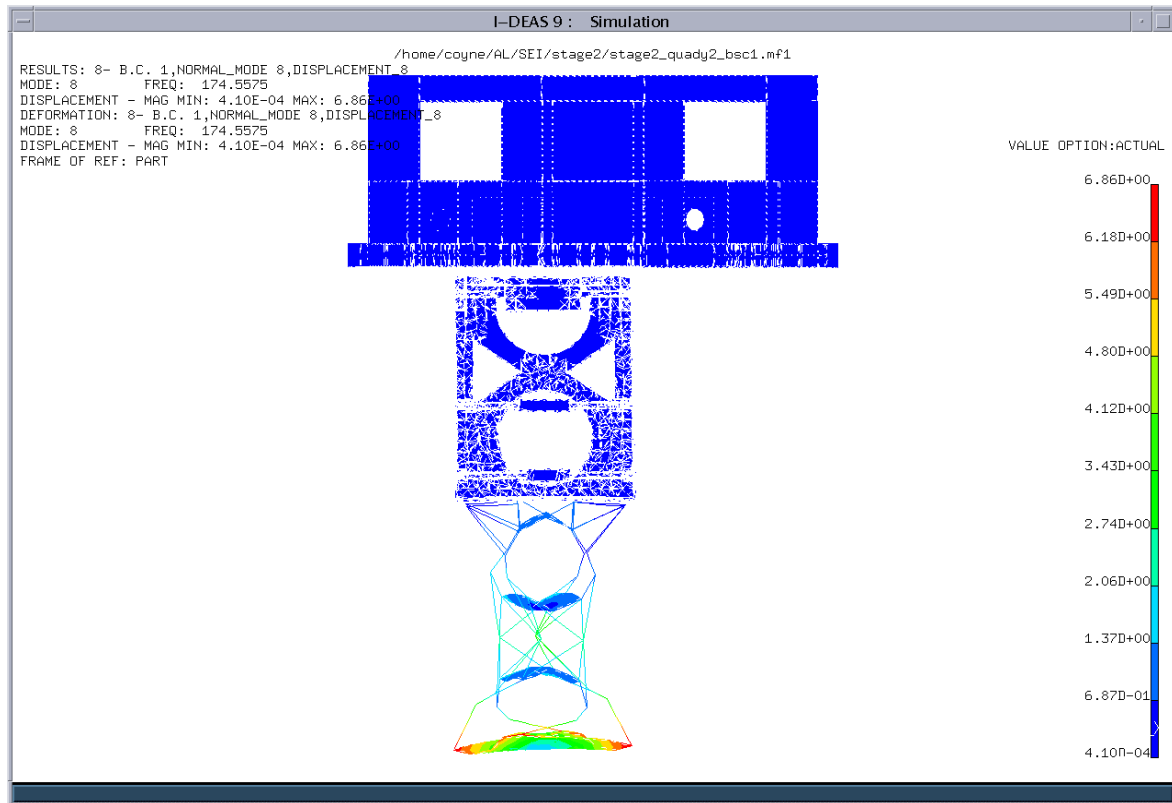
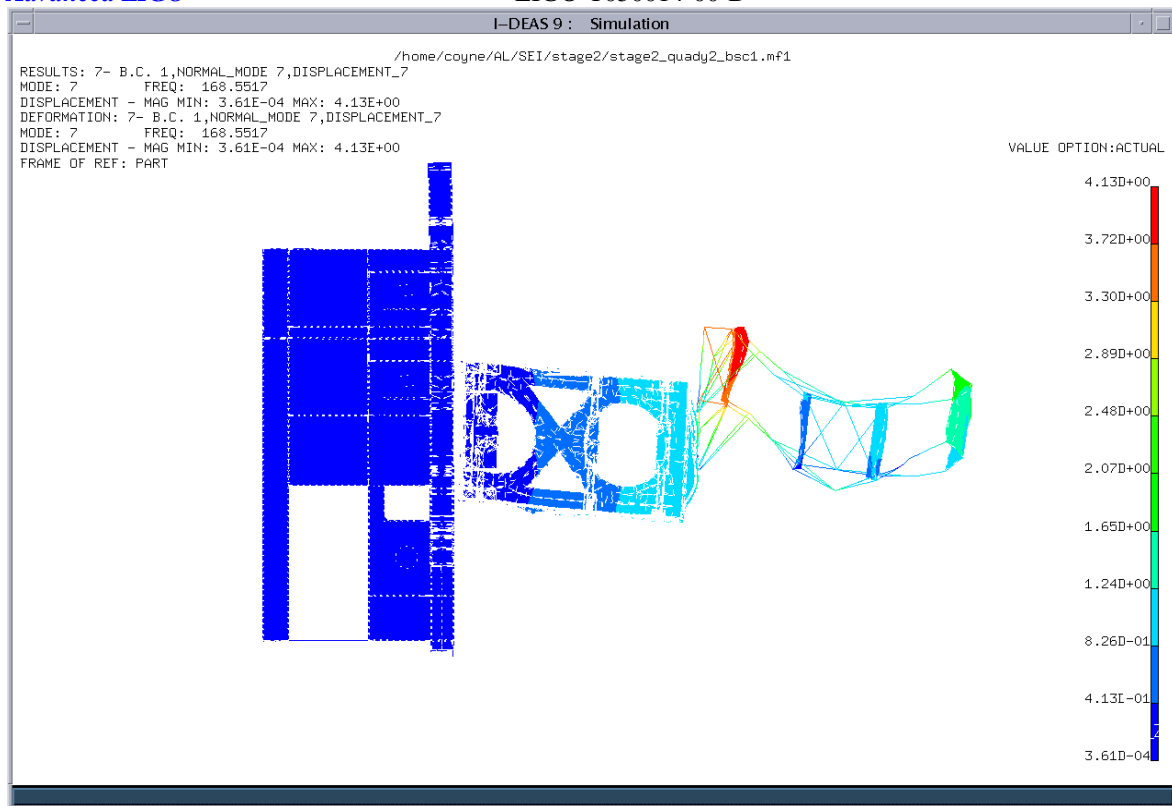


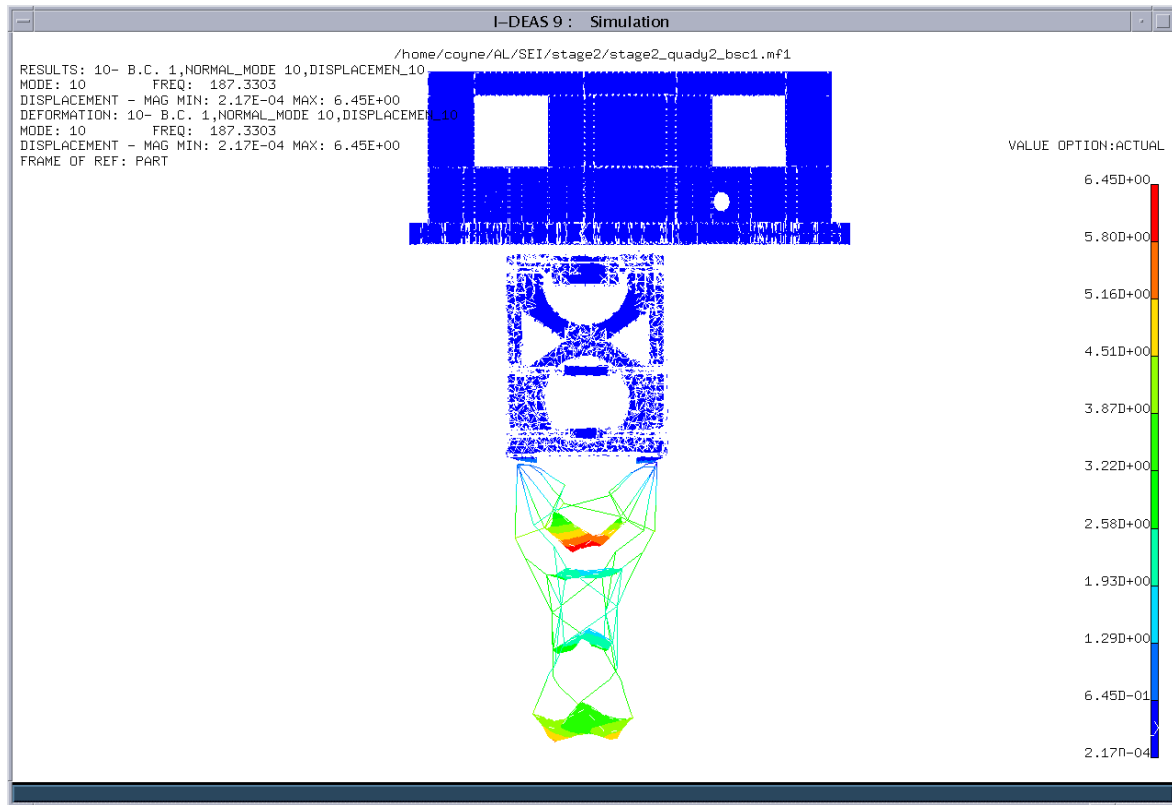
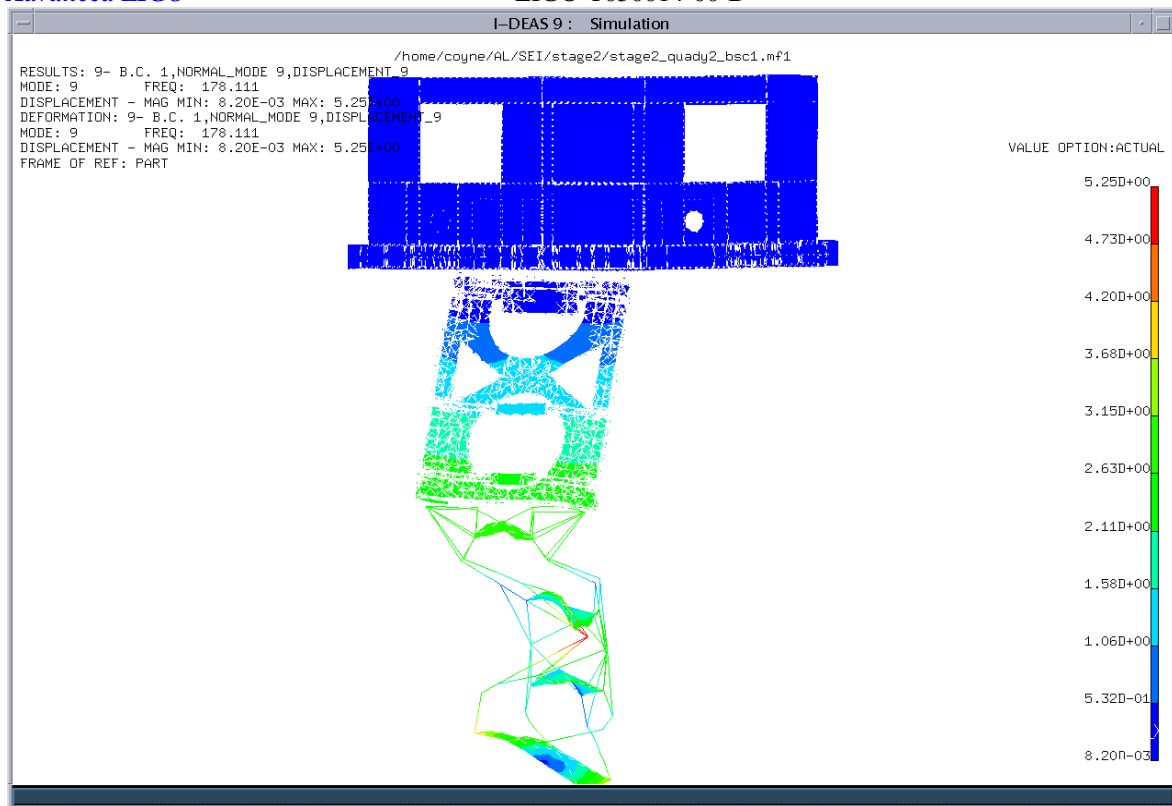
No.	Freq (Hz)	Modal Mass	Description
1	27.35	5.73	lower quad section, 1st y-bending
2	83.78	2.064	lower quad section, 1st x-bending
3	91.3	0.698	lower quad section, 2nd y-bending
4	93.26	0.358	lower quad section, 1st torsion
5	121.83	0.468	lower quad section, 2nd x-bending
6	132.68	1.084	lower quad section, 3rd y-bending
7	168.55	0.328	lower quad section, 2nd torsion
8	174.56	0.25	
9	178.11	1.119	
10	187.33	0.439	
11	195.22	8.618	
12	203.47	34.884	
13	204.68	32.161	
14	211.7	18.88	
15	214.29	35.314	
16	226.03	0.048	
17	230.49	2.217	
18	248.48	1.902	
19	250.46	5.665	
20	251.41	4.056	

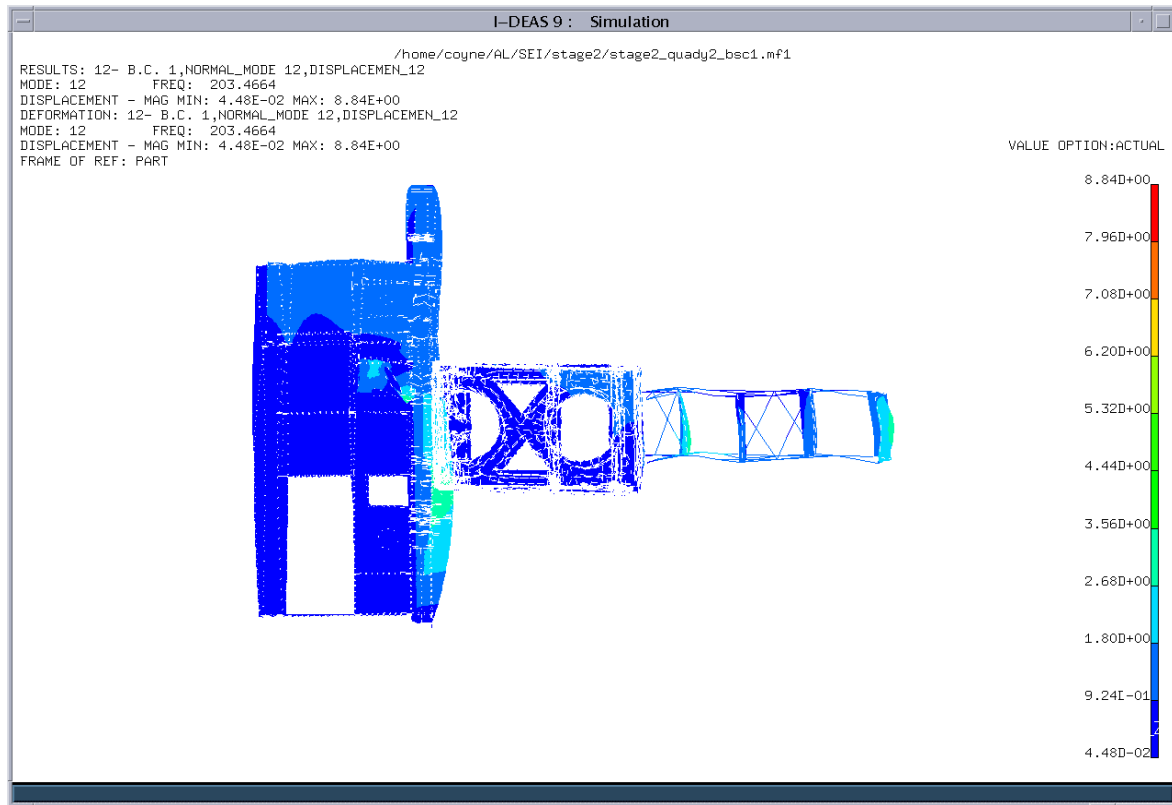
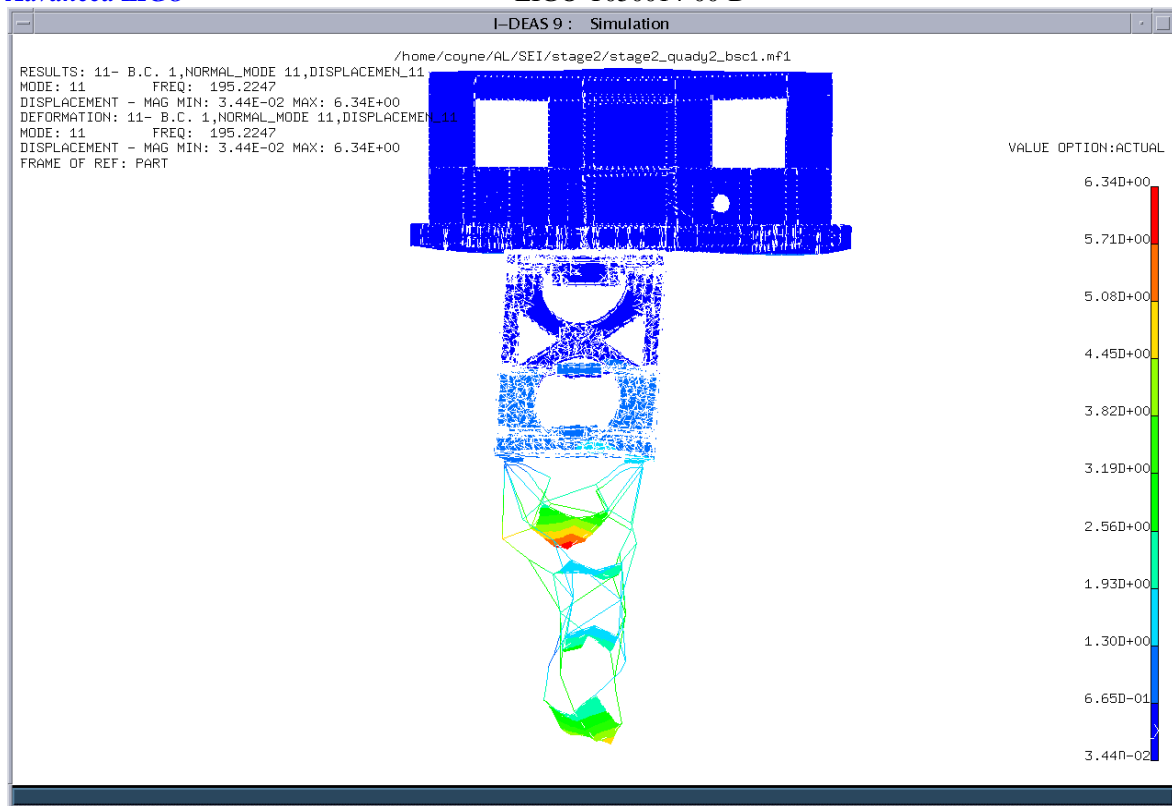


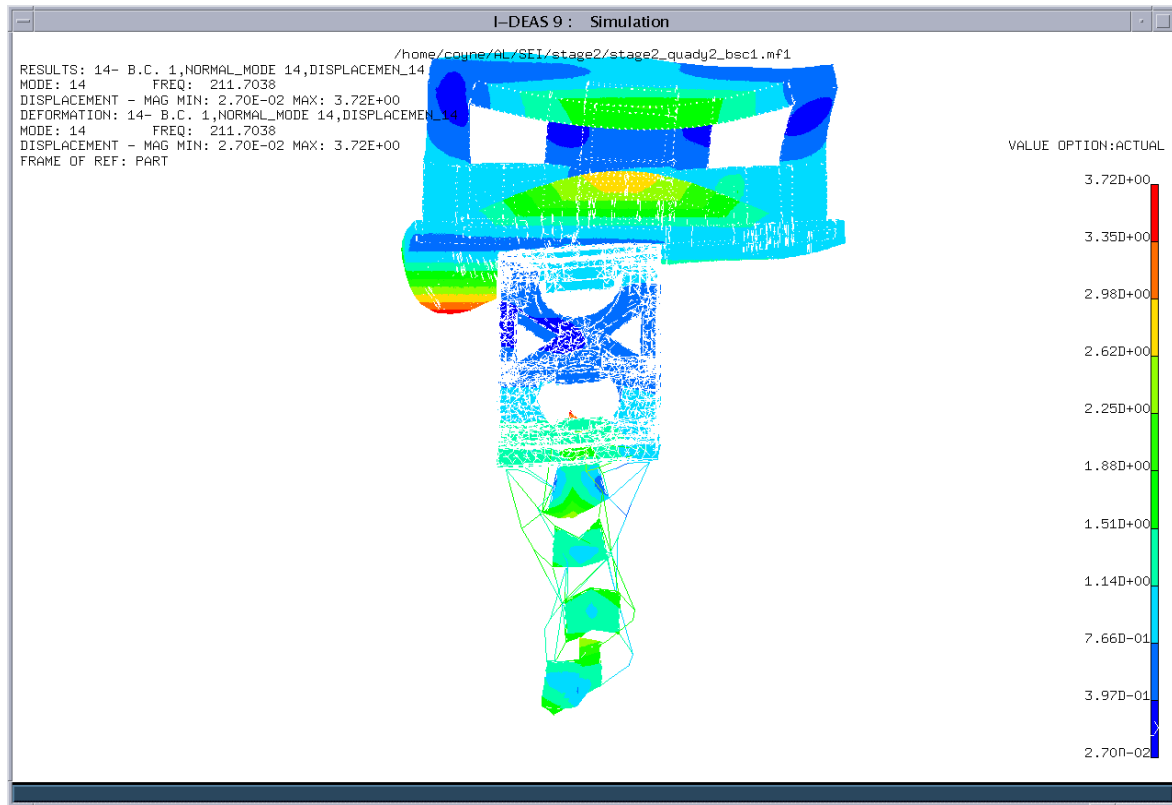
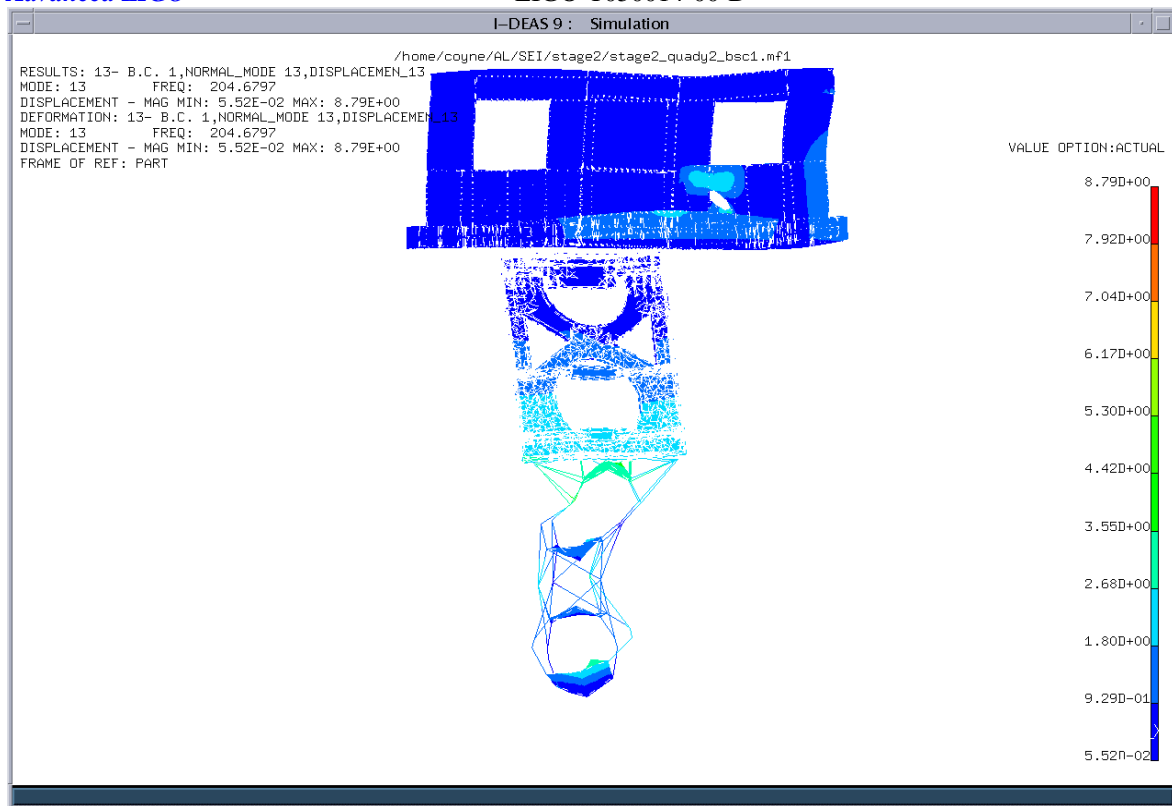


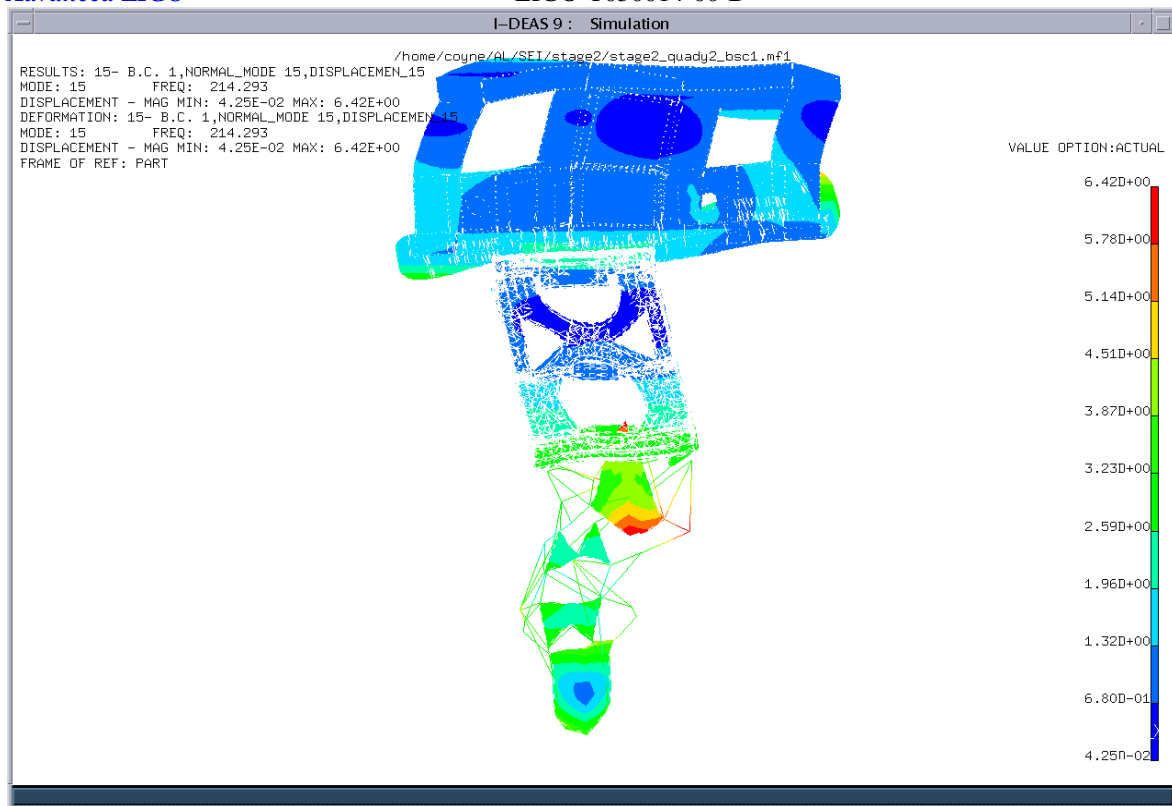


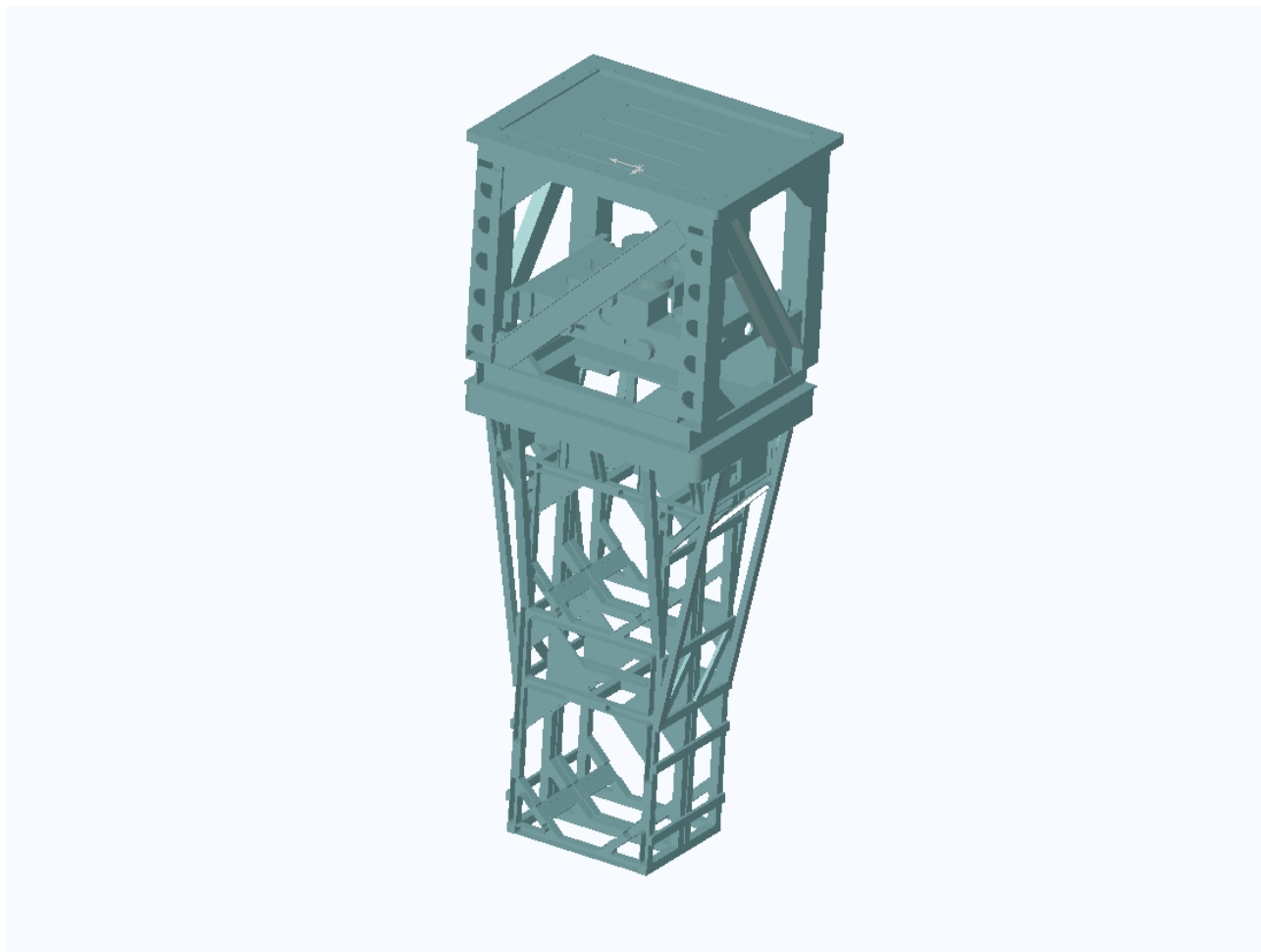


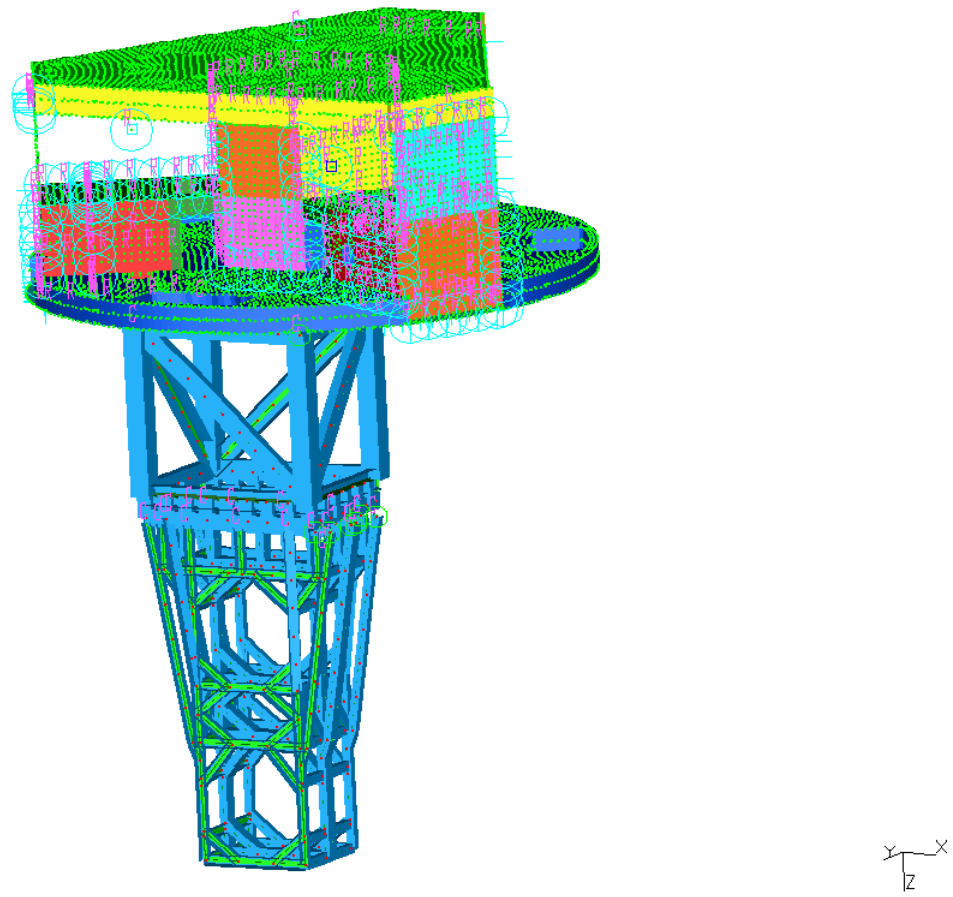


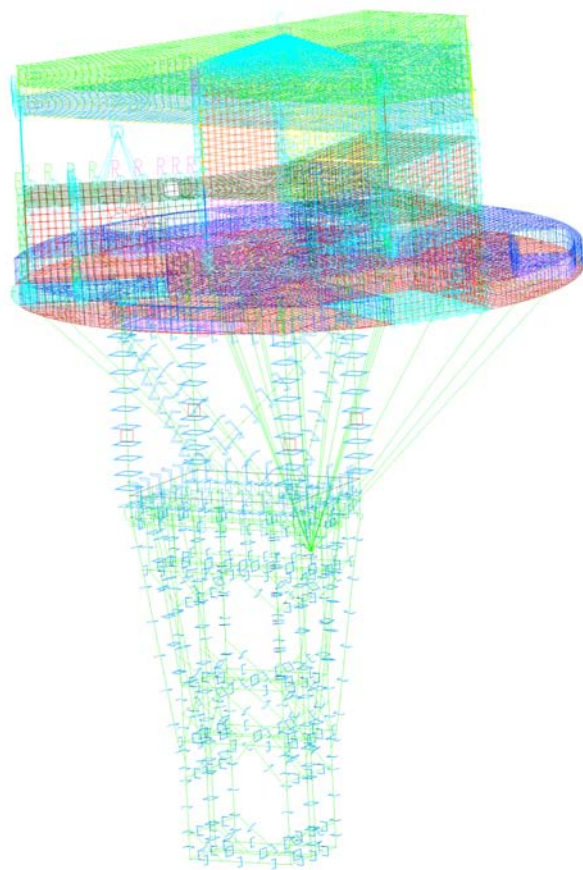












Advanced LIGO

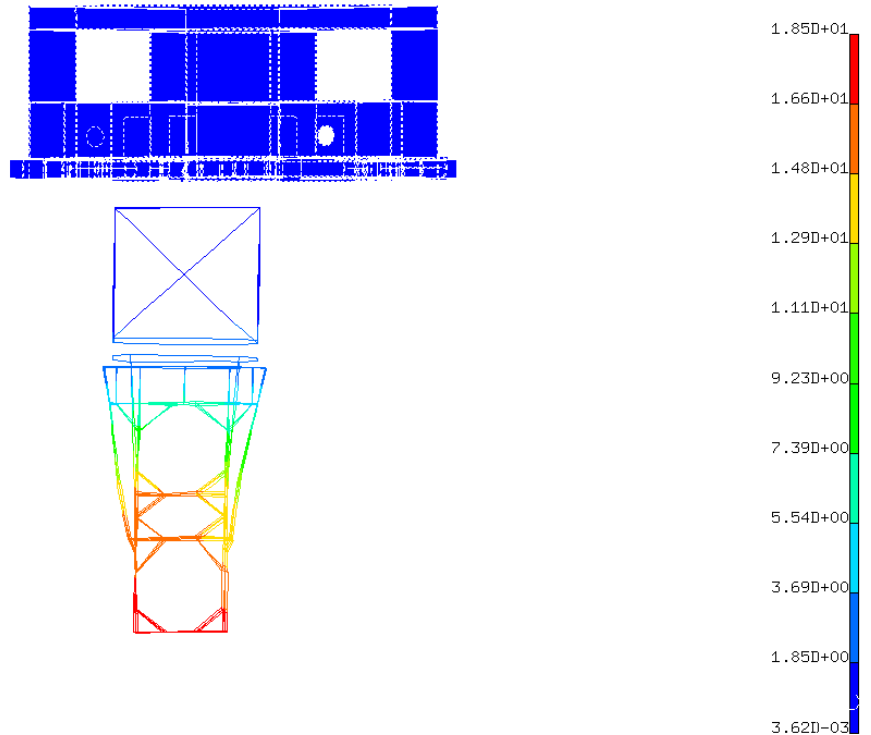
LIGO-T050014-00-D

Mode #	Frequency(Hz)	Modal Prop.			-- Damping Factors --		
	Undamped	Mass	% X-Mass	% Y-Mass	% Z-Mass	% Viscous	% Hysteretic
*3	0.0000	2266.56	18.16	0.47	0.32	0.00	0.00
*2	0.0000	6325.41	3.27	9.95	40.57	0.00	0.00
*4	0.0000	15517.9	0.09	41.29	45.71	0.00	0.00
*5	0.0001	3236.09	2.39	40.93	12.86	0.00	0.00
*1	0.0001	13294.8	75.86	0.01	0.54	0.00	0.00
*6	0.0001	5113.9	0.23	7.35	0.00	0.00	0.00
*7	81.8846	22.6946	0.00	0.00	0.00	0.00	1.00
*8	100.2360	0.0964143	0.00	0.00	0.00	0.00	1.00
*9	104.8209	0.07844484	0.00	0.00	0.00	0.00	1.00
*10	105.1081	0.0809334	0.00	0.00	0.00	0.00	1.00
*11	105.8823	0.0745193	0.00	0.00	0.00	0.00	1.00
*12	124.6958	3.25645	0.00	0.00	0.00	0.00	1.00
*13	125.7106	0.626295	0.00	0.00	0.00	0.00	1.00
*14	126.0744	0.0924677	0.00	0.00	0.00	0.00	1.00
*15	126.5679	0.0980559	0.00	0.00	0.00	0.00	1.00

*=Active

Rigid-Body Mode Frequency Tolerance (Hz)

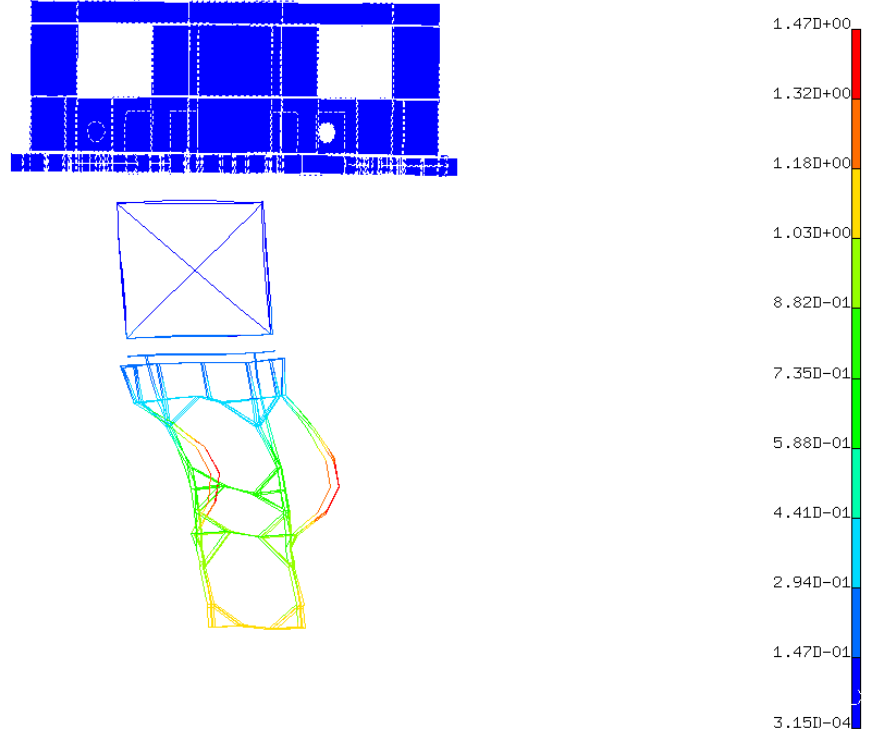
/home/coyne/AL/SEI/stage2/stage2_D040519-04.mf1
RESULTS: 7- B.C. 1,NORMAL_MODE 7,DISPLACEMENT_7
MODE: 7 FREQ: 81.88462
DISPLACEMENT - MAG MIN: 3.62E-03 MAX: 1.85E+01
DEFORMATION: 7- B.C. 1,NORMAL_MODE 7,DISPLACEMENT_7
MODE: 7 FREQ: 81.88462
DISPLACEMENT - MAG MIN: 3.62E-03 MAX: 1.85E+01
FRAME OF REF: PART



```

RESULTS: 8- B.C. 1,NORMAL_MODE 8,DISPLACEMENT_8
MODE: 8      FREQ: 100.236
DISPLACEMENT - MAG MIN: 3.15E-04 MAX: 1.47E+00
DEFORMATION: 8- B.C. 1,NORMAL_MODE 8,DISPLACEMENT_8
MODE: 8      FREQ: 100.236
DISPLACEMENT - MAG MIN: 3.15E-04 MAX: 1.47E+00
FRAME OF REF: PART

```



5 Transfer functions

5.1 Damping

For all of the transfer functions, a $Q = 100$, hysteretic loss (frequency independent) has been assumed. Typical damping values are as follows:

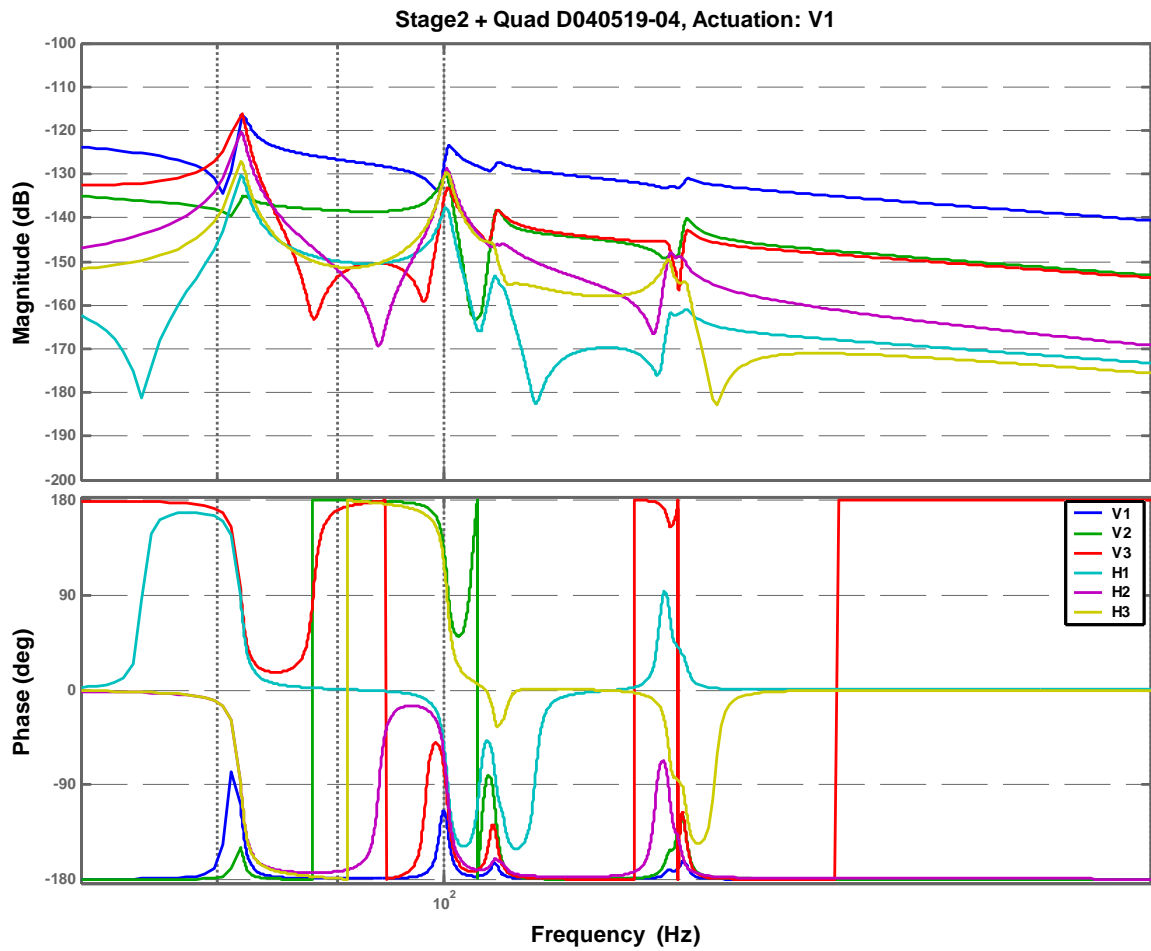
- aluminum alone (monolithic) at low stress, $Q = 380$
- initial LIGO assumed structural $Q = 100$
- From the literature, but probably at considerably higher stress than for LIGO:
- one piece construction, $Q = 50$
- welded assembly, $Q = 25$
- Riveted assembly, $Q = 12.5$
- Bolted assembly, $Q = 10$

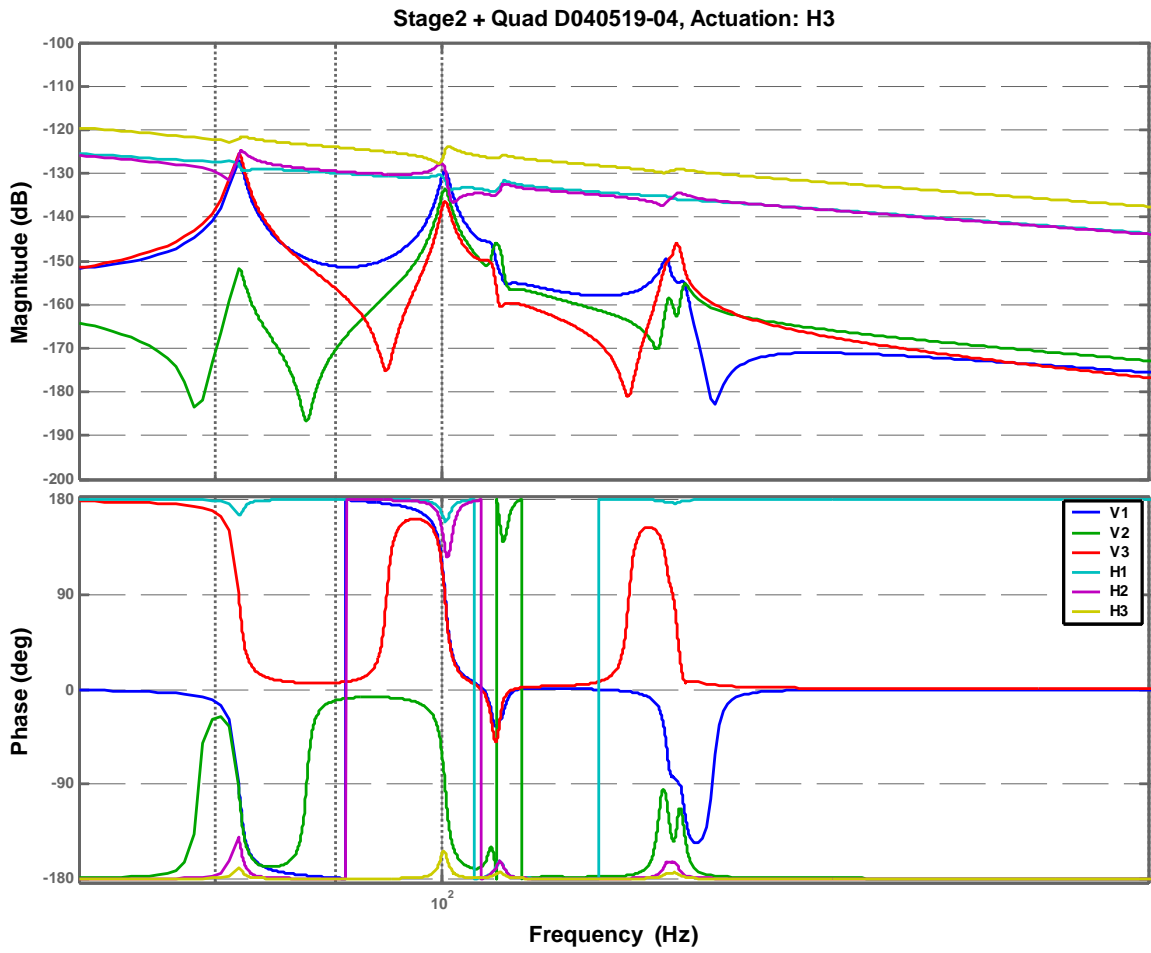
5.2 D040519-04

The transfer functions were calculated for the response of each of the 6 sensor locations in each of the 6 degrees of freedom (dof) for actuation by each of the 6 actuators ($6 \times 6 \times 6 = 216$ transfer

functions). The transfer functions were exported from the I-DEAS finite element code to Matlab in order to project the 6 dof response into the sensor direction and then to combine the transfer functions to obtain the transfer function for coordinated modal actuation (i.e. actuation along the cartesian coordinates). The Matlab m-file script for doing this conversion is given in Appendix B. The transfer functions are all given in Appendix C.

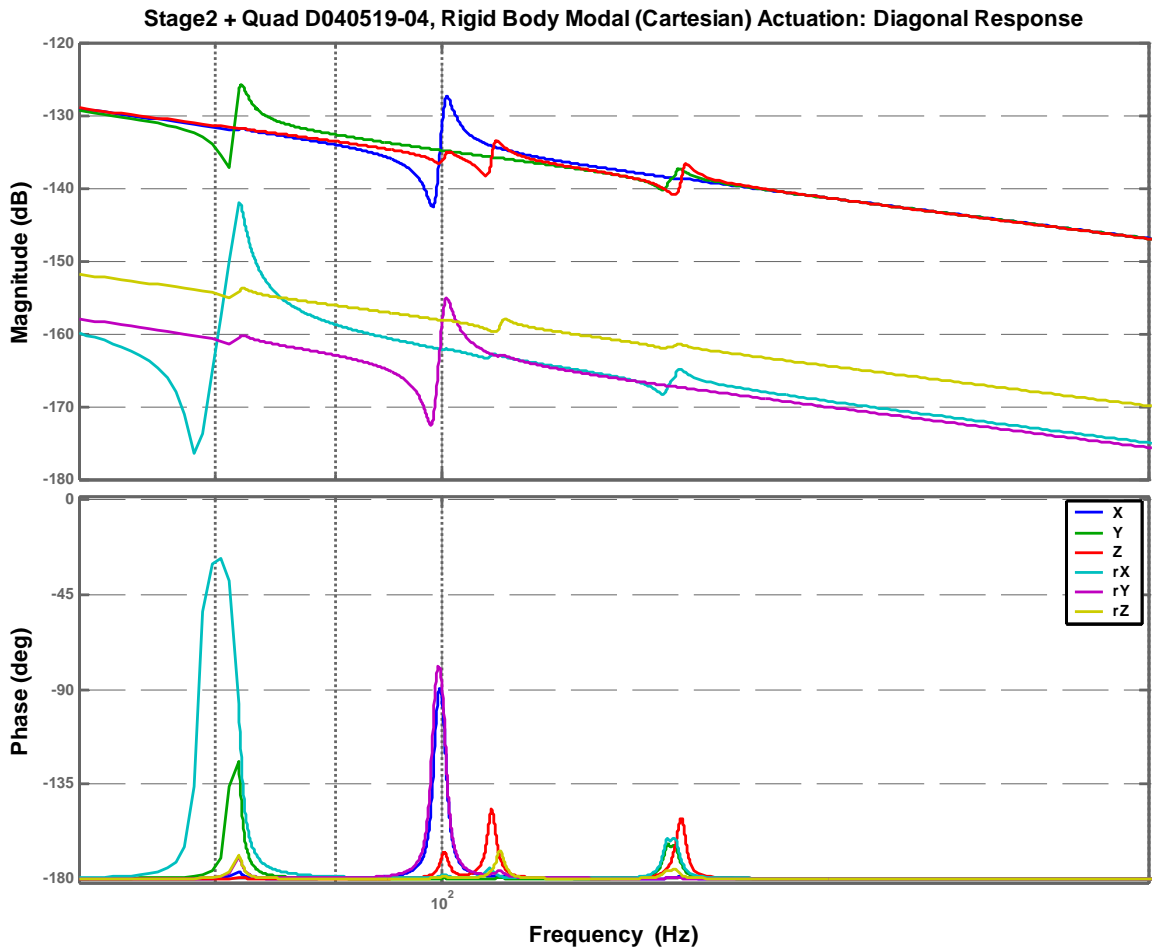
Some of the single actuator to single (non-adjacent) sensor transfer functions have significant phase lag. Examples follow: V1 actuation to V3 sensor response, H3 actuation to V3 sensor response



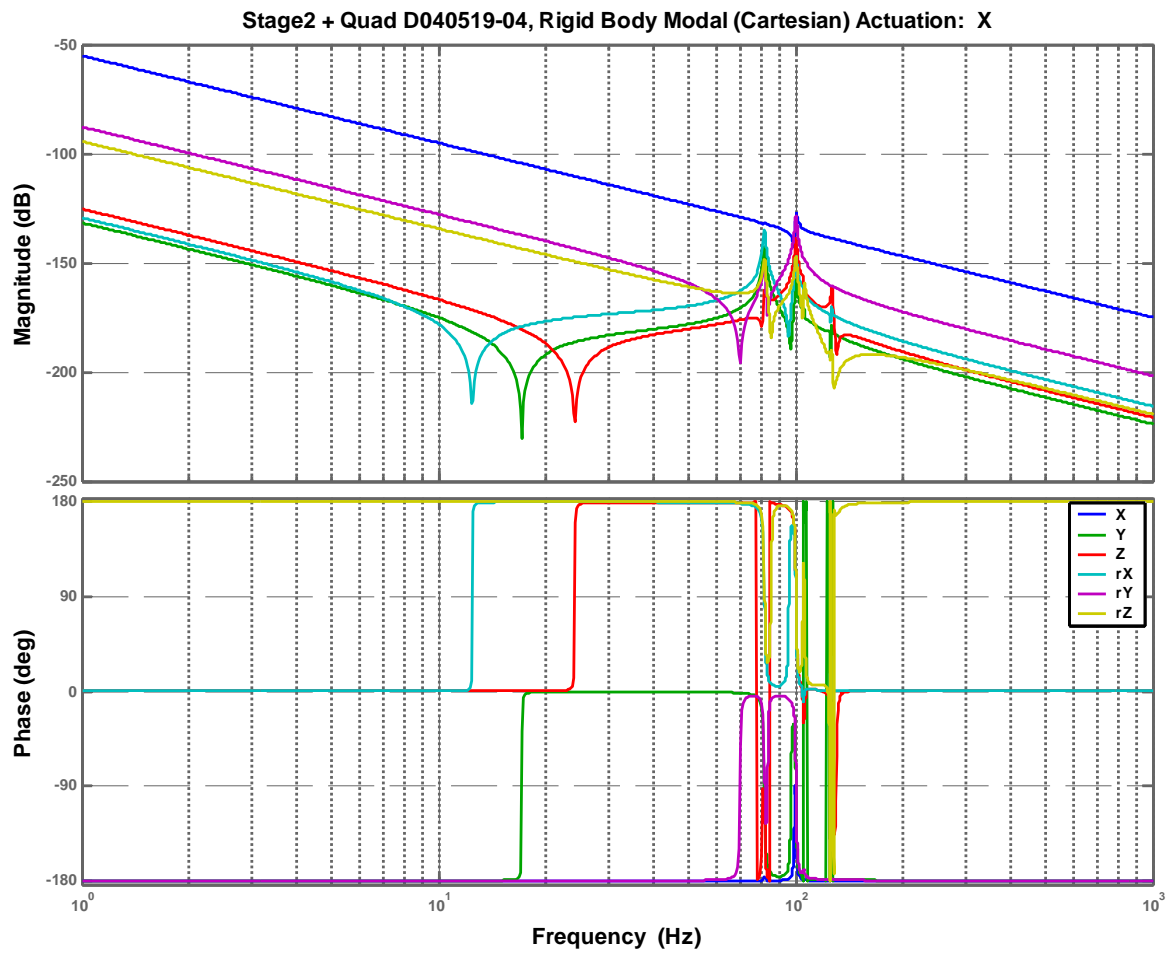


However, all of the single actuation to collocated (adjacent) sensors have zero-pole pairs and positive phase excursions associated with the payload modes.

When the modes are projected into coordinated modal actuation and sensing, all transfer functions have zero-pole pairings with positive phase perturbation, or no effect, due to the actuation force having a component in the modal generalized force direction.



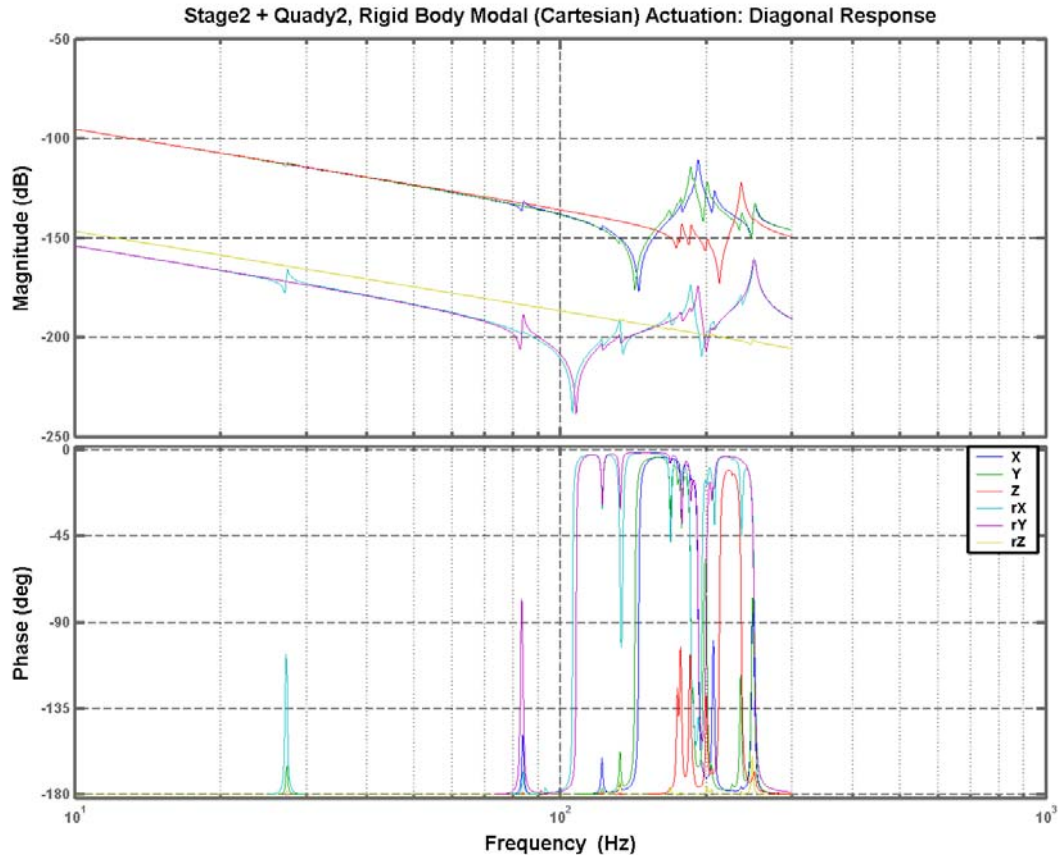
However, note that there is significant cross coupling at the payload resonances. In all of the transfer functions the rotational modes have been multiplied by the distance from the center of mass to the sensor locations, so that they can be compared to the translational modes. For example, the X-mode transfer function has significant coupling to rotation about the y-axis.



5.3 Quady2

SEI Stage2 & Quady2, Modal Actuation and Modal Sensing (displacement) transfer functions

Note: The rotational transfer functions have not been scaled by the radius to the displacement sensor in the plot below (unlike the transfer functions presented for D040519-04)



6 Conclusions and Further Work

The quadruple pendulum suspension structures are not destabilizing to the seismic isolation control system. Modal transfer functions indicate that only positive phase excursions result from the coupling of the elastic dynamics of the suspension structures to the rigid body dynamics of the seismic stage2 structure. This behavior is consistent with the interaction of a cantilevered beam coupled to a rigid body. The collocation of the sensing and actuation of the seismic stage2 system is not compromised by the addition of the suspension structure payloads.

There does appear to be significant modal cross-coupling at the suspension structure modes. In order to reduce the effect of this cross-coupling and to avoid the complication and (slight) reduction in gain due to the presence of these zero-pole pairs in band, it is recommended that the first mode of the suspension structure be designed to be somewhat above the upper unity gain frequency of the seismic isolation system. The planned SEI upper unity gain frequency is 60 Hz.

The current working baseline (see section 1) of a first suspension structure mode > 100 Hz seems reasonable. Moreover, if this requirement is not met, then the effect on the seismic control system may be minor.

Future work:

- [needed] More careful consideration of the effect of the modal cross-coupling resulting from the payload dynamics on the SEI control system design.
- [needed] Use the more current ASI FEM for coupled analysis with the payloads. Better still; develop a more appropriate model for use in these dynamics studies. The current model has far too many degrees of freedom (more appropriate for a stress analysis).
- [not essential] Use a higher fidelity model for the SUS quad structure, D040519-04. The relatively simple finite element beam model used herein has a first frequency of 82 Hz whereas more detailed solid element FEMs indicate a first frequency closer to 100 Hz. The simple FEM used here also has some local modes which likely do not exist in the real structure.
- [needed] Develop a full stage 0, 1, 2 and suspension system (pendulums and structure) model and use it to export a state space model for control system work in Matlab.
- [not essential] Study the effect of a small footprint payload with a more significant lower end mass (such as the current concept for a pickoff mirror). While there is likely to be significant elastic coupling in this scenario, the result should not compromise the collocation of the SEI sensing and actuation.



LASER INTERFEROMETER GRAVITATIONAL WAVE OBSERVATORY

7 Appendix A: Beam and Rigid Body Mass Model

Simple Model of a SEI Payload

SEI Stage 2 is modeled as a rigid mass with 6 degrees of freedom and an inertia matrix, In
Payload is modeled as a uniform cross-section, Euler beam cantilevered (with zero relative rotation boundary condition) from the SEI Stage2 optic table.

■ Initialization

```
In[1]:= Off[General::"spell"]
Off[General::"spell1"]
<< Graphics`Graphics`
<< Miscellaneous`Units`

In[5]:= logGrid = Join[Table[{Log[10, j], {GrayLevel[0.8]}}, {j, 1, 10, 1}],
Table[{Log[10, j], {GrayLevel[0.8]}}, {j, 10, 100, 10}],
Table[{Log[10, j], {GrayLevel[0.8]}}, {j, 100, 1000, 100}] // N;
```

SEI Stage2 Model

Ms2 = stage2 mass, kg

fs = horizontal force applied to stage 2 center of mass (c.m.), N

ys = horizontal displacement of the stage2 c.m., m

Tfsys = transmissibility from fs to ys, m/N

```
In[6]:= Ms2 = 2536 - 2 57;
```

```
In[7]:= 14.48 386.4
```

```
Out[7]= 5595.07
```

Stage 2 Mass:

FEM mass = 5591 lb = 2536 kg

ASI Tech Memo 200009022-A, mass = 5757 lb

```
In[8]:= Convert[5591 Pound, Kilogram]
```

```
Out[8]= 2536.03 Kilogram
```

```
In[9]:= lbm2kg = Convert[1 Pound, Kilogram];
in2m = Convert[1 Inch, Meter];
```

FEM moment of inertia values, (lbf-s^2/in) in^2 :

```
In[11]:= Ixx = 11170.;
Iyy = Ixx;
Izz = 5315;
```

FEM moment of inertia values, kg m^2 :

```
In[14]:= conversionFactor = 386.4 lbm2kg[[1]] in2m[[1]]^2;
Ixx = Ixx conversionFactor;
Iyy = Iyy conversionFactor;
Izz = Izz conversionFactor;
```

```
In[18]:= Is2 = {{Ixx, 0, 0},
{0, Iyy, 0},
{0, 0, Izz}};
MatrixForm[Is2]
```

```
Out[19]//MatrixForm=

$$\begin{pmatrix} 1263.06 & 0 & 0 \\ 0 & 1263.06 & 0 \\ 0 & 0 & 600.998 \end{pmatrix}$$

```

```
In[20]:= Clear[Tfsys];
Tfsys[f_] := -3 / (Ms2 (2 Pi f)^2);
```

Quad SUS Payload Model

Y = elastic modulus, Pa

del = damping factor = 1/Q

a = beam length, m

dens = material density, kg/m^3

A = cross-sectional area, m^2

rho = dens * A, effective beam lineal density, kg/m

r = radius of gyration of the quad beam cross-section, m

Ib = area moment of inertia for the beam, m^4

mu = eigenvalue for 1st bending mode of cantilevered beam

Vroot = shear force at the beam root for a unit lateral displacement of the beam root as a function of frequency, Pa/m

Mroot = moment at the beam root for a unit lateral displacement of the beam root as a function of frequency, Pa-m/m

```

In[26]:= y[x_] := Ps Cosh[ns x] + Qs Cos[ns x] + Rs Sinh[ns x] + Ss Sin[ns x];

In[27]:= y[x]

Out[27]= Qs Cos[ns x] + Ps Cosh[ns x] + Ss Sin[ns x] + Rs Sinh[ns x]

In[28]:= baseTranslationBoundaryConditions =
  {y[0] == y0, y'[0] == alpha, y''[a] == 0, y''''[a] == 0};

In[29]:= soln = Simplify[
  Solve[baseTranslationBoundaryConditions, {Ps, Qs, Rs, Ss}]]

Out[29]= { {Ps → (ns y0 + Cosh[a ns] (ns y0 Cos[a ns] + alpha Sin[a ns]) +
  (-alpha Cos[a ns] + ns y0 Sin[a ns]) Sinh[a ns]) /
  (2 (ns + ns Cos[a ns] Cosh[a ns])), 
  Qs → (ns y0 + Cosh[a ns] (ns y0 Cos[a ns] - alpha Sin[a ns]) +
  (alpha Cos[a ns] - ns y0 Sin[a ns]) Sinh[a ns]) /
  (2 (ns + ns Cos[a ns] Cosh[a ns])), 
  Rs → (alpha + Cosh[a ns] (alpha Cos[a ns] - ns y0 Sin[a ns]) -
  (ns y0 Cos[a ns] + alpha Sin[a ns]) Sinh[a ns]) /
  (2 (ns + ns Cos[a ns] Cosh[a ns])), 
  Ss → (alpha + Cosh[a ns] (alpha Cos[a ns] + ns y0 Sin[a ns]) +
  (ns y0 Cos[a ns] + alpha Sin[a ns]) Sinh[a ns]) /
  (2 (ns + ns Cos[a ns] Cosh[a ns]))} }

In[30]:= z = Simplify[y[a] / y[0]] /. soln

Out[30]= { 
$$\frac{ns y0 \cos[a \text{ ns}] + ns y0 \cosh[a \text{ ns}] + alpha \sin[a \text{ ns}] + alpha \sinh[a \text{ ns}]}{ns y0 + ns y0 \cos[a \text{ ns}] \cosh[a \text{ ns}]}$$
 }

In[31]:= Simplify[y[0]] /. soln

Out[31]= {y0}

In[32]:= Simplify[y'[0]] /. soln

Out[32]= {alpha}

In[33]:= mb = Convert[0.6635 PoundForce Second^2 / Inch, Kilogram][[1]]

Out[33]= 116.197

In[34]:= a = 1.96;
del = 0.01;
rho = mb / a;
YAlu = 69 10^9;
Y = YAlu;
densAlu = 2700;
dens = densAlu;
A = rho / dens // N

Out[41]= 0.021957

```

```
In[42]:= Ib = 2.7 10^-4;
r = Sqrt[Ib / A]
```

```
Out[43]= 0.110891
```

```
In[44]:= ns = ((2 Pi f)^2 dens / (Y r^2 (1 + I del))) ^ 0.25;
```

first beam mode frequency, f1 (Hz)

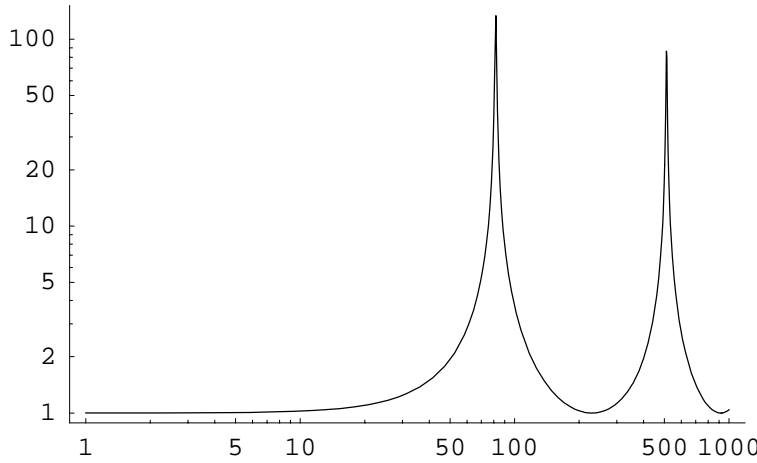
```
In[45]:= mu = 1.875;
f1 = (mu^2 / (2 Pi)) Sqrt[Y Ib / (rho a^4)]
```

```
Out[46]= 81.6485
```

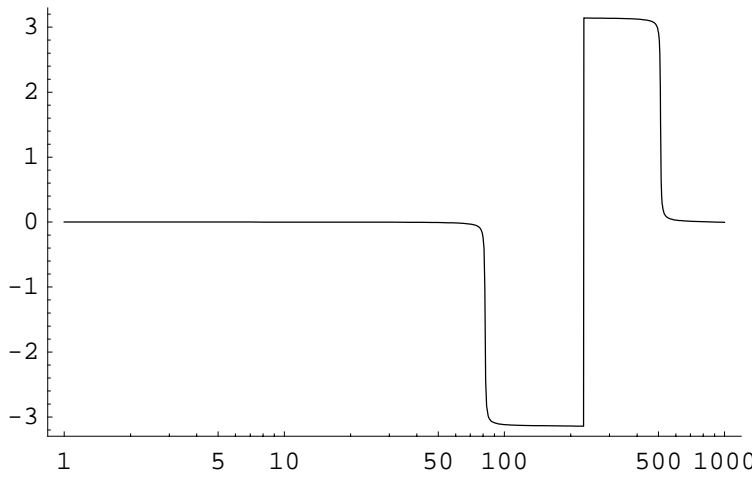
```
In[47]:= Clear[z];
z[f_] := Simplify[y[a] / y[0] /. soln /. alpha -> 0];
z[f]
```

```
Out[49]= {Cos[1.96 ((0.000125615 - 1.25615*10^-6 I) f^2)^0.25] +
Cosh[1.96 ((0.000125615 - 1.25615*10^-6 I) f^2)^0.25]] /
(1 + Cos[1.96 ((0.000125615 - 1.25615*10^-6 I) f^2)^0.25]
Cosh[1.96 ((0.000125615 - 1.25615*10^-6 I) f^2)^0.25])}
```

```
In[50]:= LogLogPlot[Evaluate[Abs[z[f]]], {f, 1, 1000}];
```



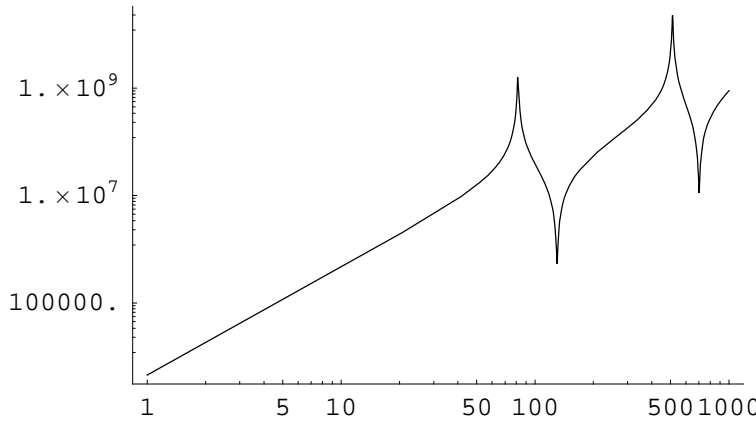
```
In[51]:= LogLinearPlot[Evaluate[Arg[z[f]]], {f, 1, 1000}];
```



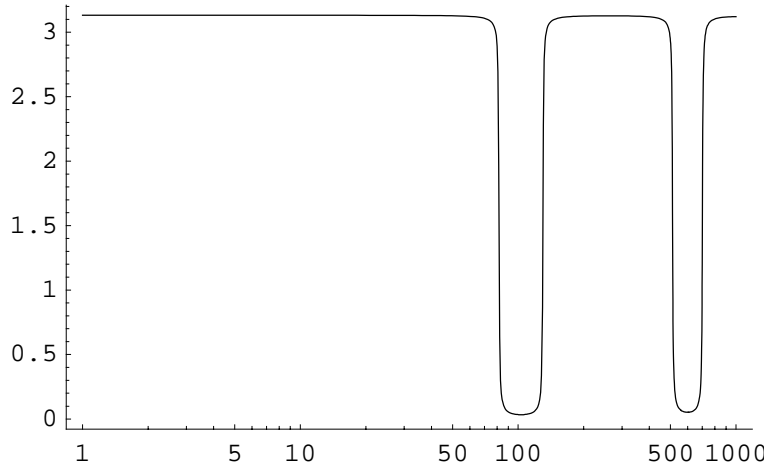
```
In[52]:= Clear[V];
V[x_, f_] :=
  Evaluate[Simplify[(Y I b y'''[x] / y0) /. soln /. alpha -> 0]];
Clear[Vroot];
Vroot[f_] := Simplify[V[0, f]];
Vroot[f]
```

$$\text{Out[56]} = \left\{ \left(\left((0.000125615 - 1.25615 \times 10^{-6} i) f^2 \right)^{0.75} \right. \right. \\ \left. \left. (-1.863 \times 10^7 \cosh[1.96 ((0.000125615 - 1.25615 \times 10^{-6} i) f^2)^{0.25}] \right. \right. \\ \left. \left. \sin[1.96 ((0.000125615 - 1.25615 \times 10^{-6} i) f^2)^{0.25}] - \right. \right. \\ \left. \left. 1.863 \times 10^7 \cos[1.96 ((0.000125615 - 1.25615 \times 10^{-6} i) f^2)^{0.25}] \right. \right. \\ \left. \left. \sinh[1.96 ((0.000125615 - 1.25615 \times 10^{-6} i) f^2)^{0.25}] \right) \right) / \\ \left(1. + \cos[1.96 ((0.000125615 - 1.25615 \times 10^{-6} i) f^2)^{0.25}] \right. \\ \left. \left. \cosh[1.96 ((0.000125615 - 1.25615 \times 10^{-6} i) f^2)^{0.25}] \right) \right\}$$

```
In[57]:= LogLogPlot[Evaluate[Abs[Vroot[f]]], {f, 1, 1000}];
```



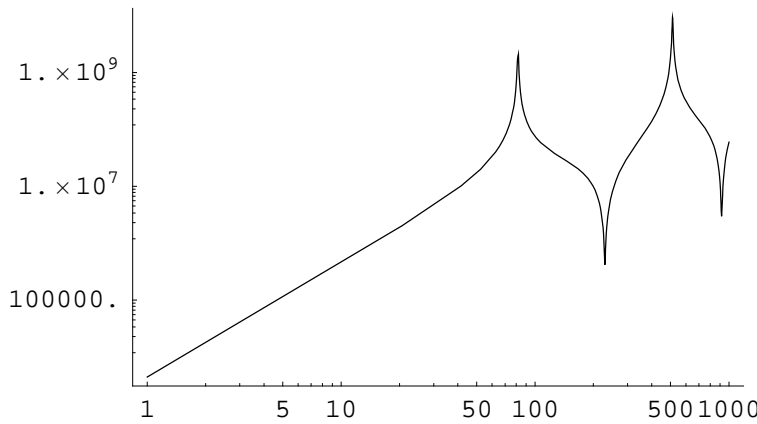
In[58]:= LogLinearPlot[Evaluate[Arg[Vroot[f]]], {f, 1, 1000}];



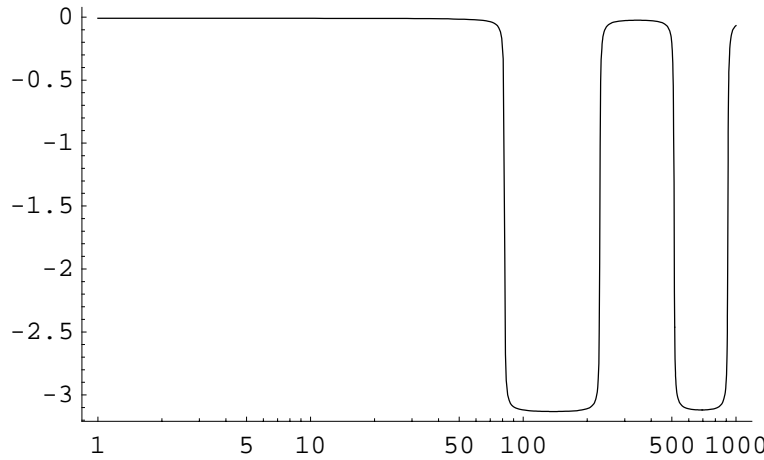
In[59]:= Clear[Momenty];
 Momenty[x_, f_] :=
 Evaluate[Simplify[(Y I b y''[x] / y0) /. soln /. alpha → 0]];
 Clear[Mrooty];
 Mrooty[f_] := Simplify[Momenty[0, f]];
 Mrooty[f]

$$\text{Out[63]= } \left\{ \left((0.000125615 - 1.25615 \times 10^{-6} i) f^2 \right)^{0.5} \right. \\ \left(0. + 0. \operatorname{Cos}[1.96 ((0.000125615 - 1.25615 \times 10^{-6} i) f^2)^{0.25}] \right. \\ \left. \operatorname{Cosh}[1.96 ((0.000125615 - 1.25615 \times 10^{-6} i) f^2)^{0.25}] \right) + \\ 1.863 \times 10^7 \operatorname{Sin}[1.96 ((0.000125615 - 1.25615 \times 10^{-6} i) f^2)^{0.25}] \\ \left. \operatorname{Sinh}[1.96 ((0.000125615 - 1.25615 \times 10^{-6} i) f^2)^{0.25}] \right) / \\ \left(1. + \operatorname{Cos}[1.96 ((0.000125615 - 1.25615 \times 10^{-6} i) f^2)^{0.25}] \right. \\ \left. \operatorname{Cosh}[1.96 ((0.000125615 - 1.25615 \times 10^{-6} i) f^2)^{0.25}] \right) \}$$

In[64]:= LogLogPlot[Evaluate[Abs[Mrooty[f]]], {f, 1, 1000}];



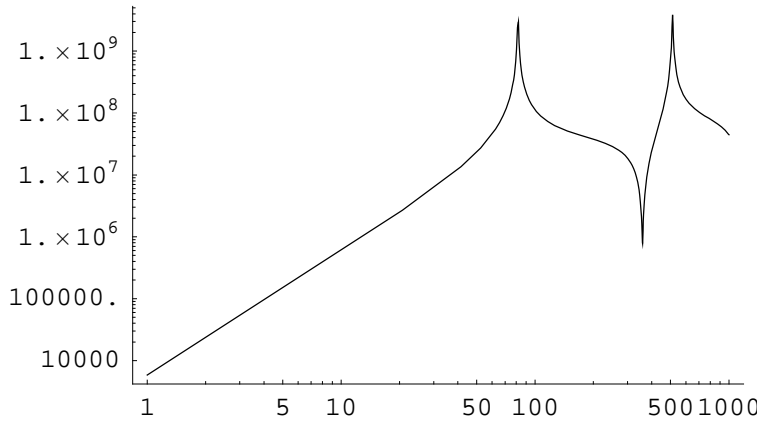
```
In[65]:= LogLinearPlot[Evaluate[Arg[Mrooty[f]]], {f, 1, 1000}];
```



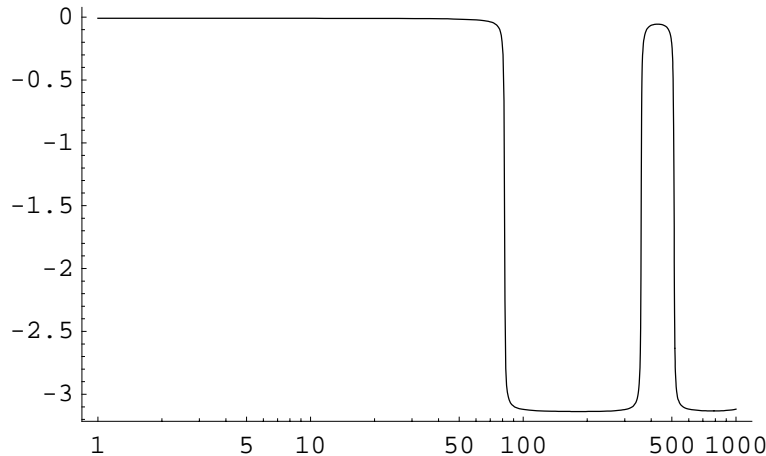
```
In[66]:= Clear[Momentalpha];
Momentalpha[x_, f_] :=
Evaluate[Simplify[(Y I b y''[x] / alpha) /. soln /. y0 → 0]];
Clear[Mroota];
Mroota[f_] := Simplify[Momentalpha[0, f]];
Mroota[f]
```

$$\text{Out[70]= } \left\{ \left(\left(0.000125615 - 1.25615 \times 10^{-6} i \right) f^2 \right)^{0.25} \left(1.863 \times 10^7 \cosh \left[1.96 \left(\left(0.000125615 - 1.25615 \times 10^{-6} i \right) f^2 \right)^{0.25} \right] \sin \left[1.96 \left(\left(0.000125615 - 1.25615 \times 10^{-6} i \right) f^2 \right)^{0.25} \right] - 1.863 \times 10^7 \cos \left[1.96 \left(\left(0.000125615 - 1.25615 \times 10^{-6} i \right) f^2 \right)^{0.25} \right] \sinh \left[1.96 \left(\left(0.000125615 - 1.25615 \times 10^{-6} i \right) f^2 \right)^{0.25} \right] \right) \right) / \left(1. + \cos \left[1.96 \left(\left(0.000125615 - 1.25615 \times 10^{-6} i \right) f^2 \right)^{0.25} \right] \cosh \left[1.96 \left(\left(0.000125615 - 1.25615 \times 10^{-6} i \right) f^2 \right)^{0.25} \right] \right) \}$$

```
In[71]:= LogLogPlot[Evaluate[Abs[Mroota[f]]], {f, 1, 1000}];
```



```
In[72]:= LogLinearPlot[Evaluate[Arg[Mroota[f]]], {f, 1, 1000}];
```



Combined [SEI Stage2 + Quad SUS Payload] Model

- Translation: Stage2 center of mass coincident with SUS structure beam root

```
In[73]:= Ms2 = 2536;
```

```
In[74]:= Convert[14.48 PoundForce Second^2 / Inch, Kilogram]
```

```
Out[74]= 2535.84 Kilogram
```

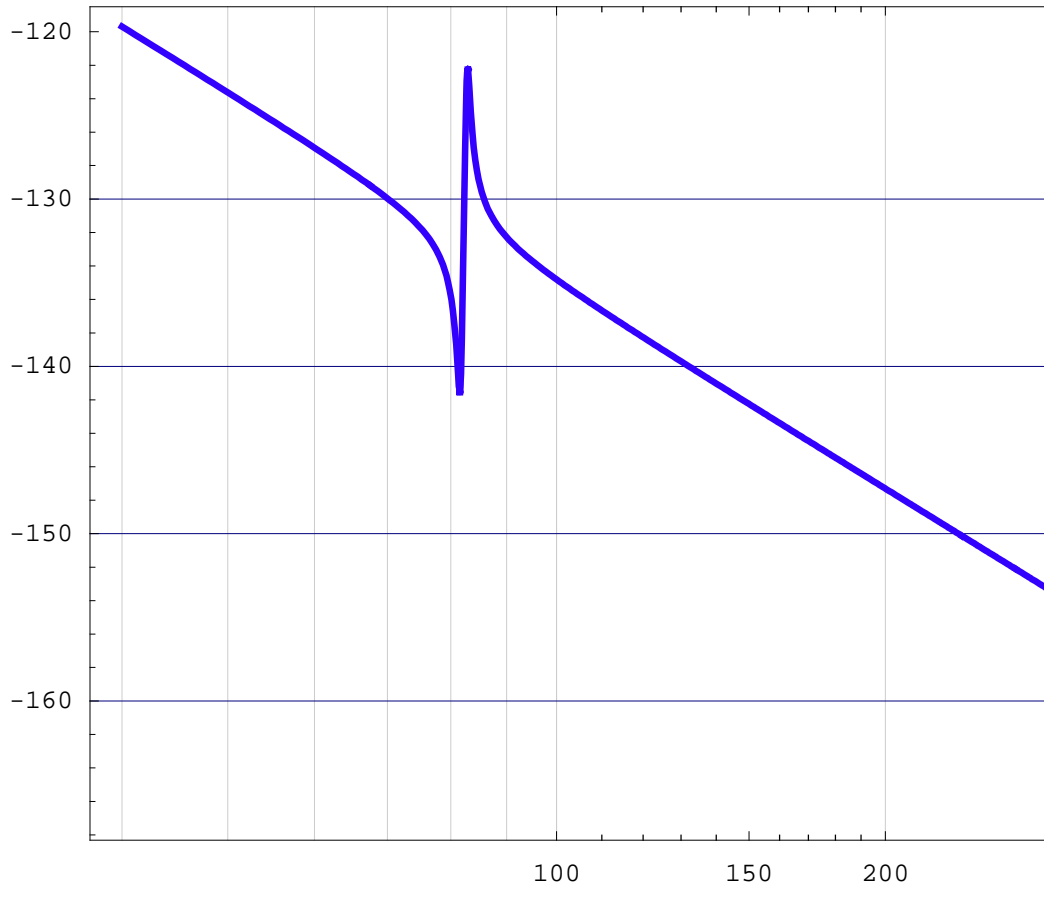
```
In[80]:= Clear[TrbFy];
TrbFy[f_] := -1 / (Ms2 (2 Pi f)^2);
```

translation transfer function is in units of m/N

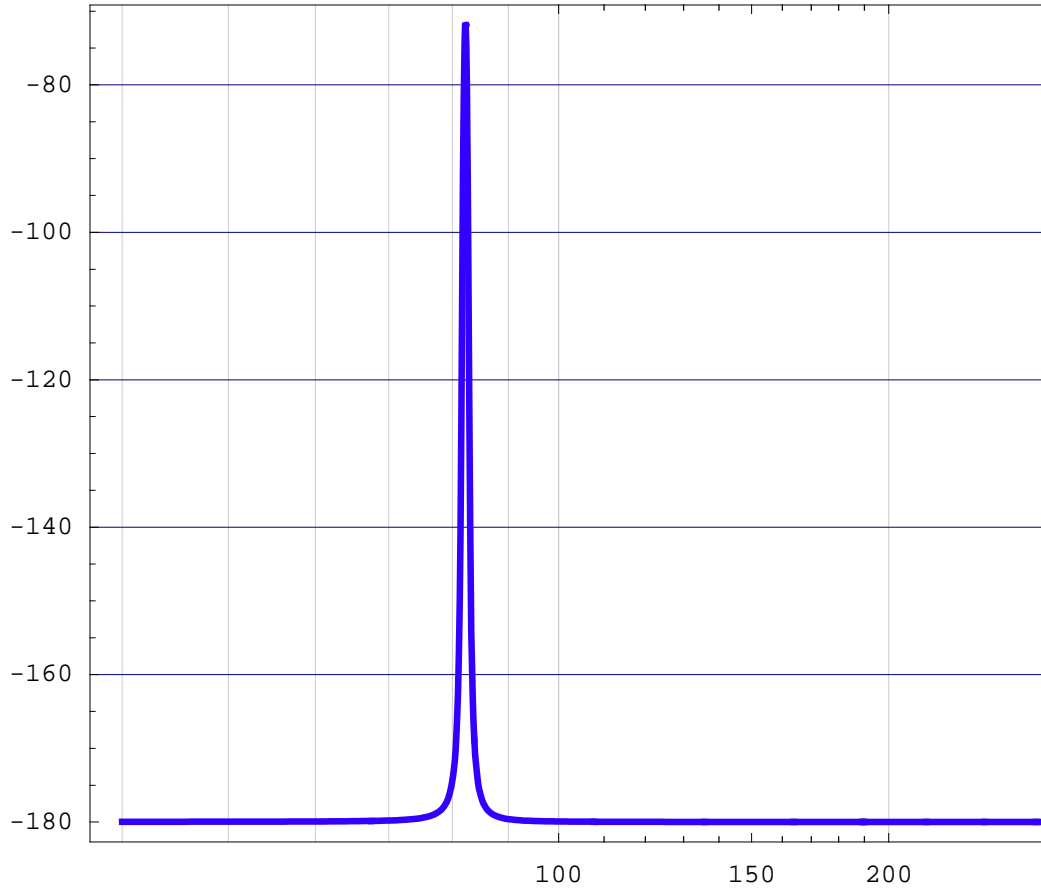
```
In[82]:= Clear[T];
T[f_] := Evaluate[TrbFy[f] / (1 + TrbFy[f] Vroot[f])]
```

plot translation transfer function in units of in/lbf to compare with FEA

```
In[122]:= conversionFactor = Convert[1 Meter, Inch][[1]]  
          Convert[1 PoundForce, Newton][[1]];  
plotTrans1m = LogLinearPlot[Evaluate[  
  20 Log[10, conversionFactor Abs[T[f]]]], {f, 40, 600},  
  PlotRange → All, PlotDivision → 1000, PlotPoints → 1000,  
  PlotStyle → {{Hue[0.7], Thickness[0.005]}},  
  DisplayFunction → Identity];  
Show[plotTrans1m, GridLines → {logGrid, Automatic},  
 Frame → True, DisplayFunction → $DisplayFunction];
```

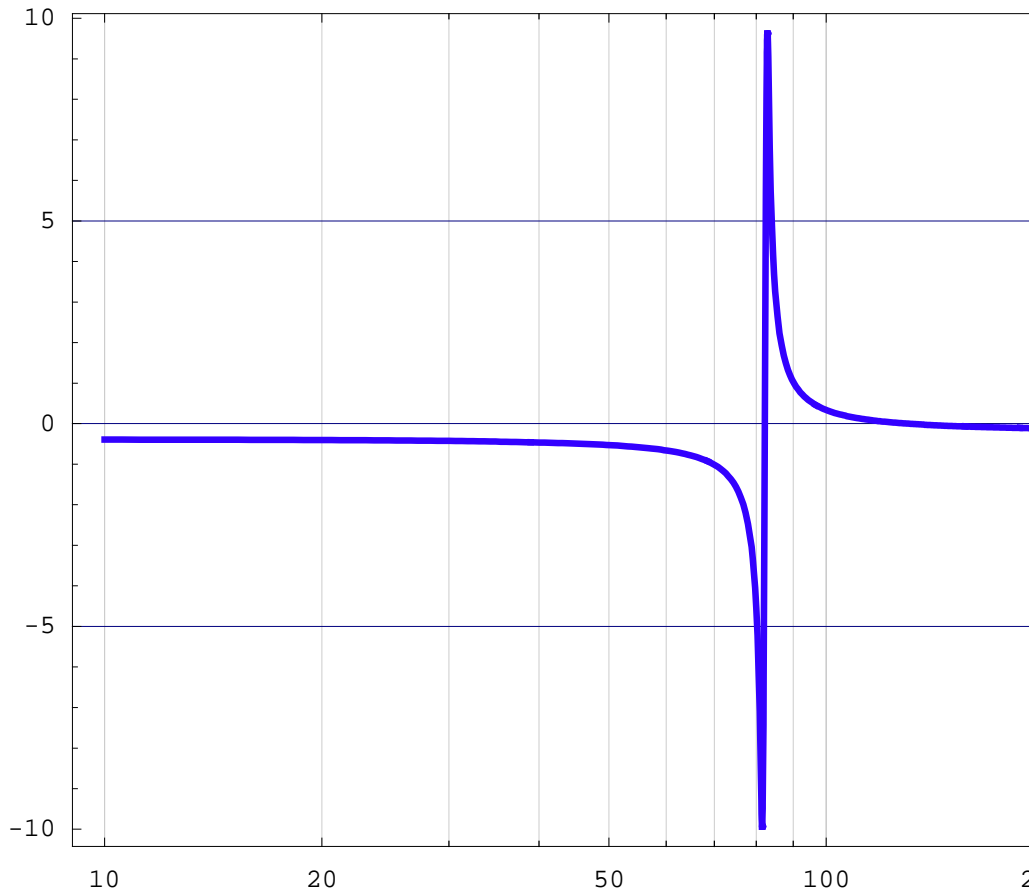


```
In[125]:= plotTrans1p = LogLinearPlot[Evaluate[(180 / Pi) Arg[T[f]]],  
{f, 40, 600}, PlotRange -> All, PlotDivision -> 1000,  
PlotPoints -> 1000, PlotStyle -> {{Hue[0.7], Thickness[0.005]}},  
DisplayFunction -> Identity];  
Show[plotTrans1p, GridLines -> {logGrid, Automatic},  
Frame -> True, DisplayFunction -> $DisplayFunction];
```



```
In[89]:= Tdif[f_] := T[f] / TrbFy[f];
```

```
In[127]:= plotTransDif1m =
  LogLinearPlot[Evaluate[20 Log[10, Abs[Tdif[f]]]], {f, 10, 600}, PlotRange -> All, PlotDivision -> 1000,
  PlotPoints -> 1000, PlotStyle -> {{Hue[0.7], Thickness[0.005]}},
  DisplayFunction -> Identity];
Show[plotTransDif1m, GridLines -> {logGrid, Automatic},
 Frame -> True, DisplayFunction -> $DisplayFunction];
```



■ Rotation: Stage2 center of mass coincident with SUS structure beam

root

Rotation about a horizontal axis

```
In[100]:= Is2 = Ixx
```

```
Out[100]= 1263.06
```

```
In[101]:= ract = 0.69;
```

```
In[102]:= Clear[TrbMa];
TrbMa[f_] := -1 / (Is2 (2 Pi f)^2);
```

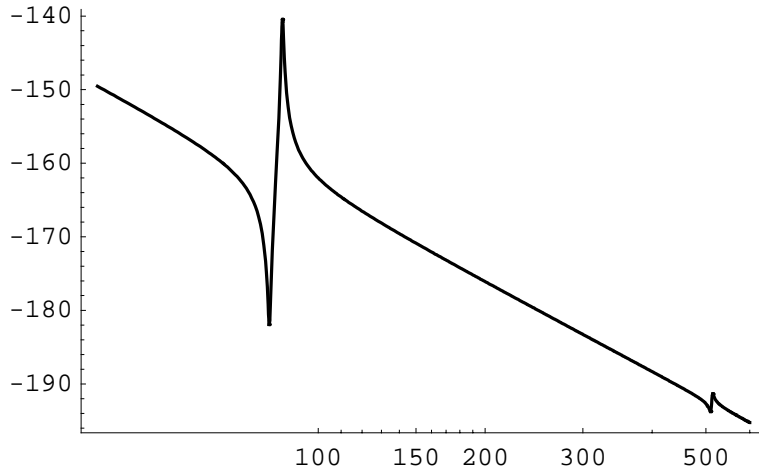
translation transfer function is in units of m/(N-m)

```
In[104]:= Clear[T1];
T1[f_] := Evaluate[TrbMa[f] ract / (1 - Mroota[f] TrbMa[f])]
```

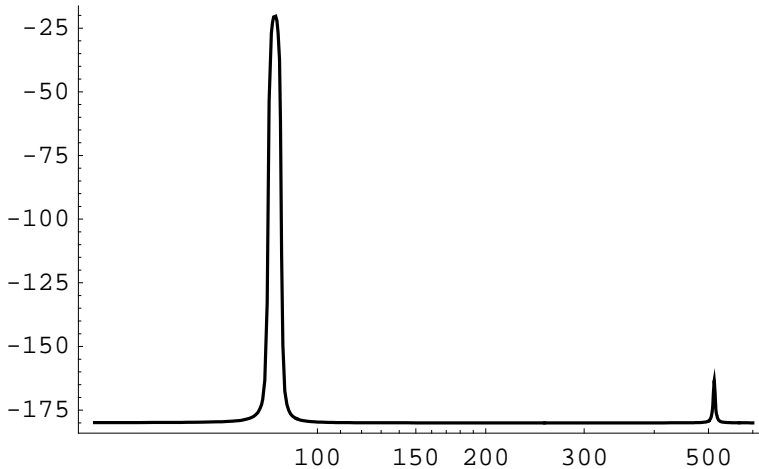
plot translation transfer function in units of in/(lbf-in) to compare with FEA

```
In[134]:= conversionFactor = Convert[1 PoundForce, Newton][[1]];
plot1m = LogLinearPlot[
  Evaluate[20 Log[10, conversionFactor Abs[T1[f]]]],
  {f, 40, 600}, PlotRange → All, PlotDivision → 100000,
  PlotPoints → 1000, PlotStyle → {Thickness[0.005]}];
```

Out[134]= 4.44822



```
In[130]:= plot1p = LogLinearPlot[Evaluate[(180 / Pi) Arg[T1[f]]],
  {f, 40, 600}, PlotRange → All, PlotStyle → {Thickness[0.005]}];
```



■ Rotation: Stage2 center of mass not coincident with SUS structure beam root

Rotation about a horizontal axis

```
In[109]:= Is2 = Ixx
```

```
Out[109]= 1263.06
```

db = distance from stage 2 center of mass, C, and the SUS structure beam root (optics table), R, (m)
(from ASI report 20009033-A)

```
In[110]:= db = 6.96 0.0254 5;
```

```
In[111]:= ract = 0.69;
```

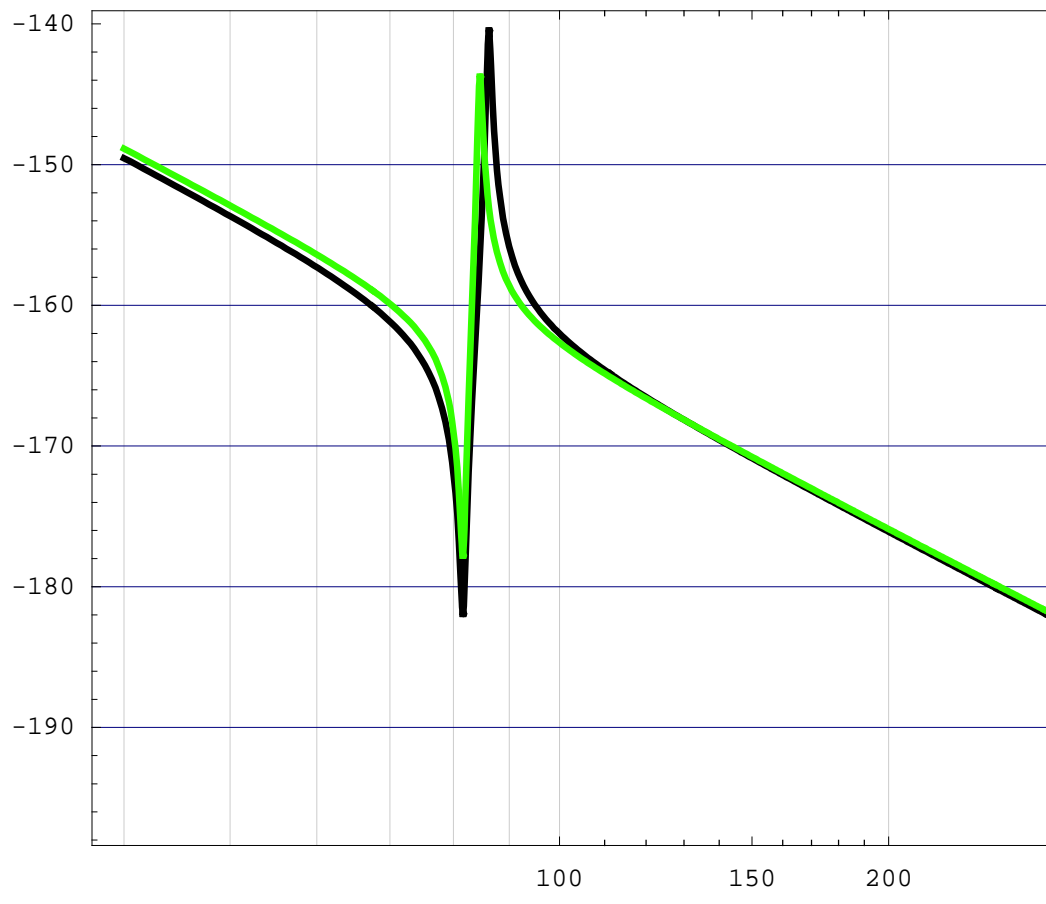
```
In[112]:= Clear[TrbMa];
TrbMa[f_] := -1 / (Is2 (2 Pi f) ^ 2);
```

translation transfer function is in units of m/(N-m)

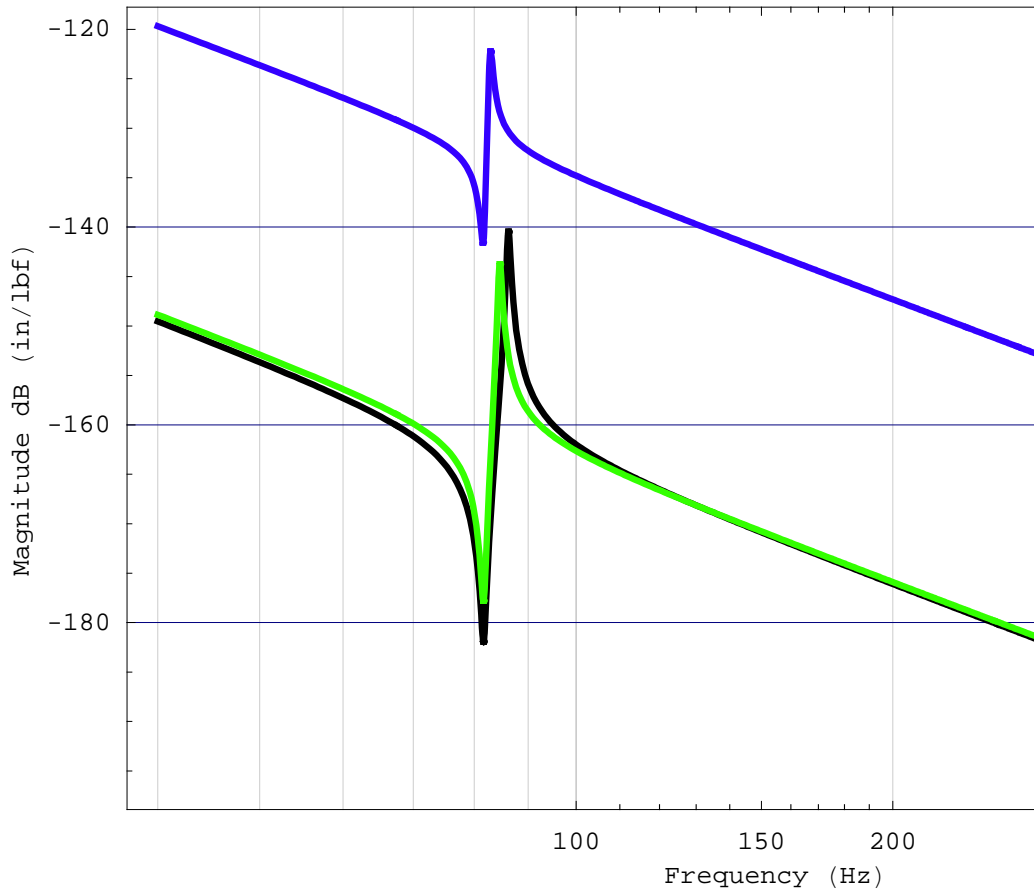
```
In[114]:= Clear[T2];
T2[f_] := Evaluate[
TrbMa[f] ract / (1 - Mroota[f] TrbMa[f] - Vroot[f] TrbMa[f] db ^ 2)]
```

plot translation transfer function in units of in/lbf-in to compare with FEA

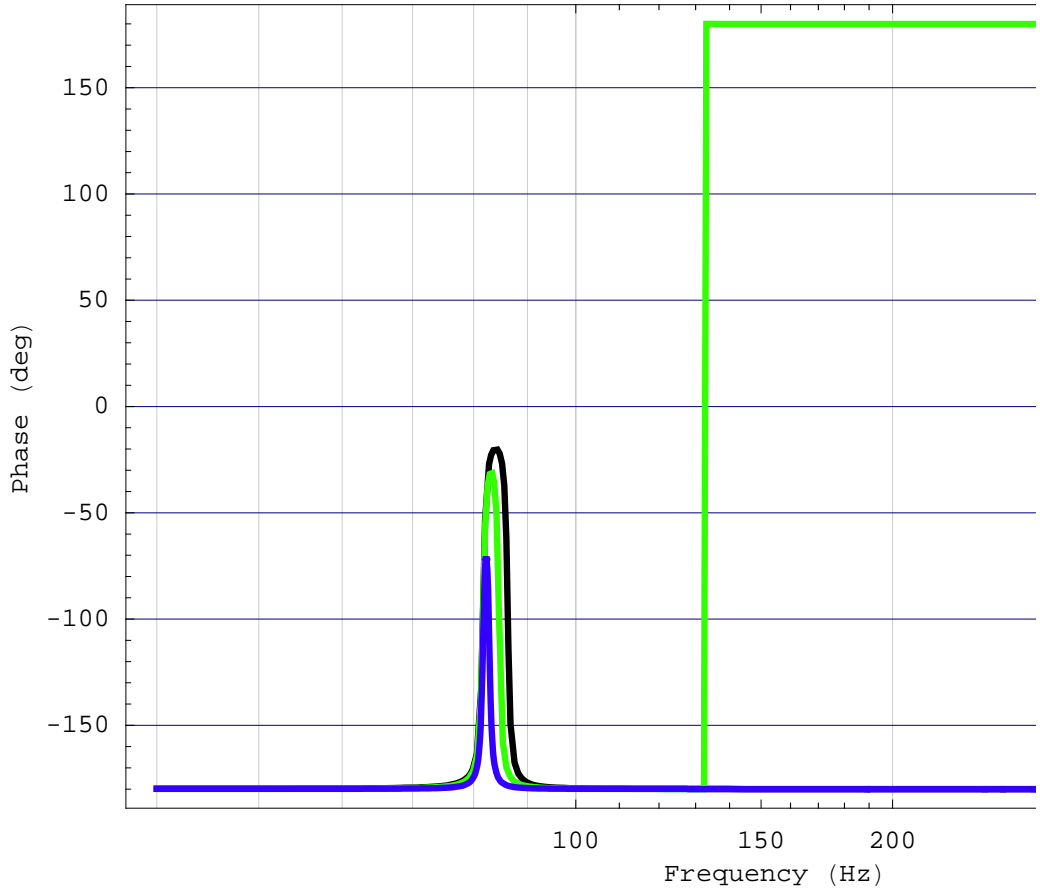
```
In[136]:= conversionFactor = Convert[1 PoundForce, Newton][[1]]
plot2m = LogLinearPlot[
  Evaluate[20 Log[10, conversionFactor Abs[T2[f]]]],
  {f, 40, 600}, PlotRange → All, PlotDivision → 100000,
  PlotPoints → 1000, PlotStyle → {{Thickness[0.005], Hue[0.3]}},
  DisplayFunction → Identity];
Show[plot1m, plot2m, DisplayFunction → $DisplayFunction,
  PlotRange → All, GridLines → {logGrid, Automatic}, Frame → True];
Out[136]= 4.44822
```



```
In[148]:= Show[plot1m, plot2m, plotTransl1m,
  DisplayFunction -> $DisplayFunction, PlotRange -> All,
  GridLines -> {logGrid, Automatic}, Frame -> True,
  FrameLabel -> {"Frequency (Hz)", "Magnitude dB (in/lbf)"}];
```



```
In[149]:= plot2p =
  LogLinearPlot[Evaluate[(180 / Pi) Arg[T2[f]]], {f, 40, 600},
    PlotRange -> All, PlotStyle -> {{Hue[0.3], Thickness[0.005]}},
    DisplayFunction -> Identity];
Show[plot1p, plot2p, plotTrans1p,
  DisplayFunction -> $DisplayFunction, PlotRange -> All,
  GridLines -> {logGrid, Automatic}, Frame -> True,
  FrameLabel -> {"Frequency (Hz)", "Phase (deg)"}];
```



8 Appendix B: Matlab Script for Modal Transfer Functions

July 6, 2005

3:52:26 PM

```
1 % MODAL SENSED RESPONSE FUNCTIONS FOR AL BSC SEI/ISI stage2 plus the quad,
2 % version D040519-04
3 % ***** stage2_D040519-04 I-DEAS model *****
4 % based upon finite element modal actuation responses (transfer functions)
5
6 % READ FEM transfer function data
7 % FEM = stage2renum
8 % Sensor transfer function sequence (based on numerical sequence of the nodes):
9 % {V2, H2, V3, H3, V1, H1}
10 % to change to desired order, {V1, V2, V3, H1, H2, H3}, use shiftindices
11 shiftindices = [5, 1, 3, 6, 2, 4];
12 % Coordinate Space Transforms:
13 % Ta2m = transform from actuator to modal (cartesian) space
14 % Tm2a = transform from modal (cartesian) to actuator space
15 % p = positional locations of Horizontal and Vertical actuators & sensors
16 %      relative to the c.g
17 % v = directional vectors for Horizontal and Vertical actuators & sensors
18 pcg = [0, 0, -8.61];
19 pV1 = [18.4, 19.86, -8.502];
20 pV2 = [-26.4, 6.005, -8.502];
21 pV3 = [8, -25.87, -8.502];
22 pH1 = [26.57, 6.1, -8.5];
23 pH2 = [-18.57, 19.96, -8.5];
24 pH3 = [-8, -26.06, -8.5];
25 dpV1 = pV1 - pcg;
26 dpV2 = pV2 - pcg;
27 dpV3 = pV3 - pcg;
28 dpH1 = pH1 - pcg;
29 dpH2 = pH2 - pcg;
30 dpH3 = pH3 - pcg;
31 vV1 = [0, 0, 1];
32 vV2 = [0, 0, 1];
33 vV3 = [0, 0, 1];
34 vH1 = [-0.223761, 0.974644, 0];
35 vH2 = [-0.73214, -0.681154, 0];
36 vH3 = [0.955969, -0.293467, 0];
37 z = zeros(1,3);
38 sensedDirection = [vV1,z; vV2,z; vV3,z; vH1,z; vH2,z; vH3,z];
39 M = [vV1, cross(dpV1, vV1);
40       vV2, cross(dpV2, vV2);
41       vV3, cross(dpV3, vV3);
42       vH1, cross(dpH1, vH1);
43       vH2, cross(dpH2, vH2);
44       vH3, cross(dpH3, vH3)];
45 Ta2m = inv(M)
46 Tm2a = transpose(Ta2m)
47 % set the number of responses, nr (6 sensors x 6 dof)
48 % cumber of columns = 1 (frequencies) + 2 x nr (real + imag)
49 nr = 36;
```

July 6, 2005

3:52:26 PM

```
50 ncol = 2*nr+1;
51
52 rdir='C:/L2/SEI/coupled_payload_dynamics/stage2_D040519_04/';
53 wdir='C:/L2/SEI/coupled_payload_dynamics/stage2_D040519_04/';
54 xferfile(1) = {'FV1_DallHV.rpt'};
55 xferfile(2) = {'FV2_DallHV.rpt'};
56 xferfile(3) = {'FV3_DallHV.rpt'};
57 xferfile(4) = {'FH1_DallHV.rpt'};
58 xferfile(5) = {'FH2_DallHV.rpt'};
59 xferfile(6) = {'FH3_DallHV.rpt'};
60
61 for j=1:6
62     % read the displacement response at each of the 6 sensors locations in each of 6 ↵
63     dof
64         fid=fopen(char(strcat(rdir,xferfile(j))), 'rt');
65         [data,count]=fscanf(fid, '%f');
66         st = fclose(fid);
67         n=size(data,1);
68         nrow=n/ncol;
69         d=reshape(data,ncol,nrow);
70         f=d(1,:);
71         r=d(2:2:ncol,:);
72         im=d(3:2:ncol,:);
73         s=r+i*im;
74         % ss(sensor, dof)
75         %sss=permute(reshape(s,6,6,nrow),[2 1 3]);
76         ss=reshape(s,6,6,nrow);
77         % reorder the sensors to {V1, V2, V3, H1, H2, H3}
78         % g(actuator, sensor, dof, freq)
79         g(j,:,:,:)=ss(shiftindices,:,:);
80         % transform g to h(actuator, sensor, freq)
81         for k=1:6
82             h(j,k,:)= sensedDirection(k,:) * squeeze(g(j,k,:,:));
83         end
84         % H(act, modal sens, freq)
85         H(j,:,:)= Ta2m * squeeze(h(j,:,:));
86     end
87
88 % plot single actuator excitation to the 6 dof response at each sensor
89 % for comparison to I-DEAS transfer function plots -- agrees!
90 % N.B: use GUI ltiview, preferences to set phase to *not* wrap
91 % 6 x 6 x 6 = 216 transfer functions
92 printFile = strcat(wdir, 'act2dof');
93 actuator = ['V1';'V2';'V3';'H1';'H2';'H3'];
94 for jact=1:6
95     sysstage2g=frd(squeeze(g(jact,:,:,:)),f,'Units','Hz');
96     for m=1:6 %sensor
97         figure;
```

July 6, 2005

3:52:26 PM

```
98      bode(sysstage2g(m,1),sysstage2g(m,2),sysstage2g(m,3),sysstage2g(m,4),sysstage2g(m,5),sysstage2g(m,6));
99      title(['Stage2 + Quad D040519-04, Actuation: ', actuator(jact,:),' , Sensor: ' ,
100     , actuator(m,:)]);
101     legend('dof X','dof Y','dof Z','dof rX','dof rY','dof rZ');
102     hfig = findall(gcf,'type','line','visible','on');
103     set(hfig,'linewidth',2.0);
104     orient landscape;
105     print('-dpssc2','-append', printFile)
106     close;
107 end
108
109
110 % plot single actuator excitation to the response at each sensor
111 % 6 x 6 = 36 transfer functions
112 sysstage2h=frd(h,f,'Units','Hz');
113 printFile = strcat(wdir,'act2sen');
114 actuator = ['V1';'V2';'V3';'H1';'H2';'H3'];
115 for m=1:6
116     figure;
117     bode(sysstage2h(m,1),sysstage2h(m,2),sysstage2h(m,3),sysstage2h(m,4),sysstage2h(m,
118     ,5),sysstage2h(m,6));
119     title(['Stage2 + Quad D040519-04, Actuation: ', actuator(m,:)]);
120     legend('V1','V2','V3','H1','H2','H3');
121     hfig = findall(gcf,'type','line','visible','on');
122     set(hfig,'linewidth',2.0);
123     orient landscape;
124     print('-dpssc2','-append', printFile)
125     close;
126 end
127
128 % HH(modal act, modal sens, freq)
129 for j=1:6
130     HH(j,:,:)=Ta2m * squeeze(H(:,j,:));
131 end
132 % DC (low freq) modal force vectors
133 real(HH(:,:,1))
134 imag(HH(:,:,1))
135
136 % plot modal actuation to modal sensed response
137 % 6 x 6 = 36 transfer functions
138 sysstage2=frd(HH,f,'Units','Hz');
139 normalize = [1, 1, 1, sqrt(dot(dpV1,dpV1)), sqrt(dot(dpV2,dpV2)), sqrt(dot(dpH1,dpH1)) ];
140 printFile = strcat(wdir,'modal_act2sen');
141 mode = [' X';' Y';' Z';'rX';'rY';'rZ'];
142 figure;
```

July 6, 2005

3:52:26 PM

```
143      bode(normalize(1)*sysstage2(1,1),normalize(2)*sysstage2(2,2),normalize(3)*sysstag e2(3,3), ...
144          normalize(4)*sysstage2(4,4),normalize(5)*sysstage2(5,5),normalize(6)*sysstage2(6,6));
145      title('Stage2 + Quad D040519-04, Rigid Body Modal (Cartesian) Actuation: Diagonal Response');
146      legend('X','Y','Z','rX','rY','rZ');
147      hfig = findall(gcf,'type','line','visible','on');
148      set(hfig,'linewidth',2.0);
149      orient landscape;
150      print('-dpsc2','-append', printFile)
151  for m=1:6
152      figure;
153      bode(normalize(1)*sysstage2(m,1),normalize(2)*sysstage2(m,2),normalize(3)*sysstag e2(m,3), ...
154          normalize(4)*sysstage2(m,4),normalize(5)*sysstage2(m,5),normalize(6)*sysstage2(m,6));
155      title(['Stage2 + Quad D040519-04, Rigid Body Modal (Cartesian) Actuation: ', mode(m,:)]);
156      legend('X','Y','Z','rX','rY','rZ');
157      hfig = findall(gcf,'type','line','visible','on');
158      set(hfig,'linewidth',2.0);
159      orient landscape;
160      print('-dpsc2','-append', printFile)
161      close;
162  end
163
164 % re-plot modal actuation to modal sensed response for 70 < f < 200 Hz
165 % 6 x 6 = 36 transfer functions
166 printFile = strcat(wdir,'modal_act2sen_zoom');
167 mode = [' X';' Y';' Z';'rX';'rY';'rZ'];
168 figure;
169 bode(normalize(1)*sysstage2(1,1),normalize(2)*sysstage2(2,2),normalize(3)*sysstag e2(3,3), ...
170          normalize(4)*sysstage2(4,4),normalize(5)*sysstage2(5,5),normalize(6)*sysstage2(6,6));
171 title('Stage2 + Quad D040519-04, Rigid Body Modal (Cartesian) Actuation: Diagonal Response');
172 legend('X','Y','Z','rX','rY','rZ');
173 set(gca,'XLim',[70 200]);
174 hfig = findall(gcf,'type','line','visible','on');
175 set(hfig,'linewidth',2.0);
176 orient landscape;
177 print('-dpsc2','-append', printFile)
178 for m=1:6
179     figure;
180     bode(normalize(1)*sysstage2(m,1),normalize(2)*sysstage2(m,2),normalize(3)*sysstag e2(m,3), ...
181          normalize(4)*sysstage2(m,4),normalize(5)*sysstage2(m,5),normalize(6)*sysstage2(m,6));
```

```
2(m,6));  
182 title(['Stage2 + Quad D040519-04, Rigid Body Modal (Cartesian) Actuation: ', mode  
(m,:)]);  
183 legend('X','Y','Z','rX','rY','rZ');  
184 set(gca,'XLim',[70 200]);  
185 hfig = findall(gcf,'type','line','visible','on');  
186 set(hfig,'linewidth',2.0);  
187 orient landscape;  
188 print('-dpsc2','-append', printFile)  
189 close;  
190 end  
191  
192  
193
```

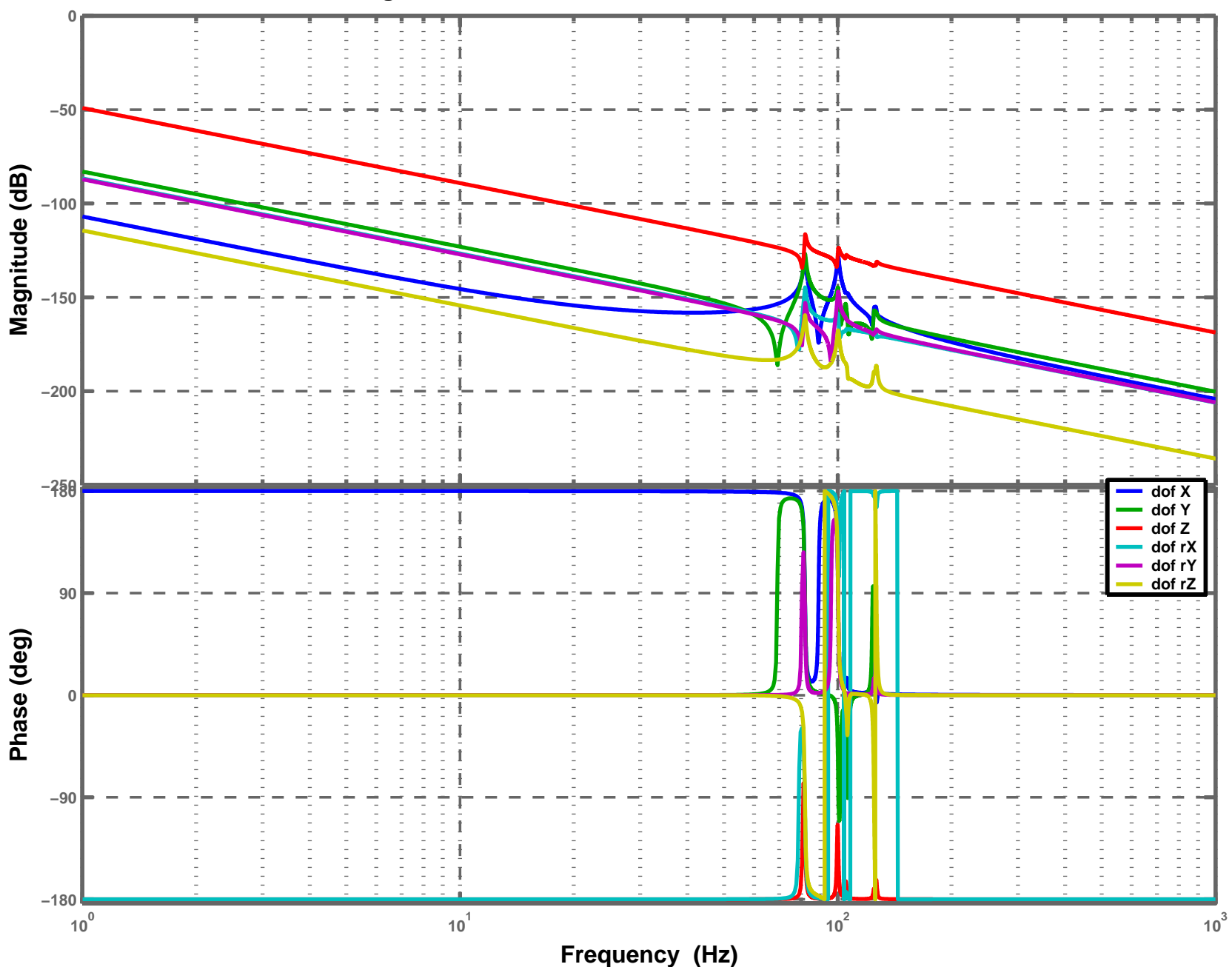
9 Appendix C: SUS D040519-04 Quad Structure Transfer functions

6 actuators x 6 degrees of freedom x 6 sensors = 216 transfer functions

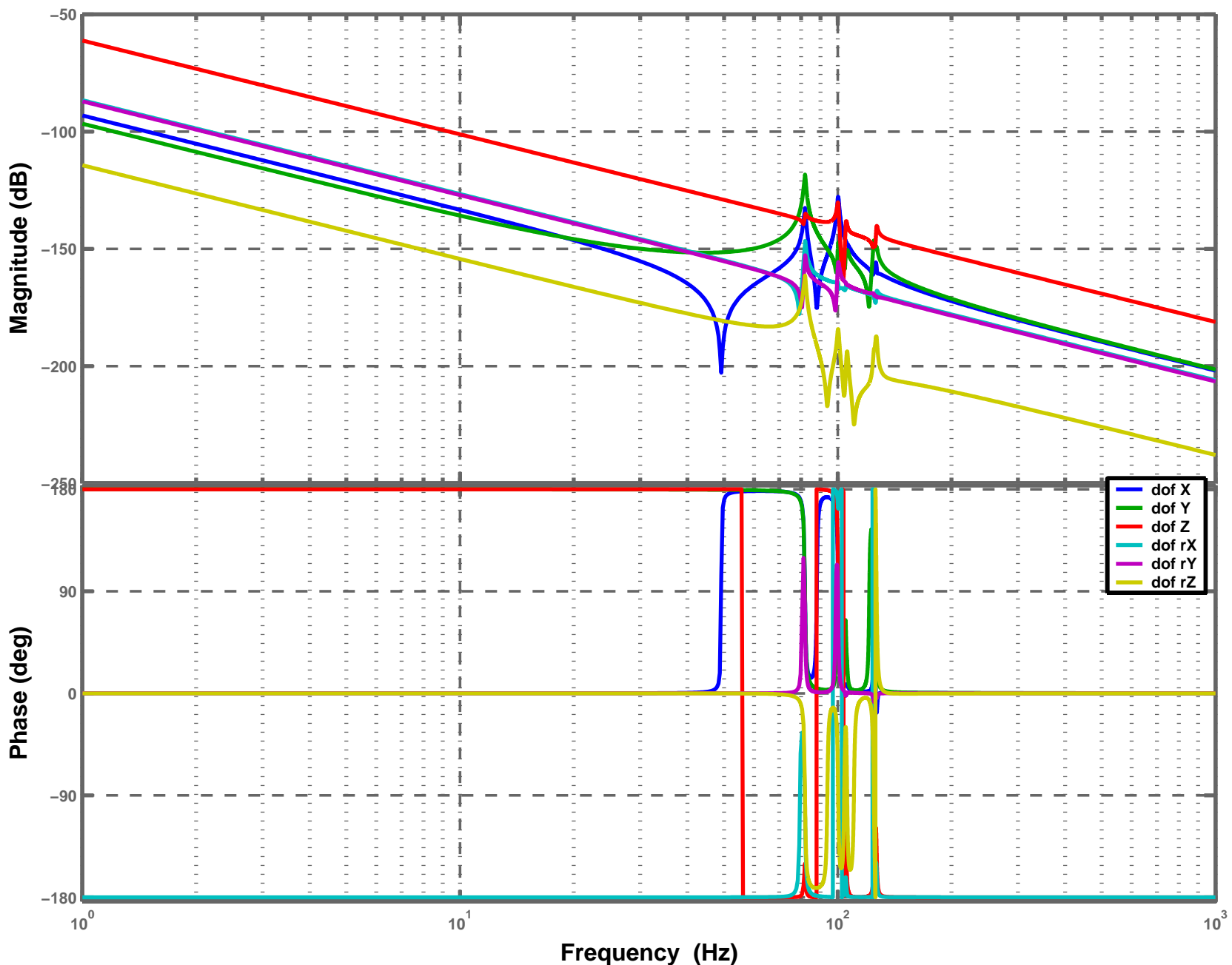
projected into 6 actuators x 6 sensor response = 36 transfer functions

projected into 6 modal actuation x 6 modal sensing = 36 transfer functions

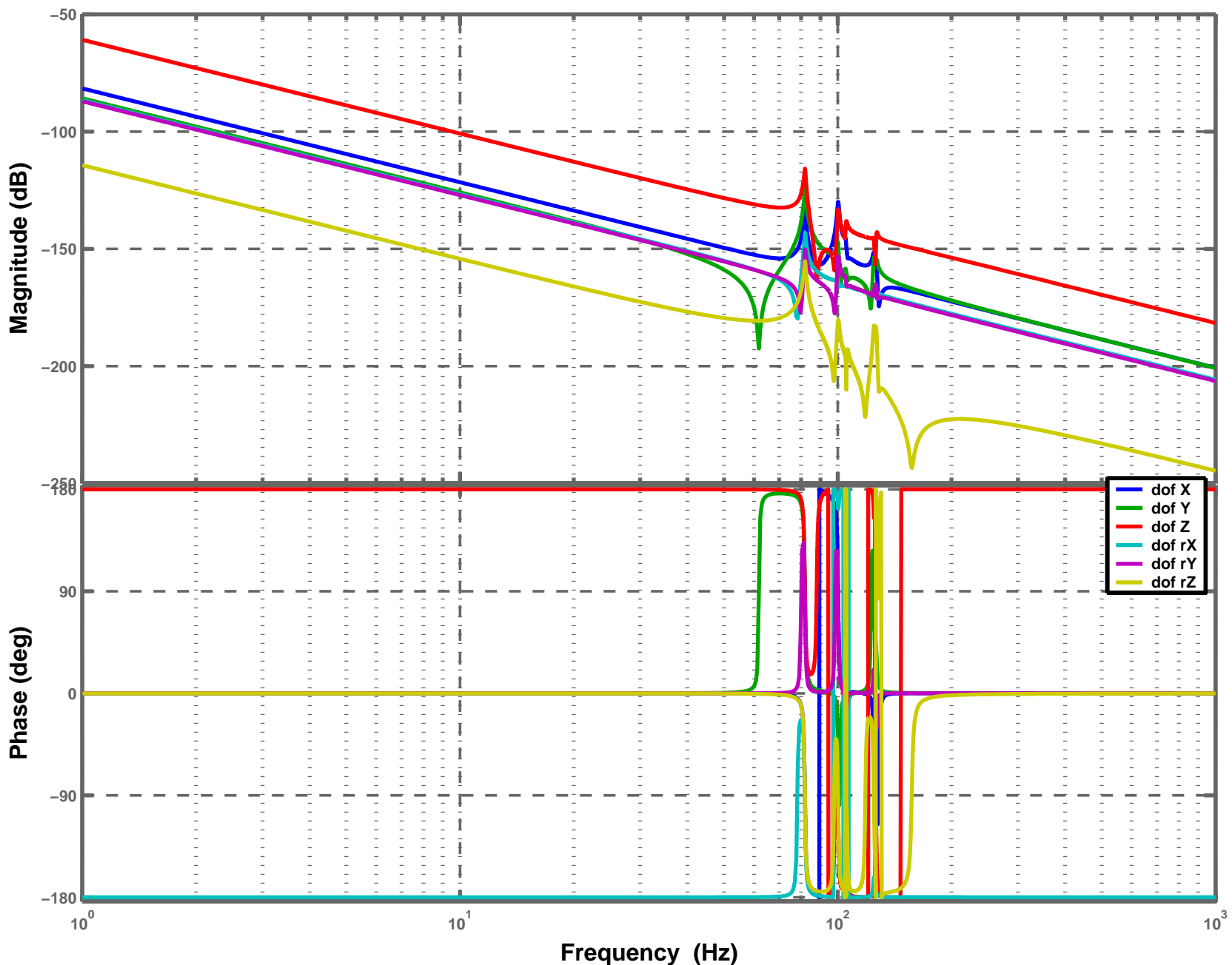
Stage2 + Quad D040519-04, Actuation: V1, Sensor: V1



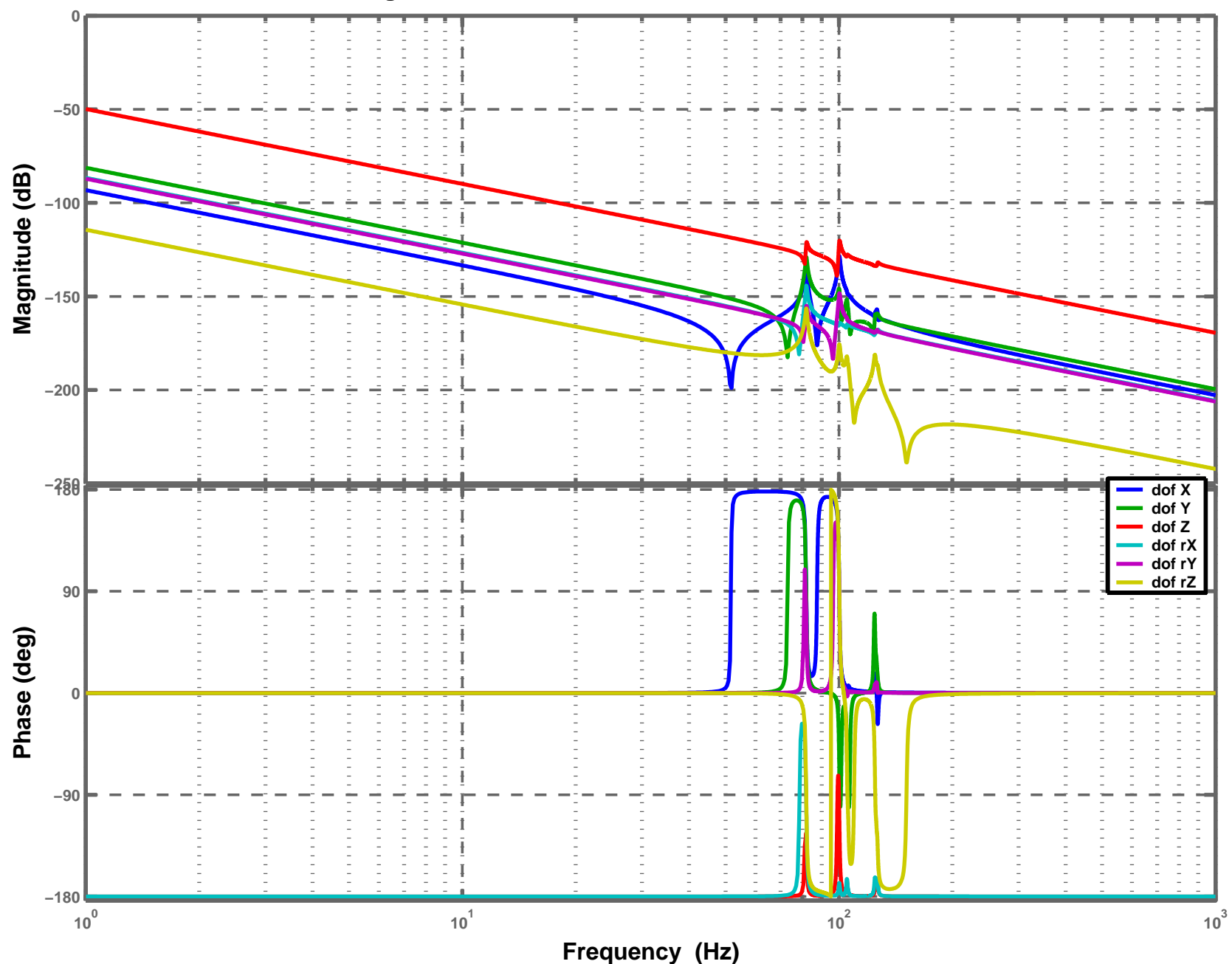
Stage2 + Quad D040519-04, Actuation: V1, Sensor: V2



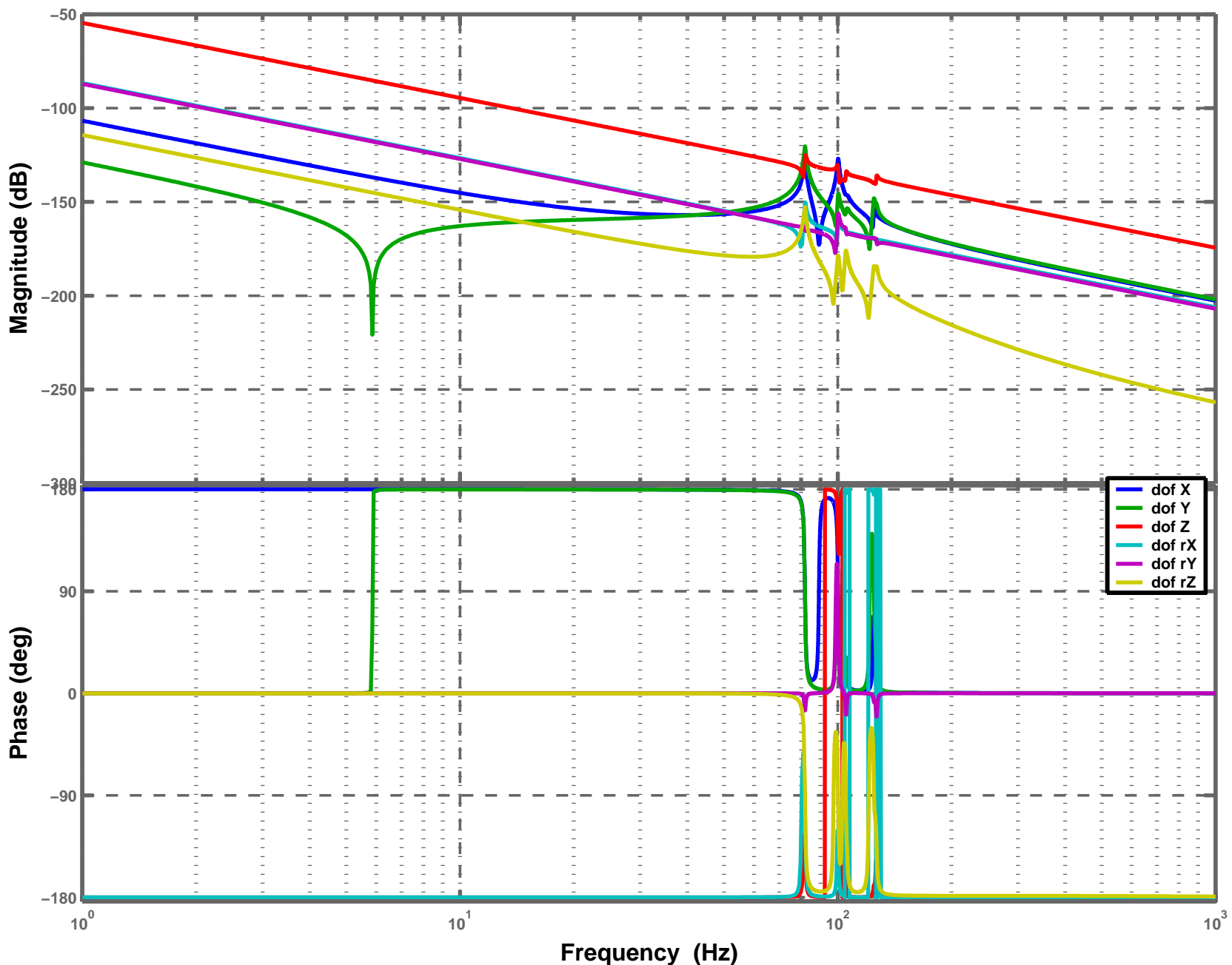
Stage2 + Quad D040519-04, Actuation: V1, Sensor: V3



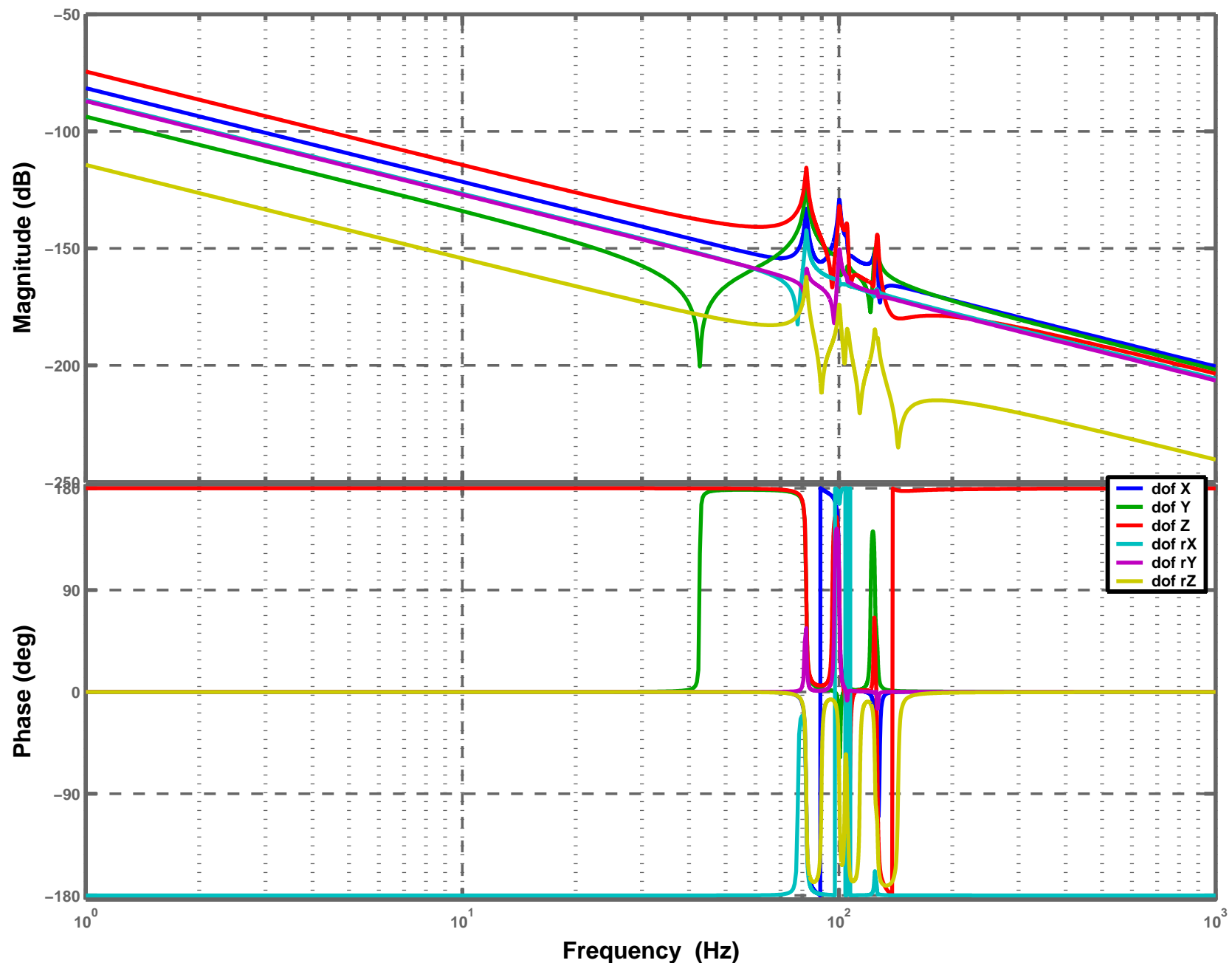
Stage2 + Quad D040519-04, Actuation: V1, Sensor: H1



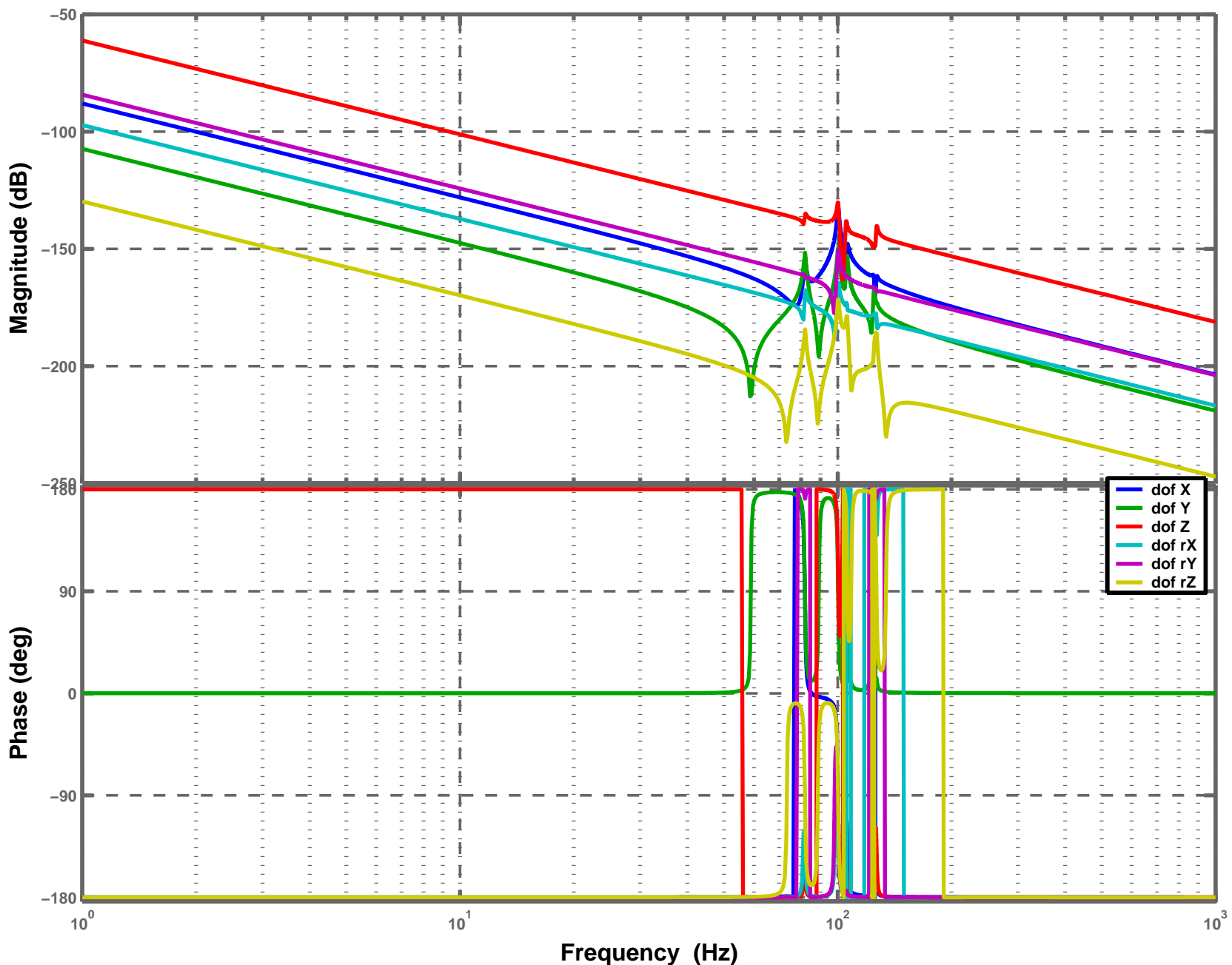
Stage2 + Quad D040519-04, Actuation: V1, Sensor: H2



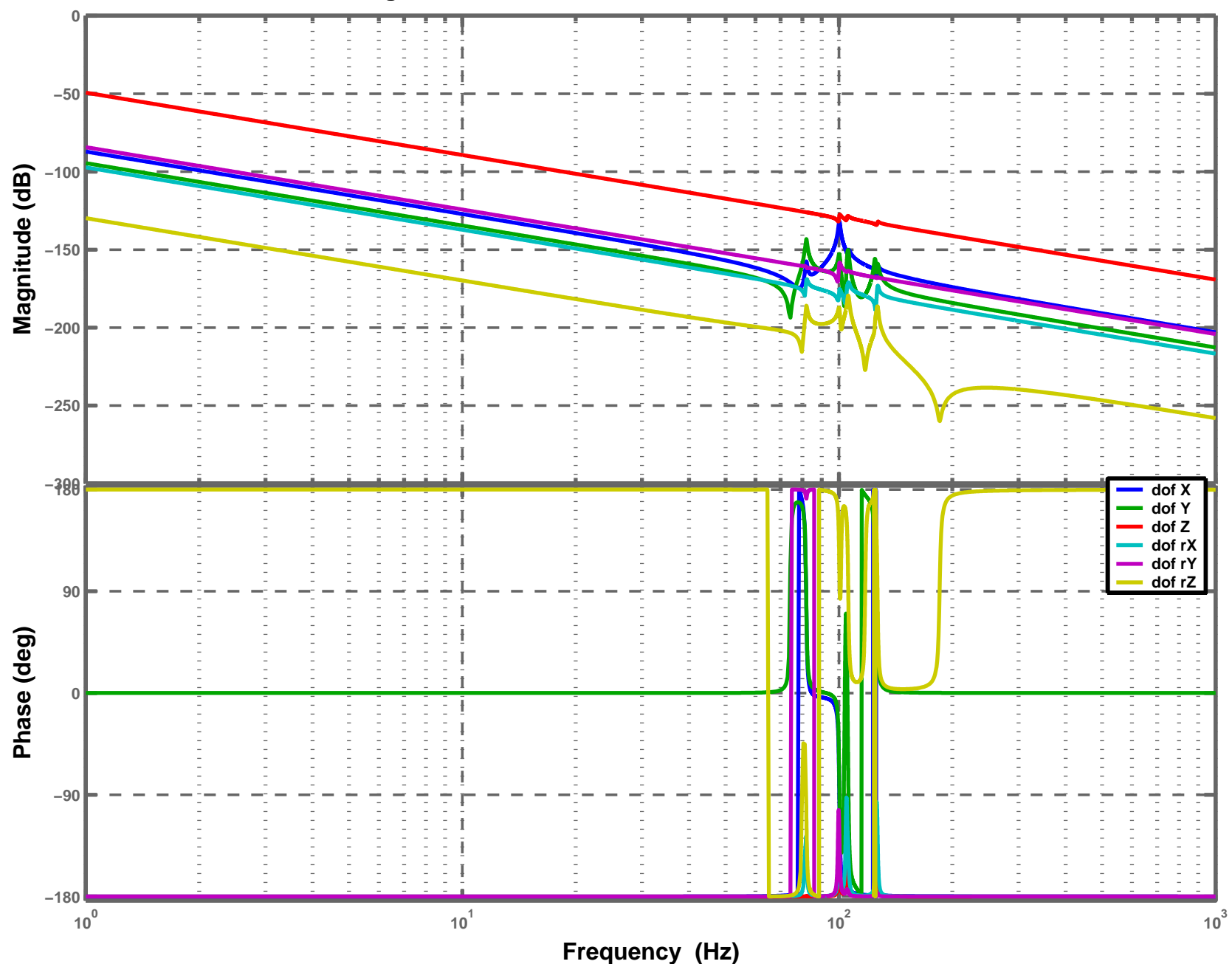
Stage2 + Quad D040519-04, Actuation: V1, Sensor: H3



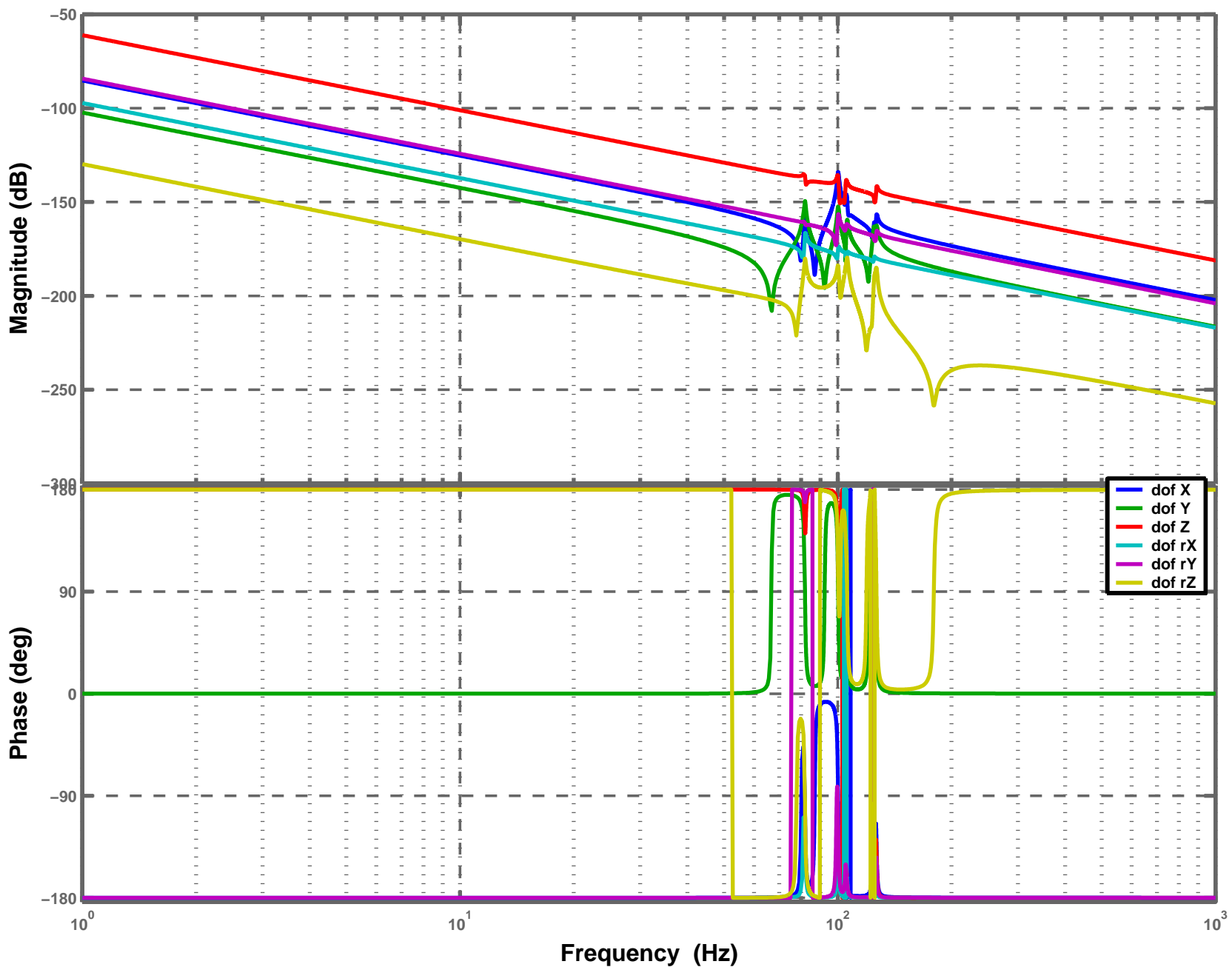
Stage2 + Quad D040519-04, Actuation: V2, Sensor: V1



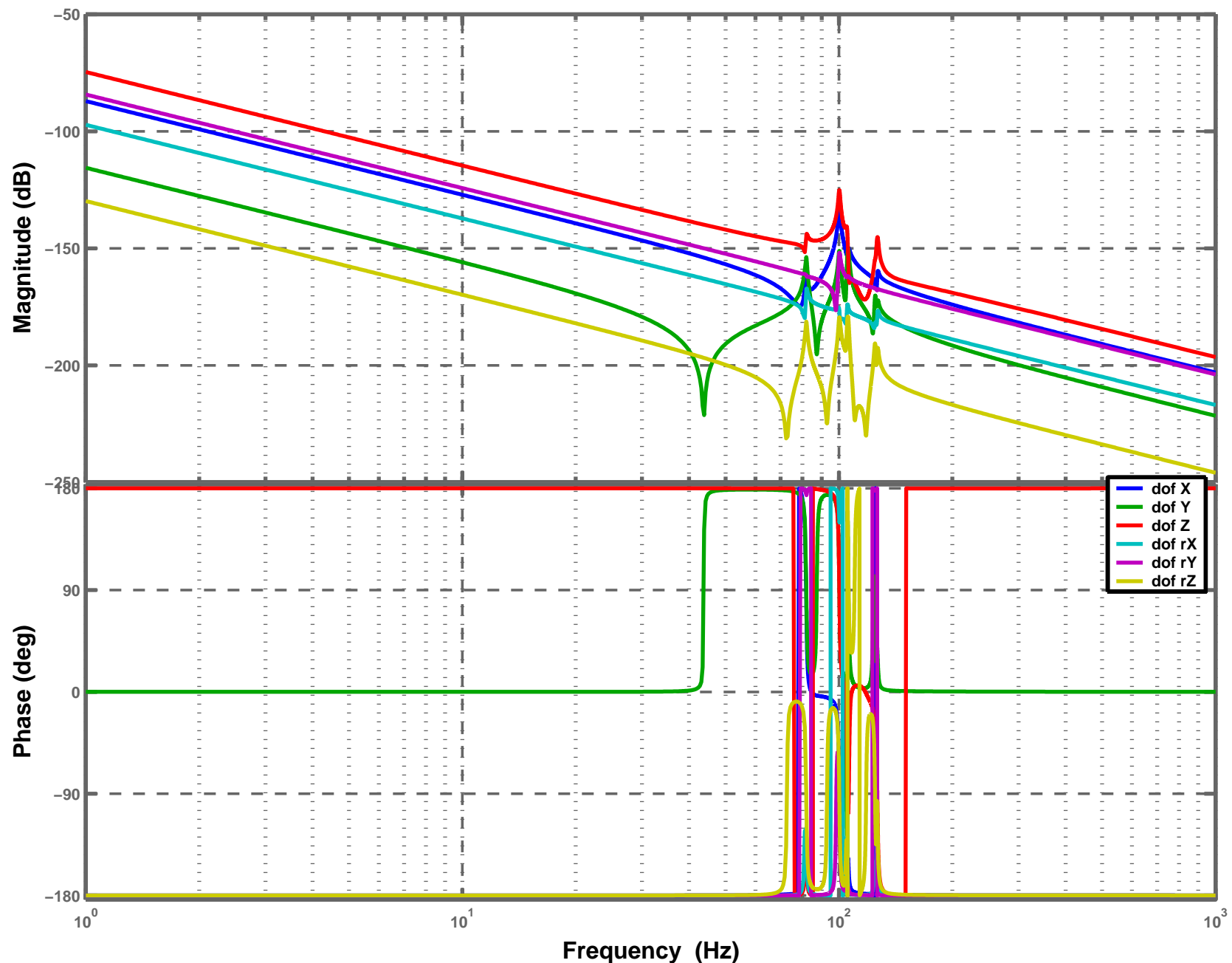
Stage2 + Quad D040519-04, Actuation: V2, Sensor: V2



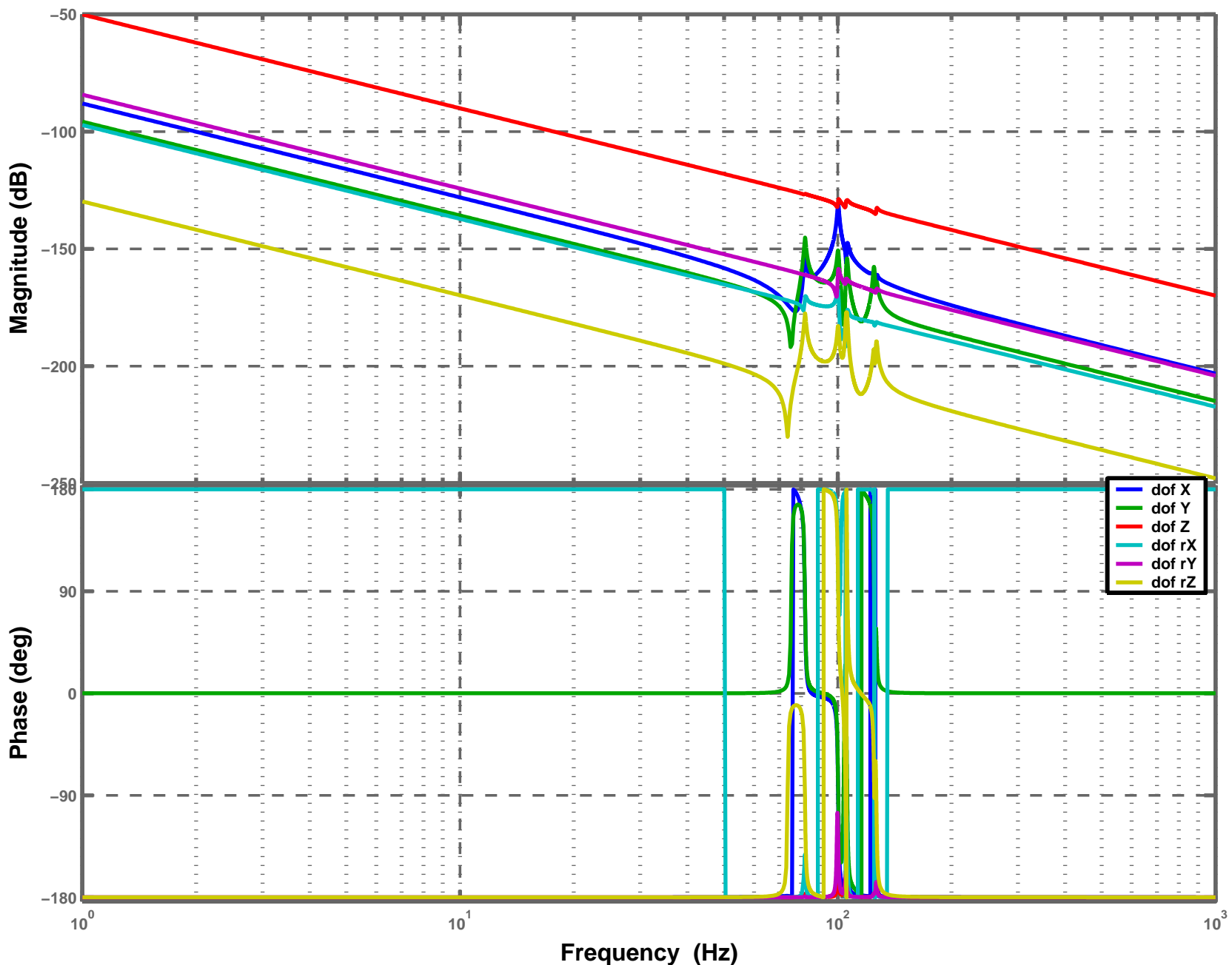
Stage2 + Quad D040519-04, Actuation: V2, Sensor: V3



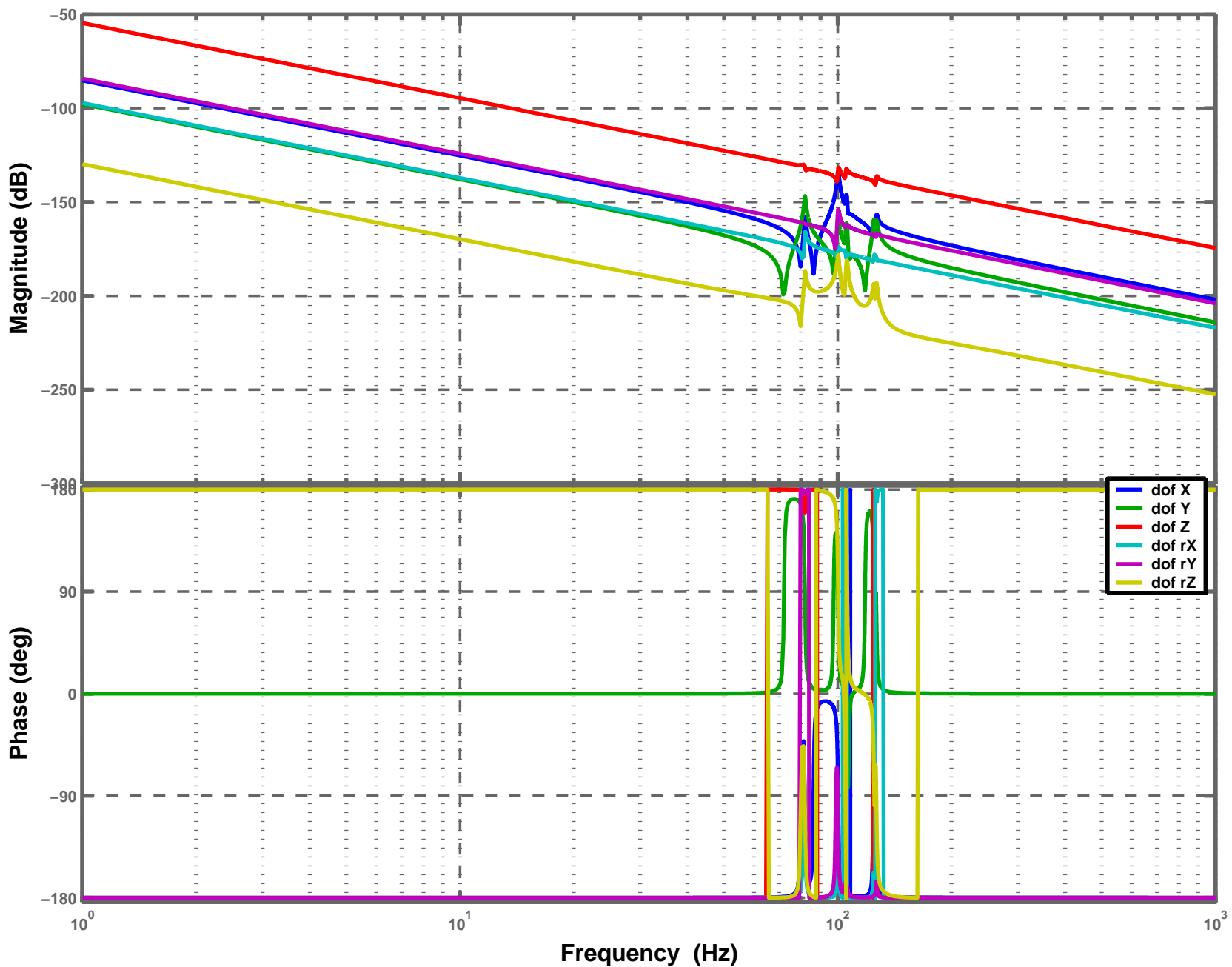
Stage2 + Quad D040519-04, Actuation: V2, Sensor: H1



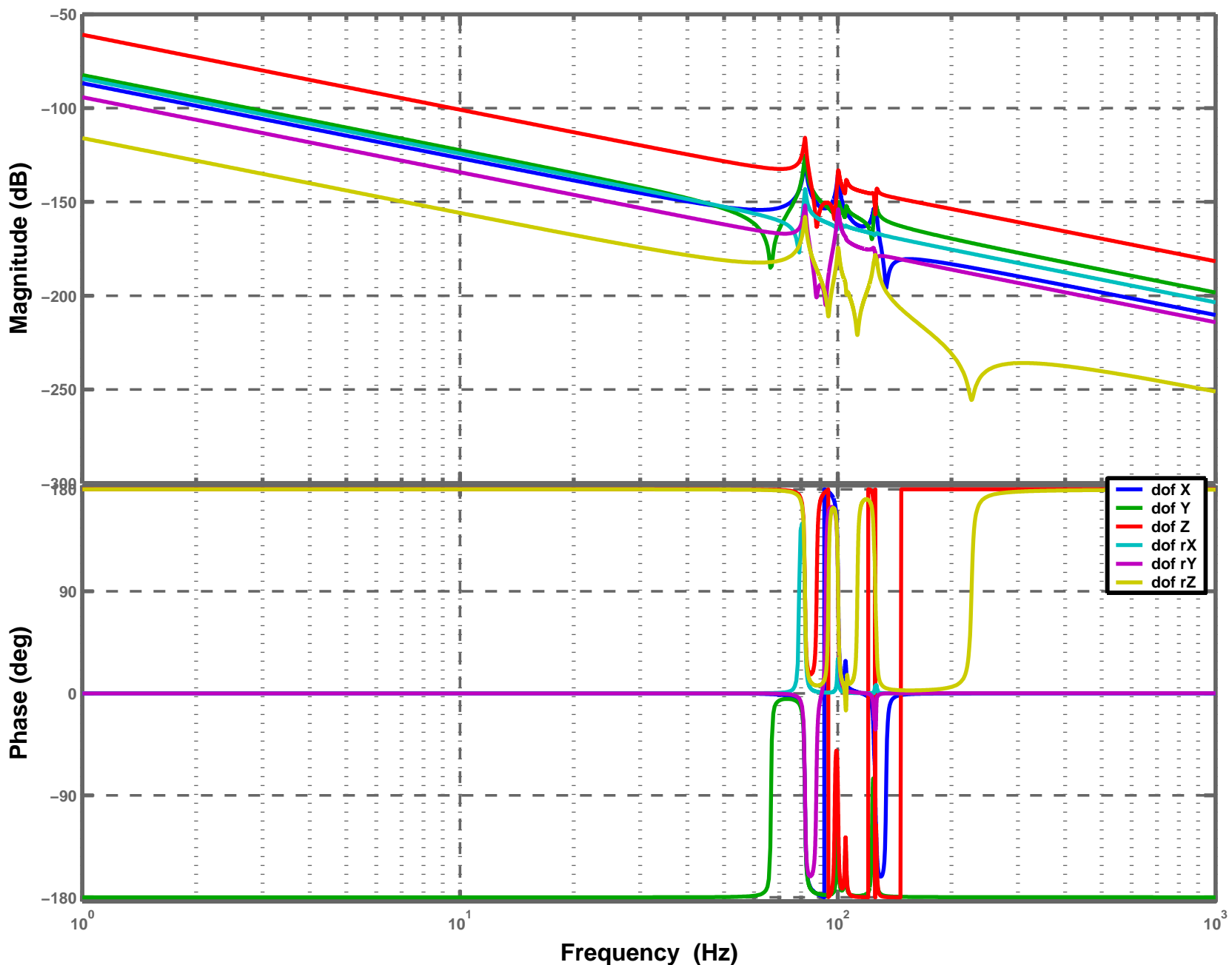
Stage2 + Quad D040519-04, Actuation: V2, Sensor: H2



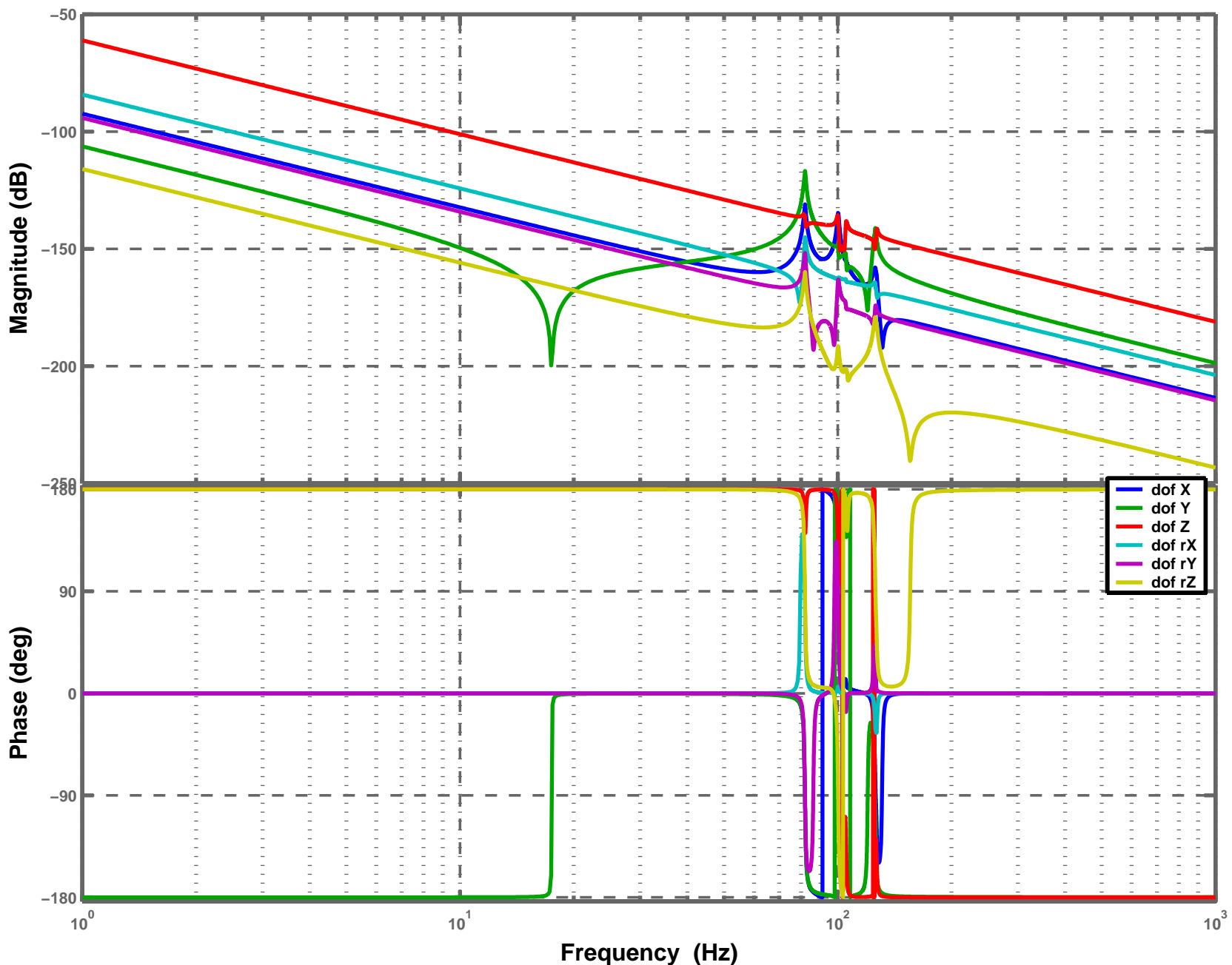
Stage2 + Quad D040519-04, Actuation: V2, Sensor: H3



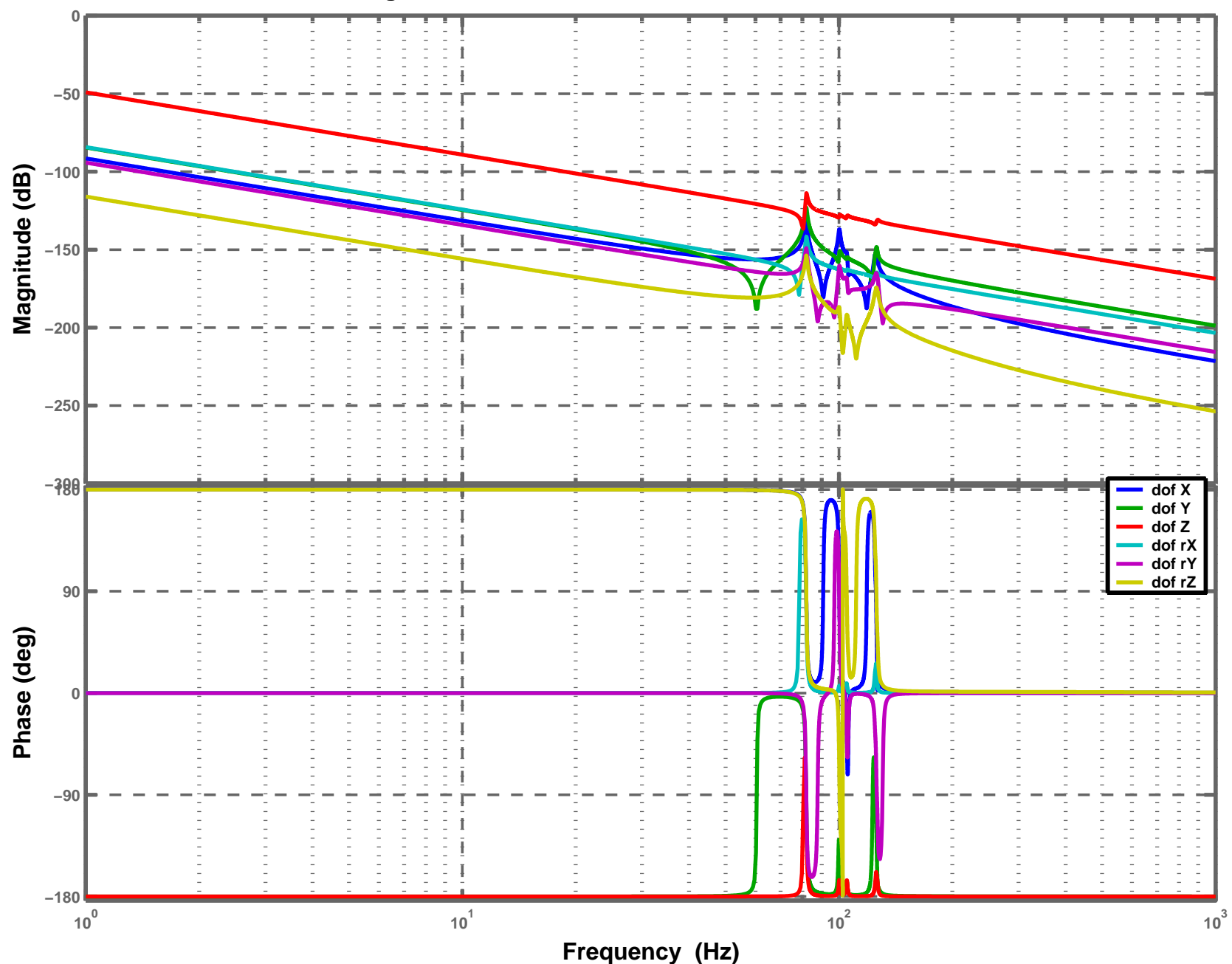
Stage2 + Quad D040519-04, Actuation: V3, Sensor: V1



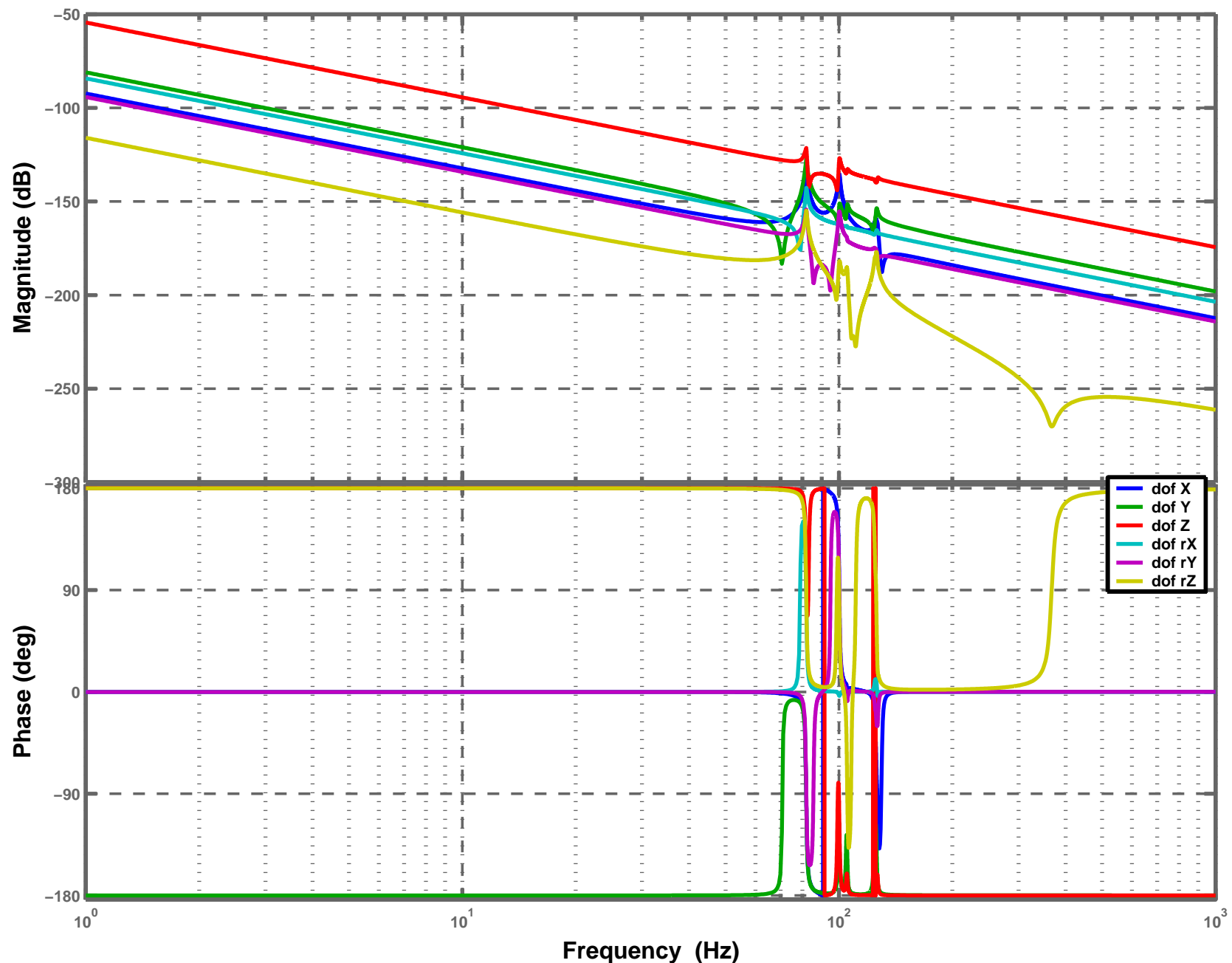
Stage2 + Quad D040519-04, Actuation: V3, Sensor: V2



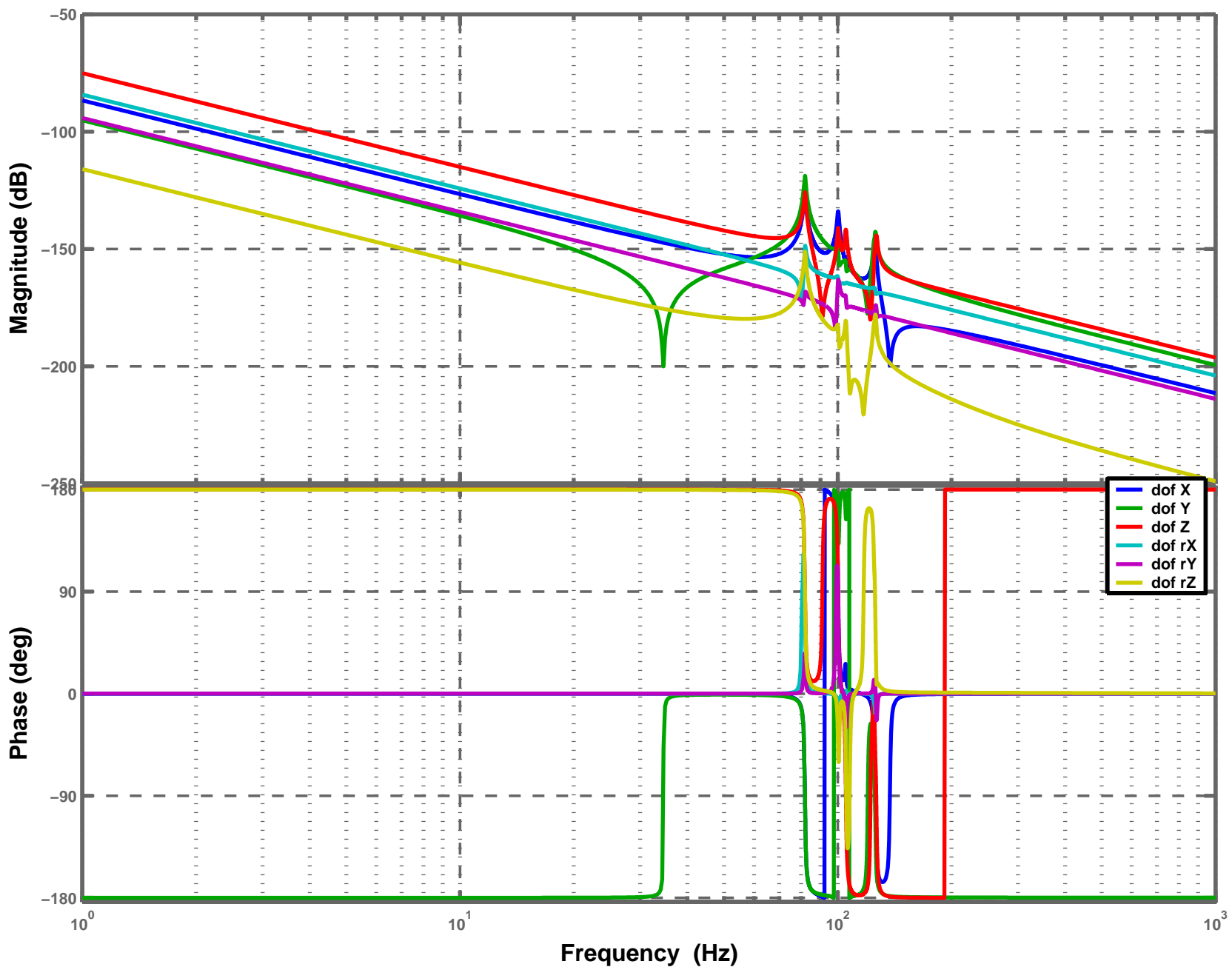
Stage2 + Quad D040519-04, Actuation: V3, Sensor: V3



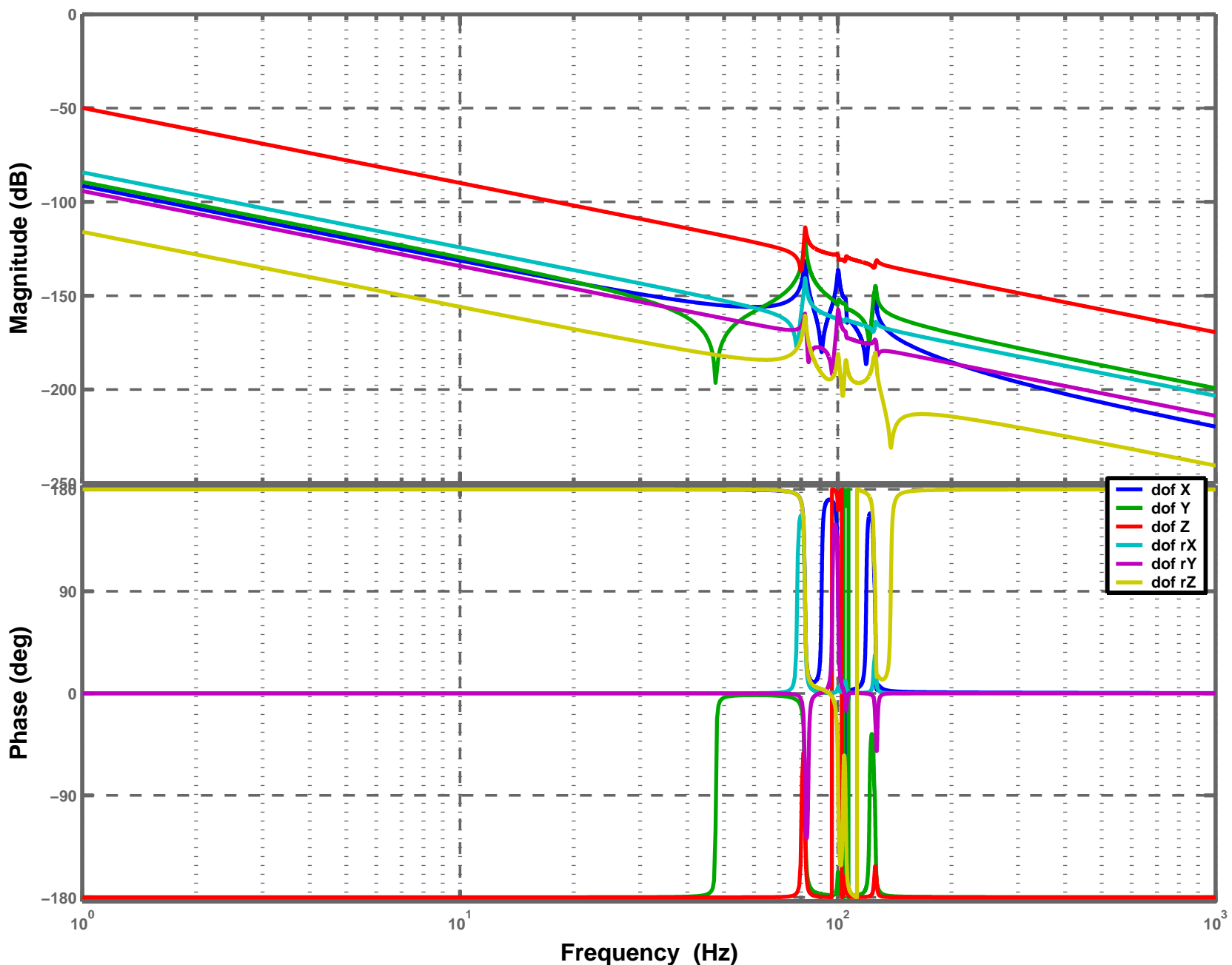
Stage2 + Quad D040519-04, Actuation: V3, Sensor: H1



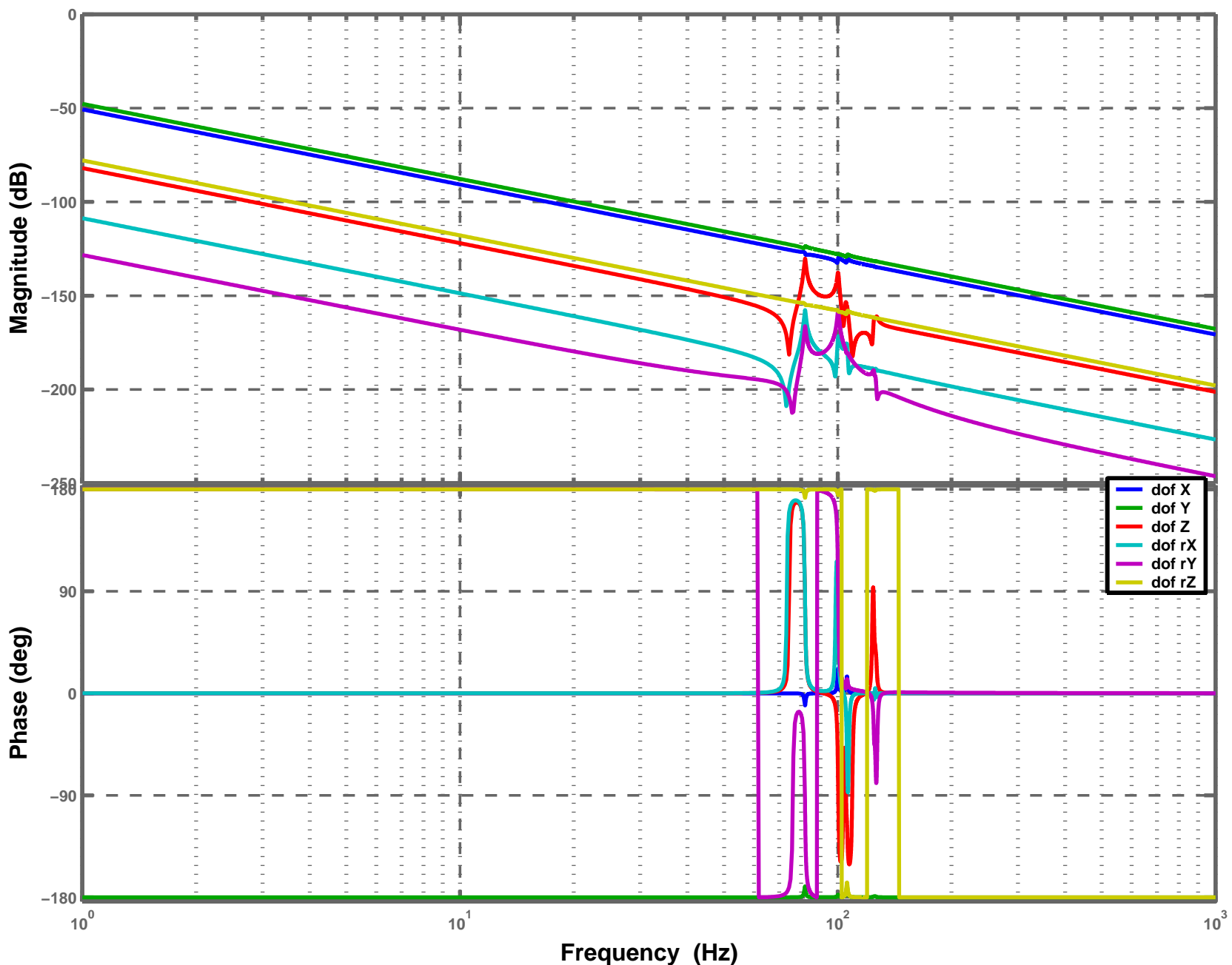
Stage2 + Quad D040519-04, Actuation: V3, Sensor: H2



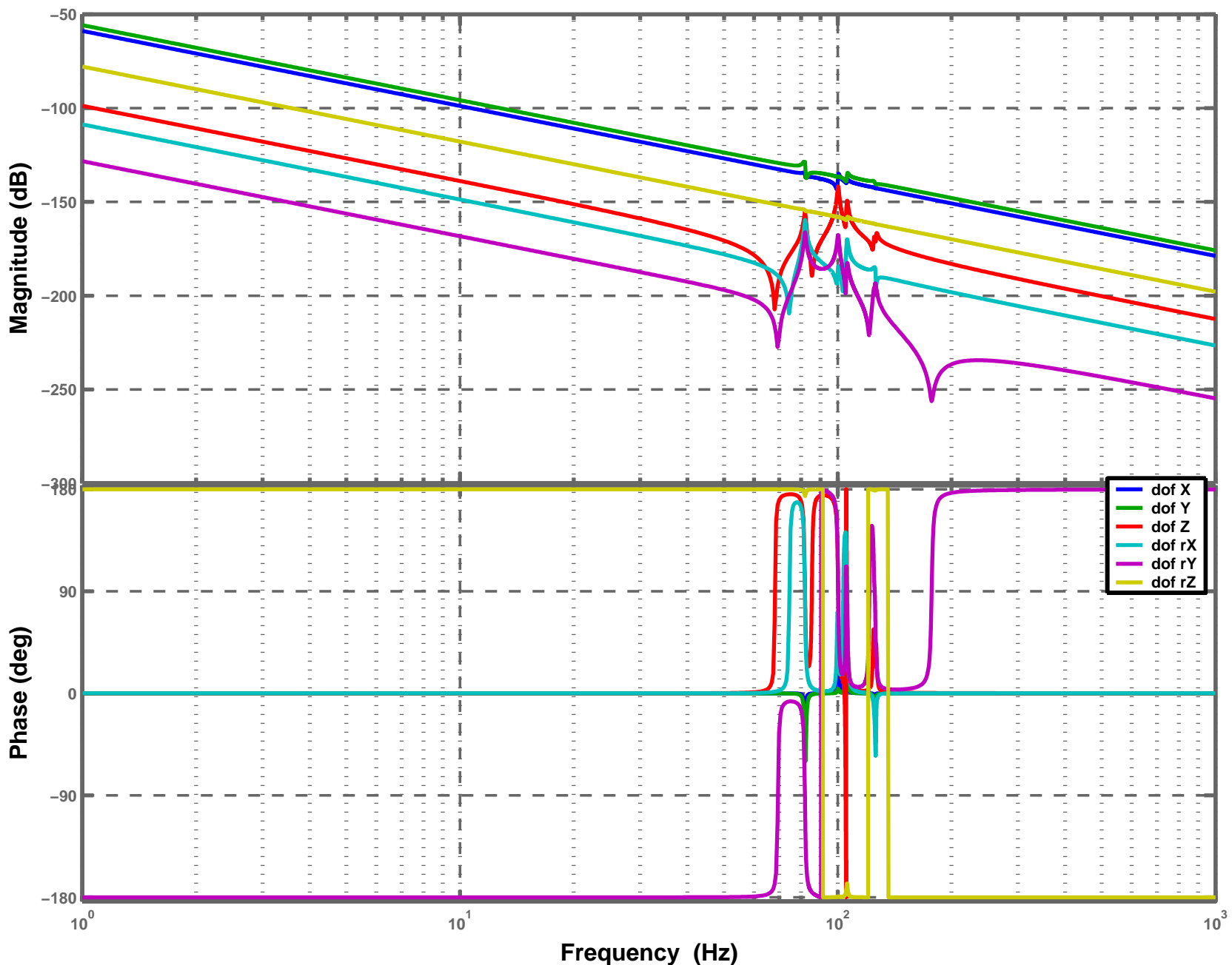
Stage2 + Quad D040519-04, Actuation: V3, Sensor: H3



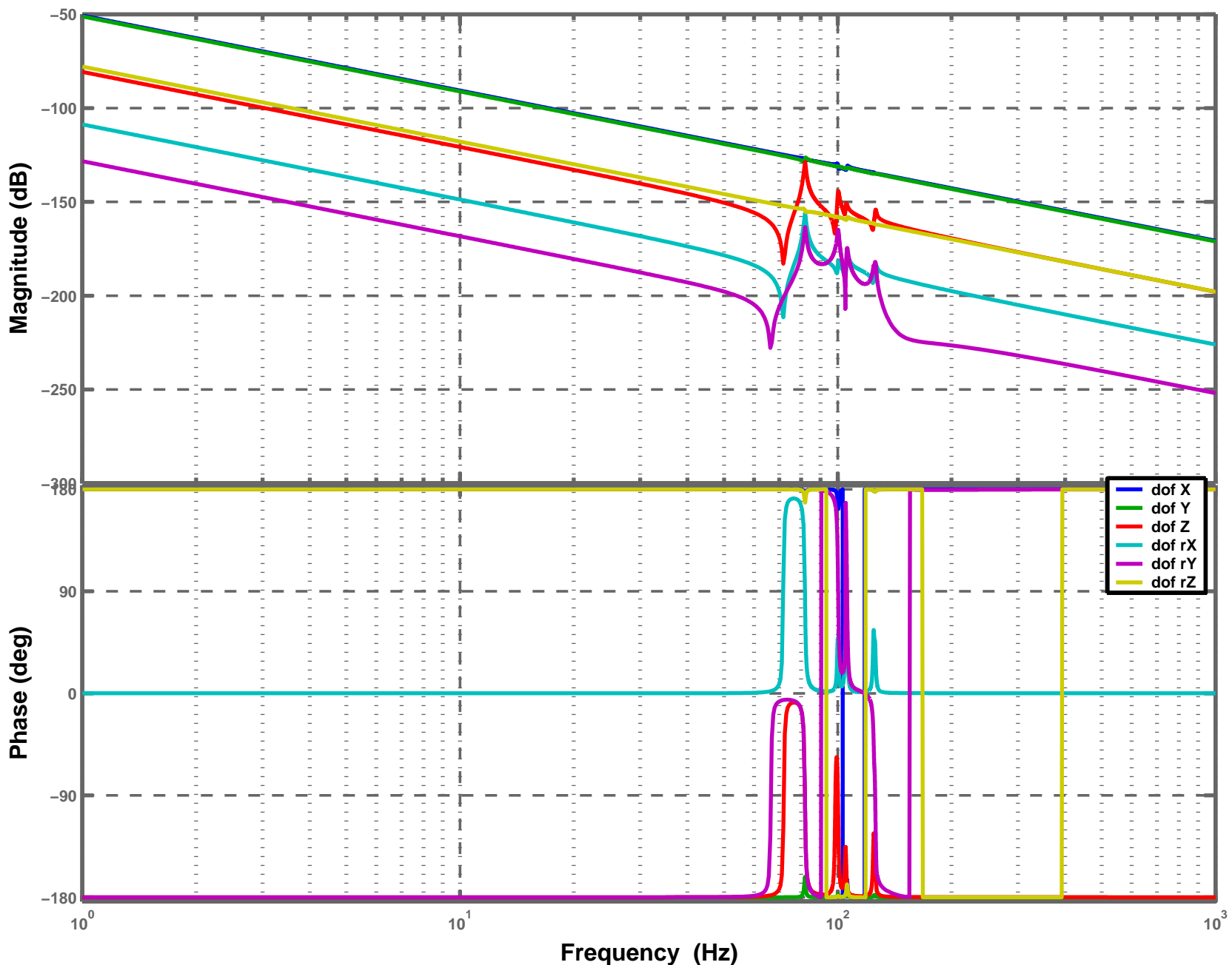
Stage2 + Quad D040519-04, Actuation: H1, Sensor: V1



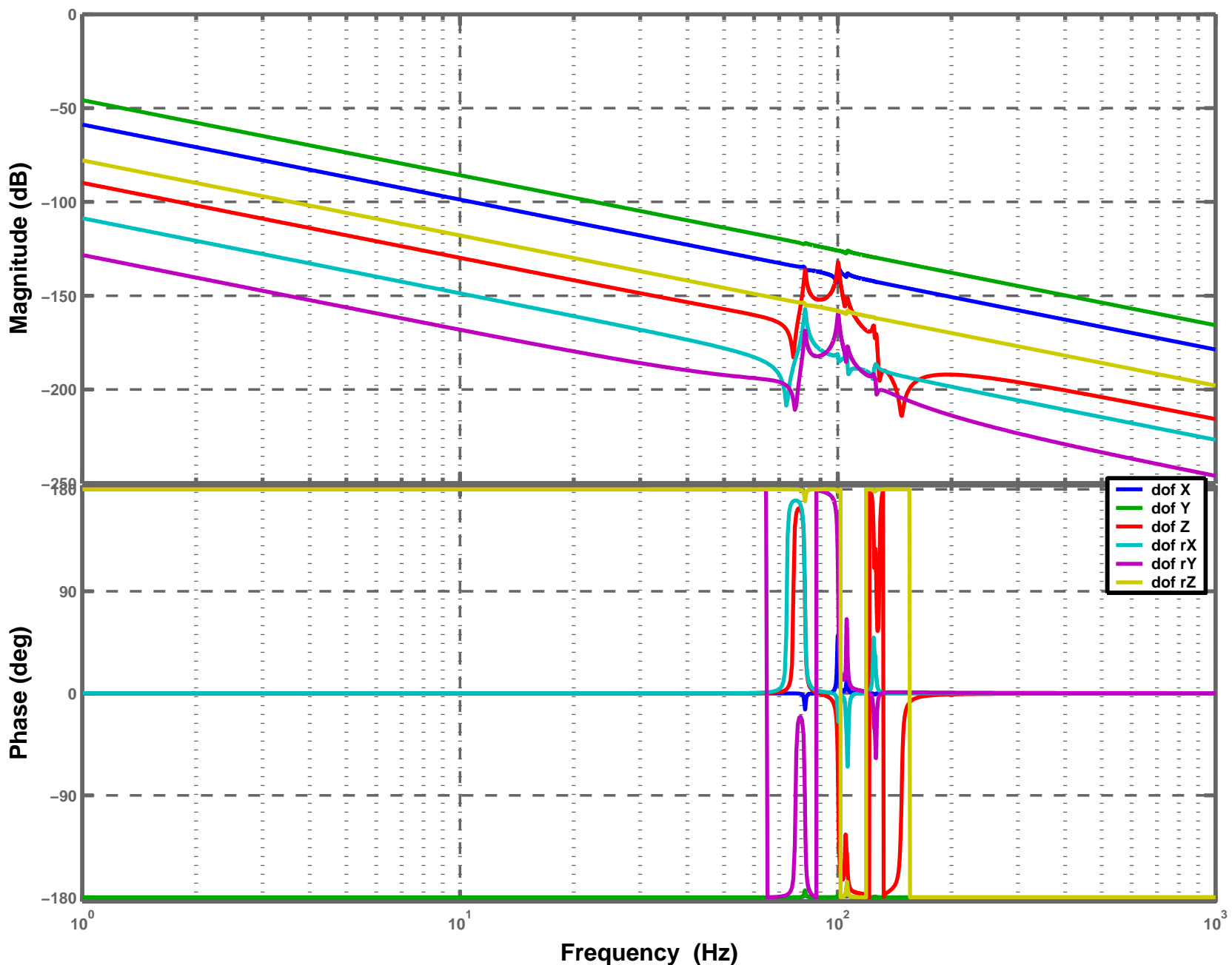
Stage2 + Quad D040519-04, Actuation: H1, Sensor: V2



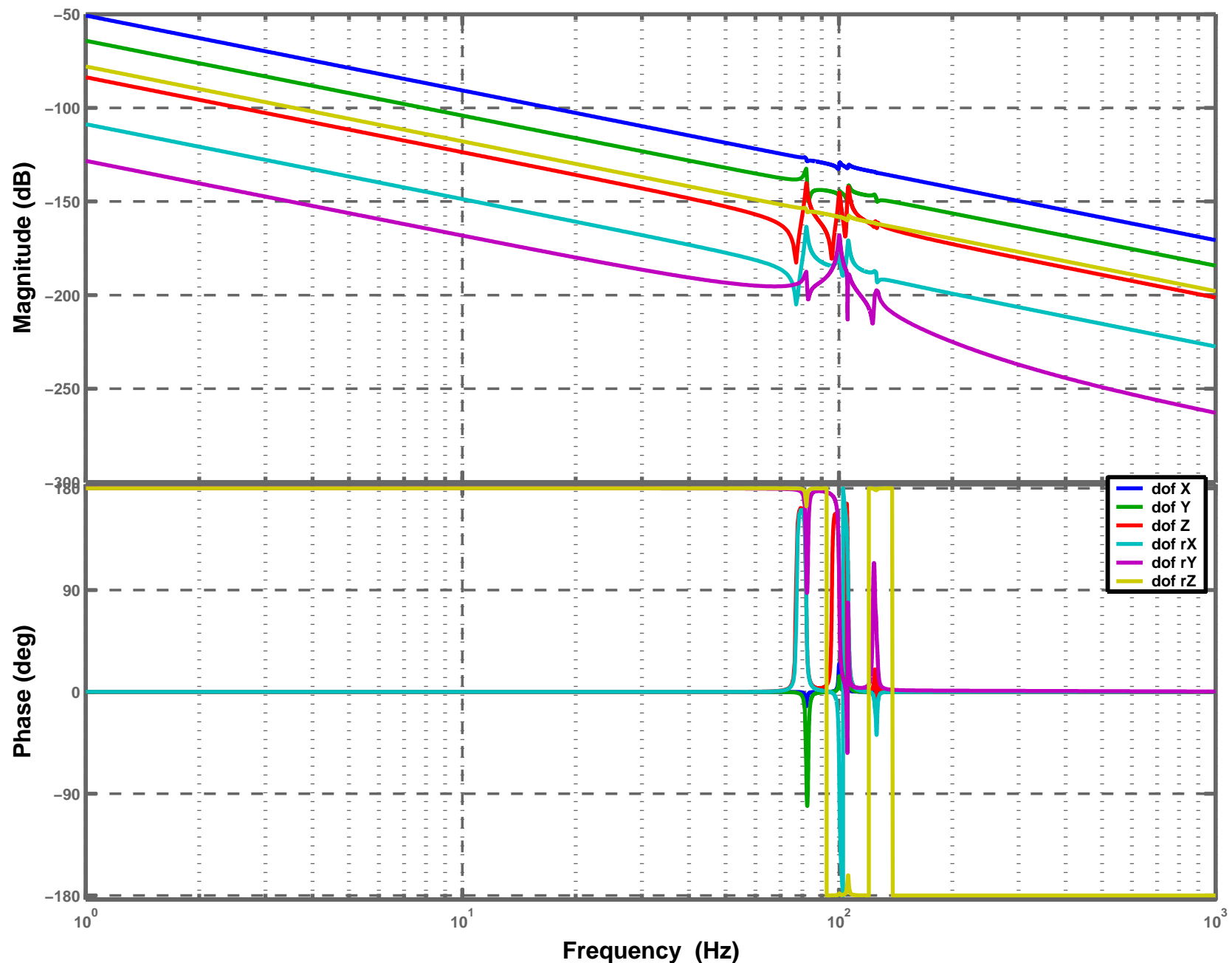
Stage2 + Quad D040519-04, Actuation: H1, Sensor: V3



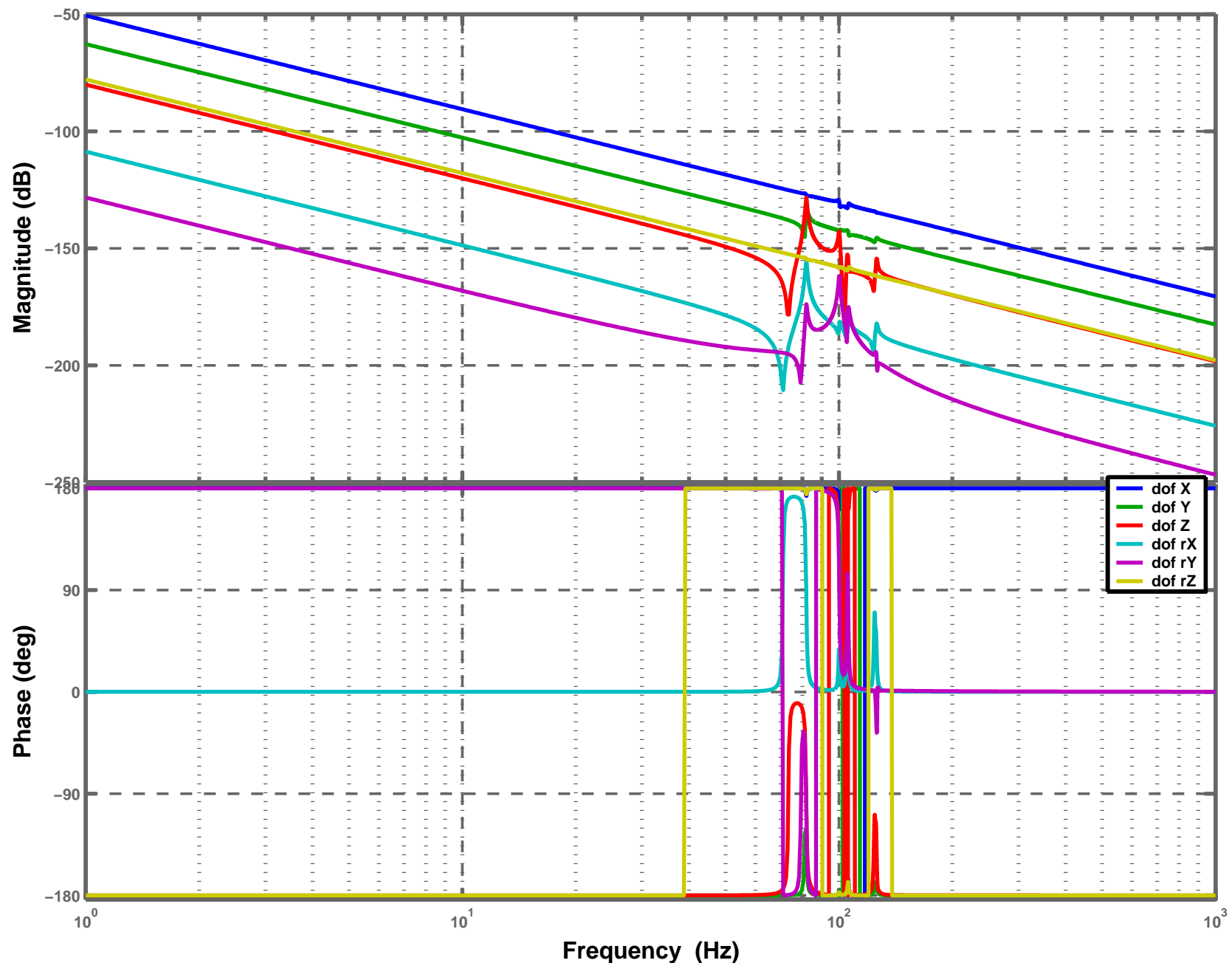
Stage2 + Quad D040519-04, Actuation: H1, Sensor: H1



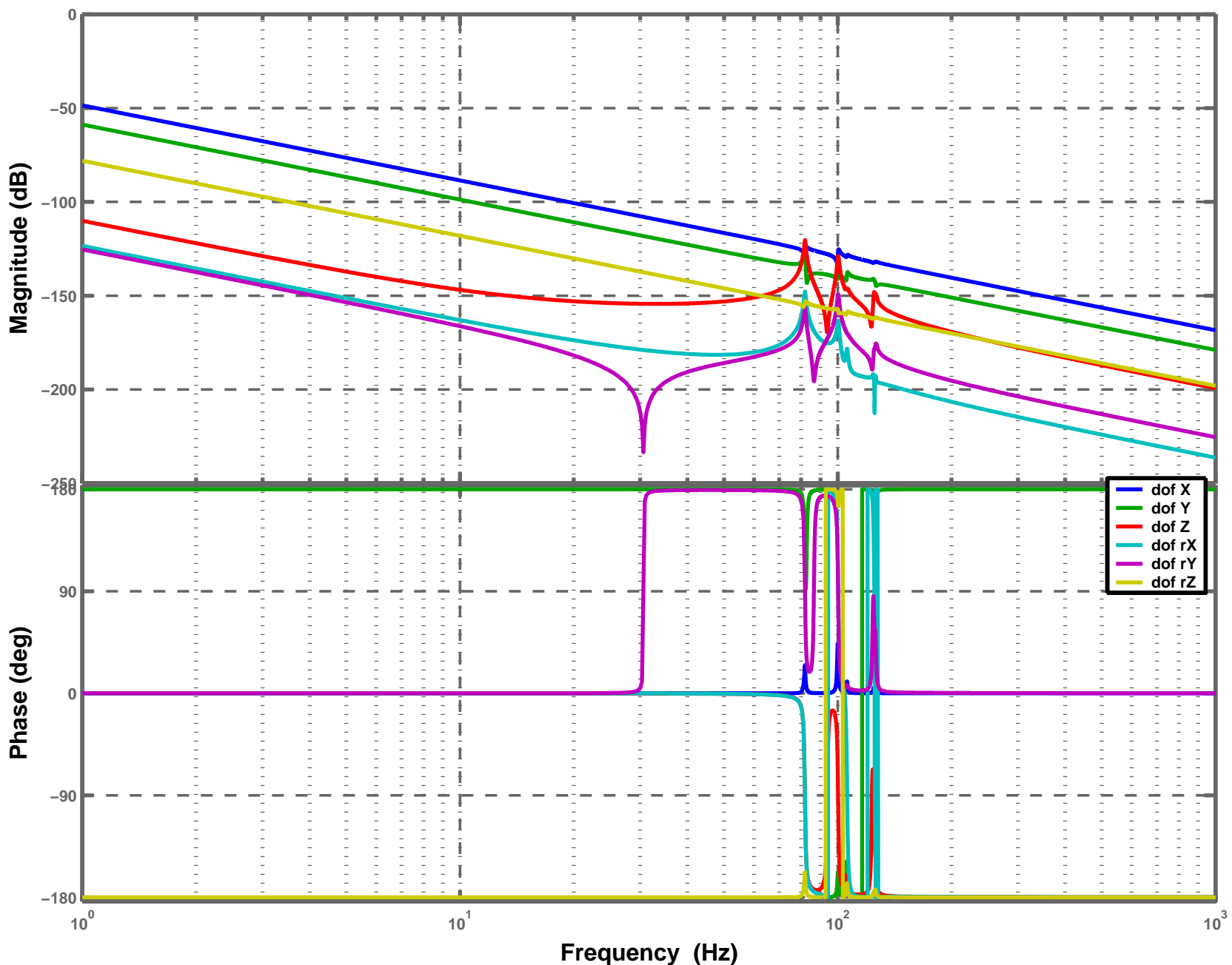
Stage2 + Quad D040519-04, Actuation: H1, Sensor: H2



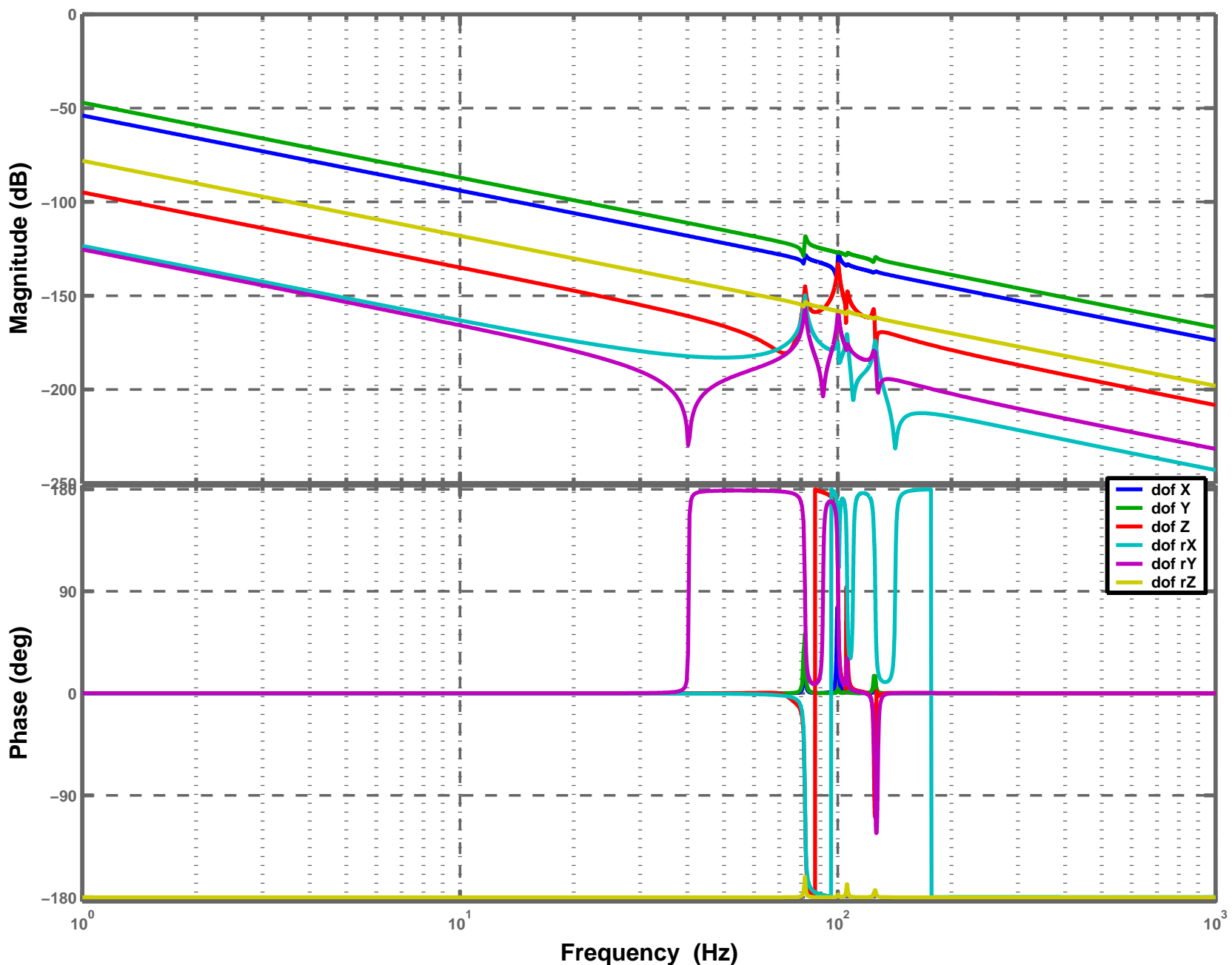
Stage2 + Quad D040519-04, Actuation: H1, Sensor: H3



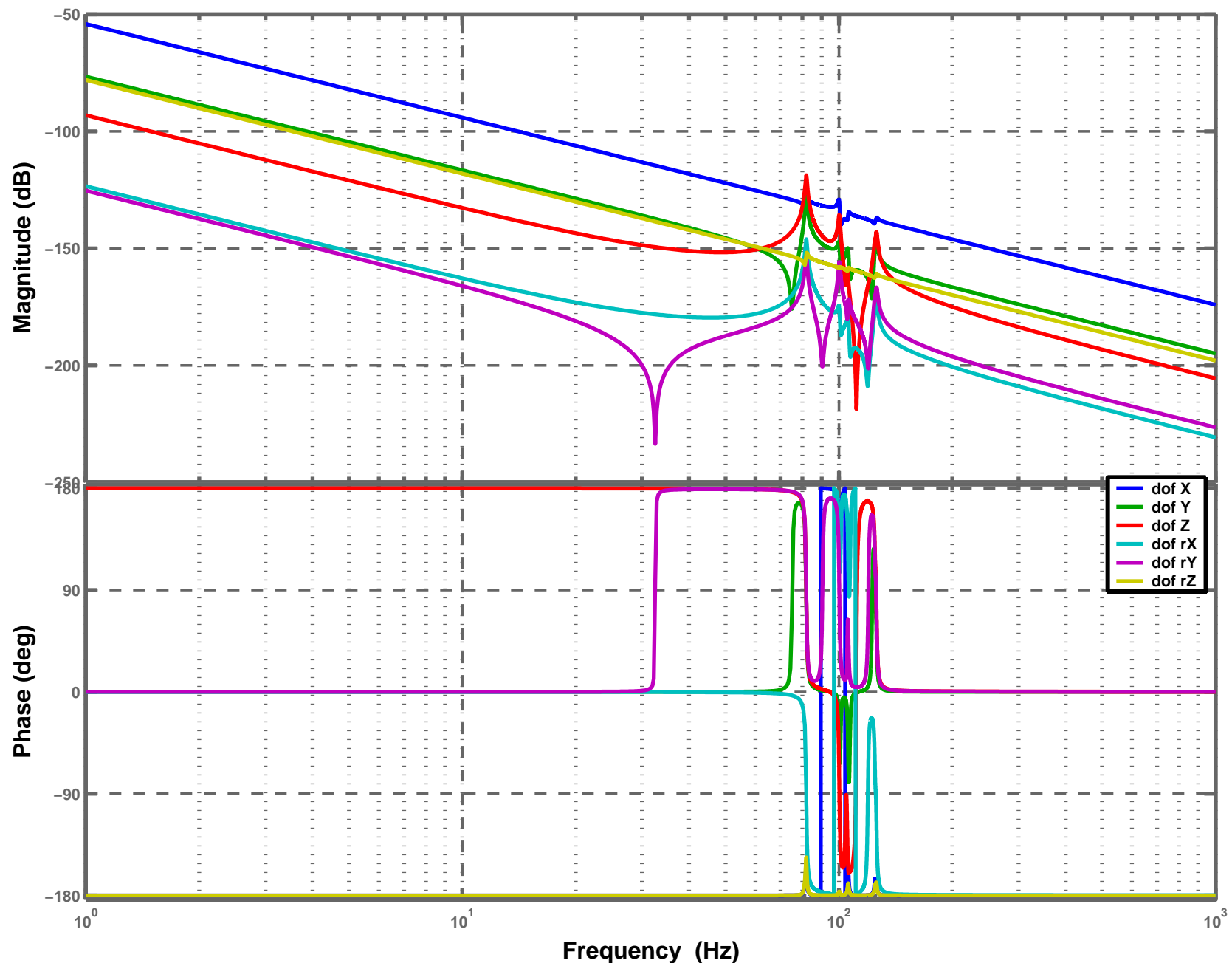
Stage2 + Quad D040519-04, Actuation: H2, Sensor: V1



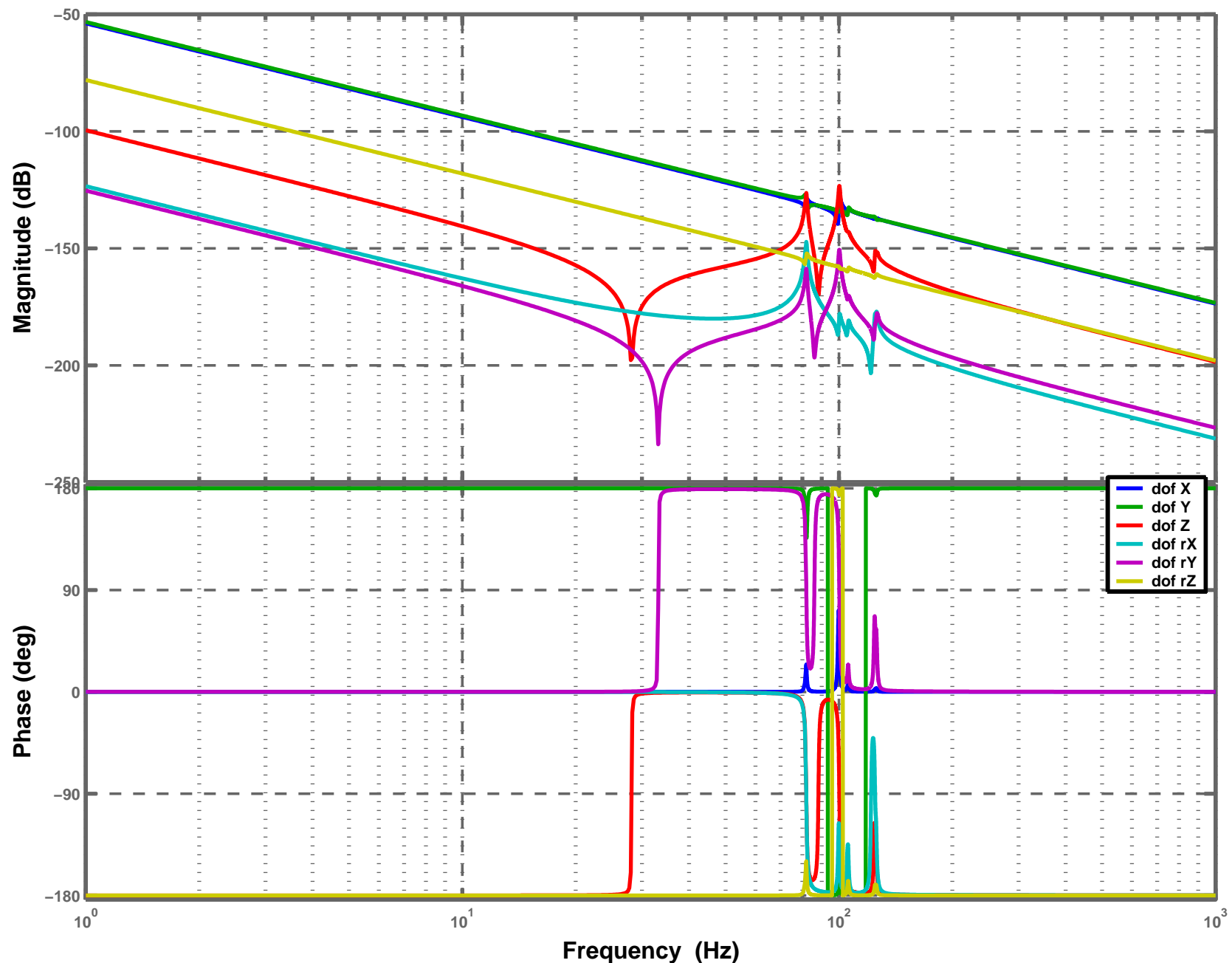
Stage2 + Quad D040519-04, Actuation: H2, Sensor: V2



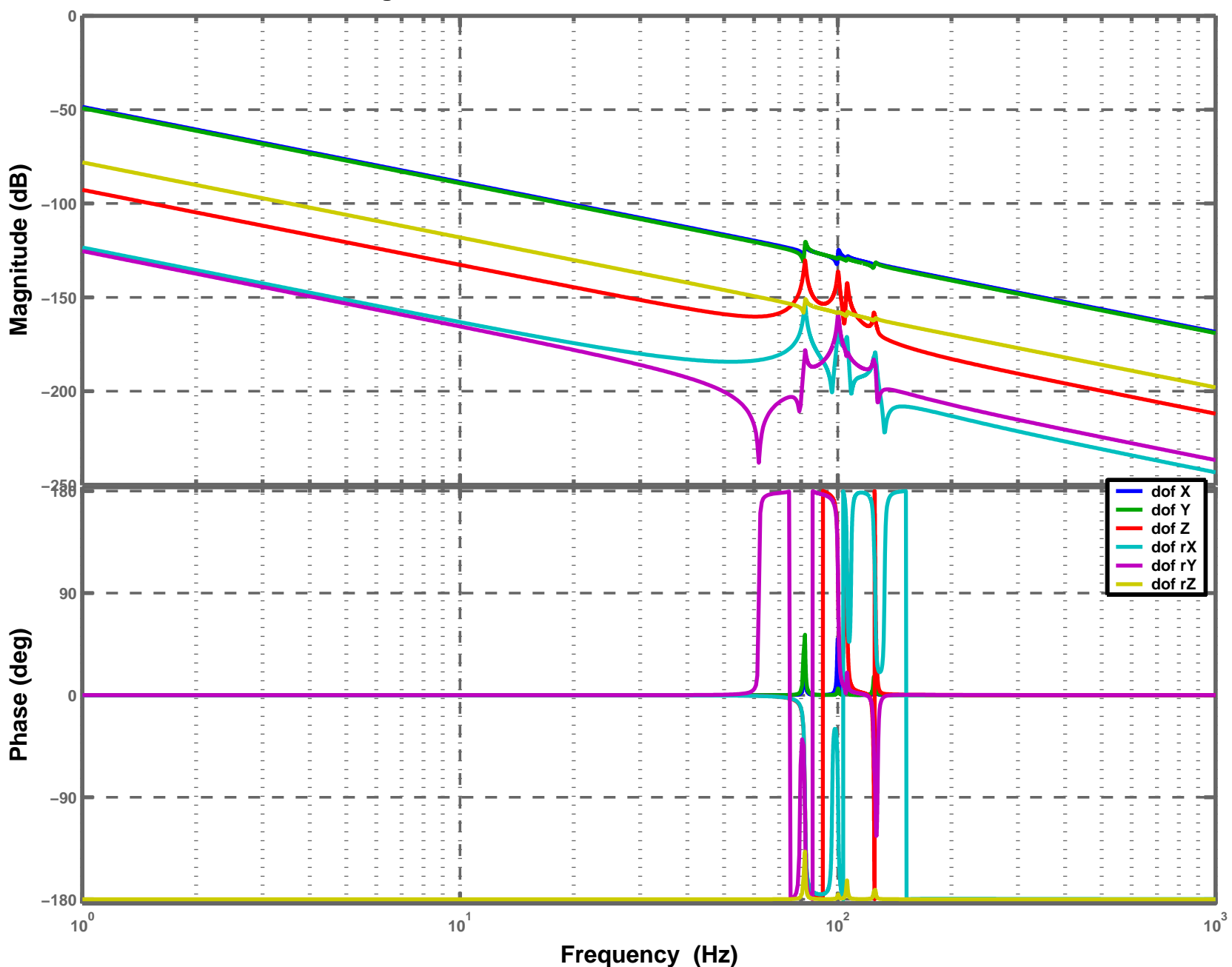
Stage2 + Quad D040519-04, Actuation: H2, Sensor: V3



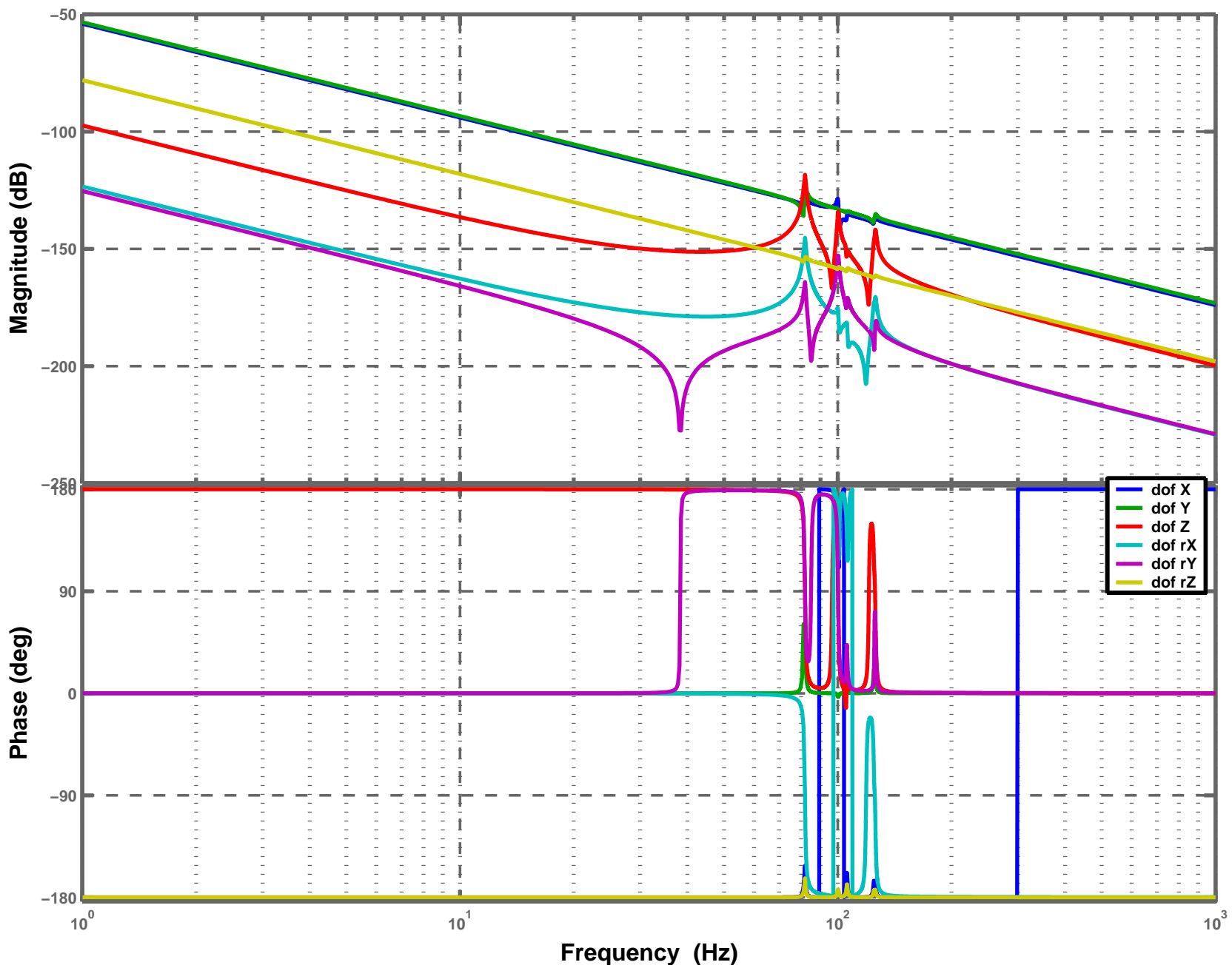
Stage2 + Quad D040519-04, Actuation: H2, Sensor: H1



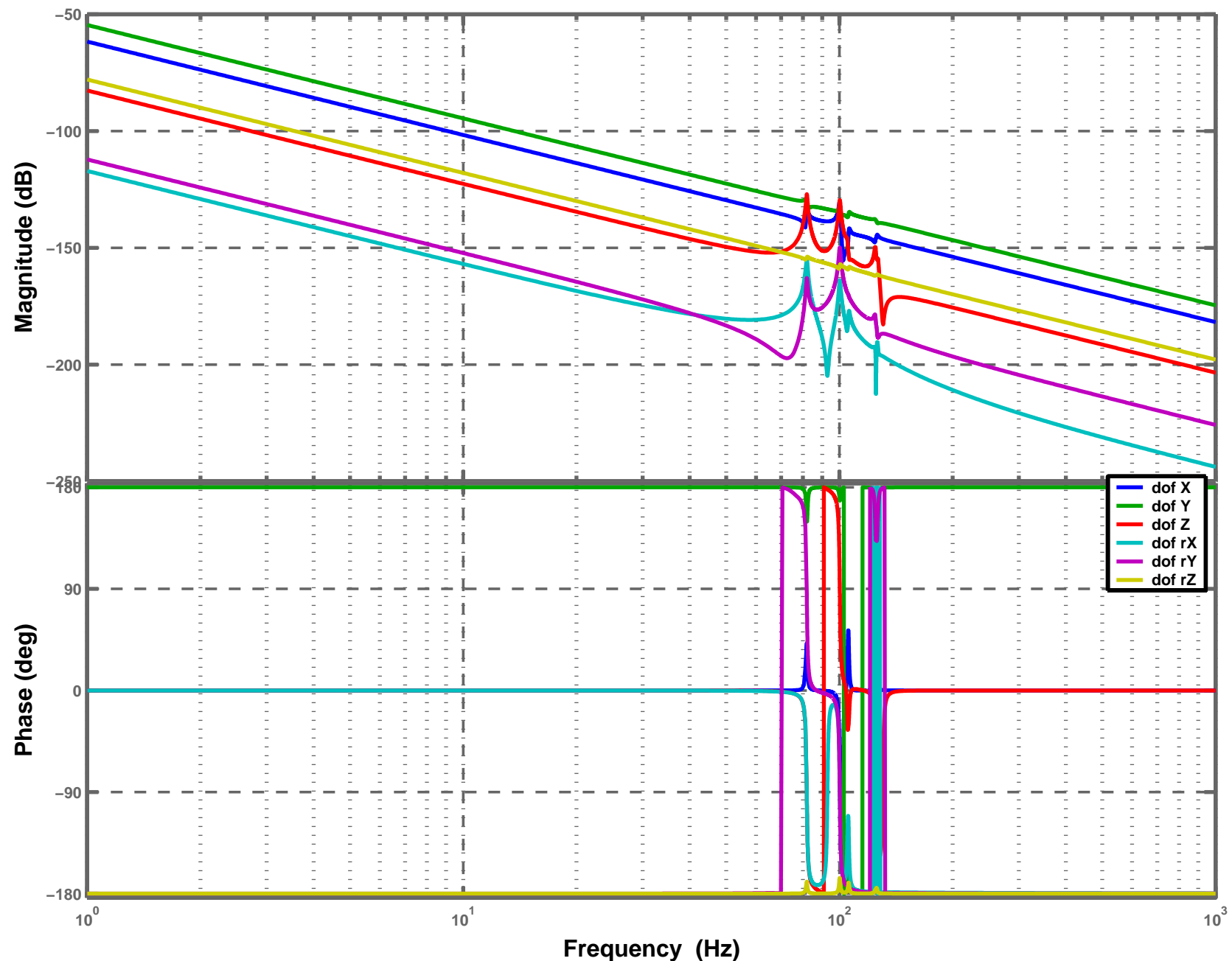
Stage2 + Quad D040519-04, Actuation: H2, Sensor: H2



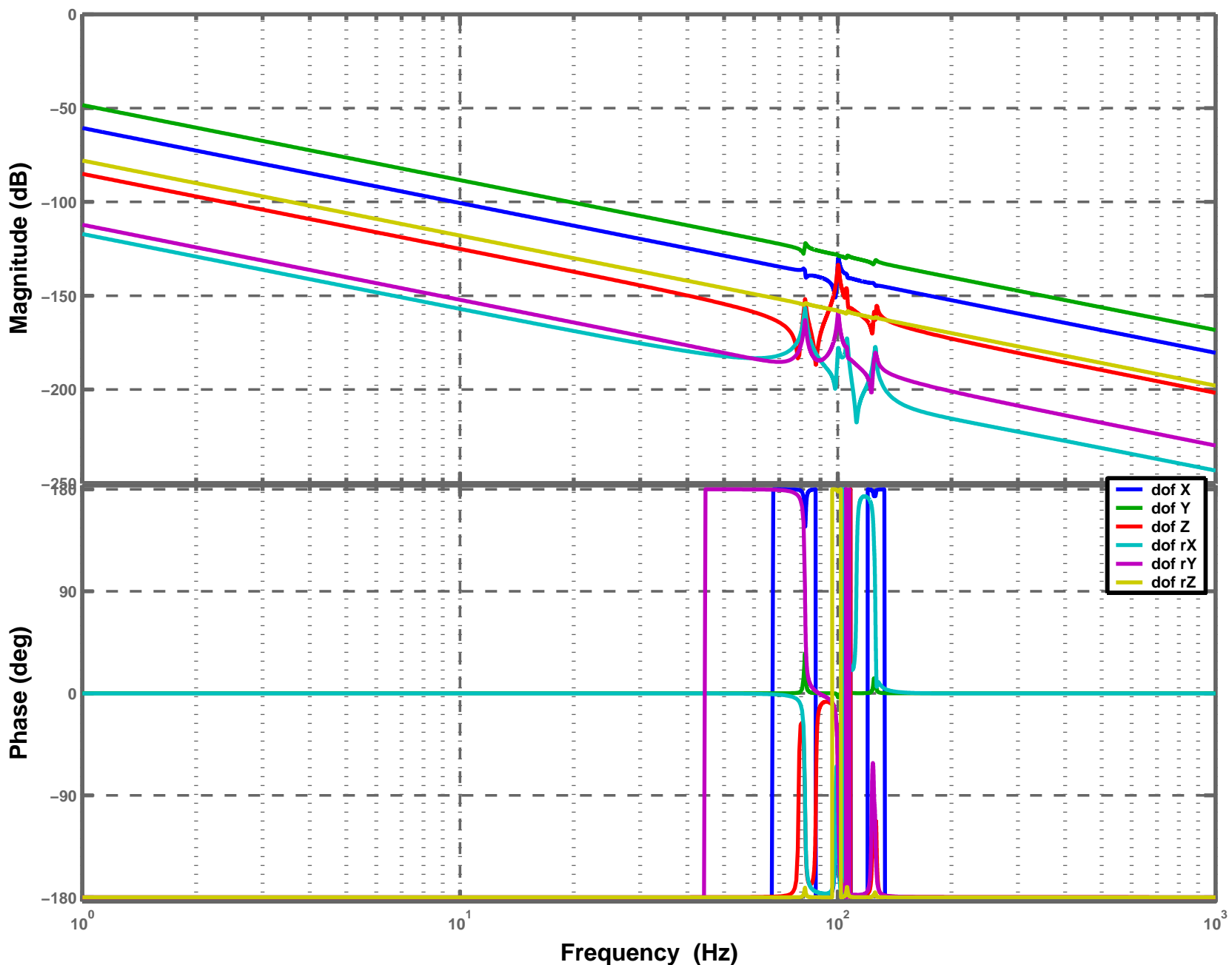
Stage2 + Quad D040519-04, Actuation: H2, Sensor: H3



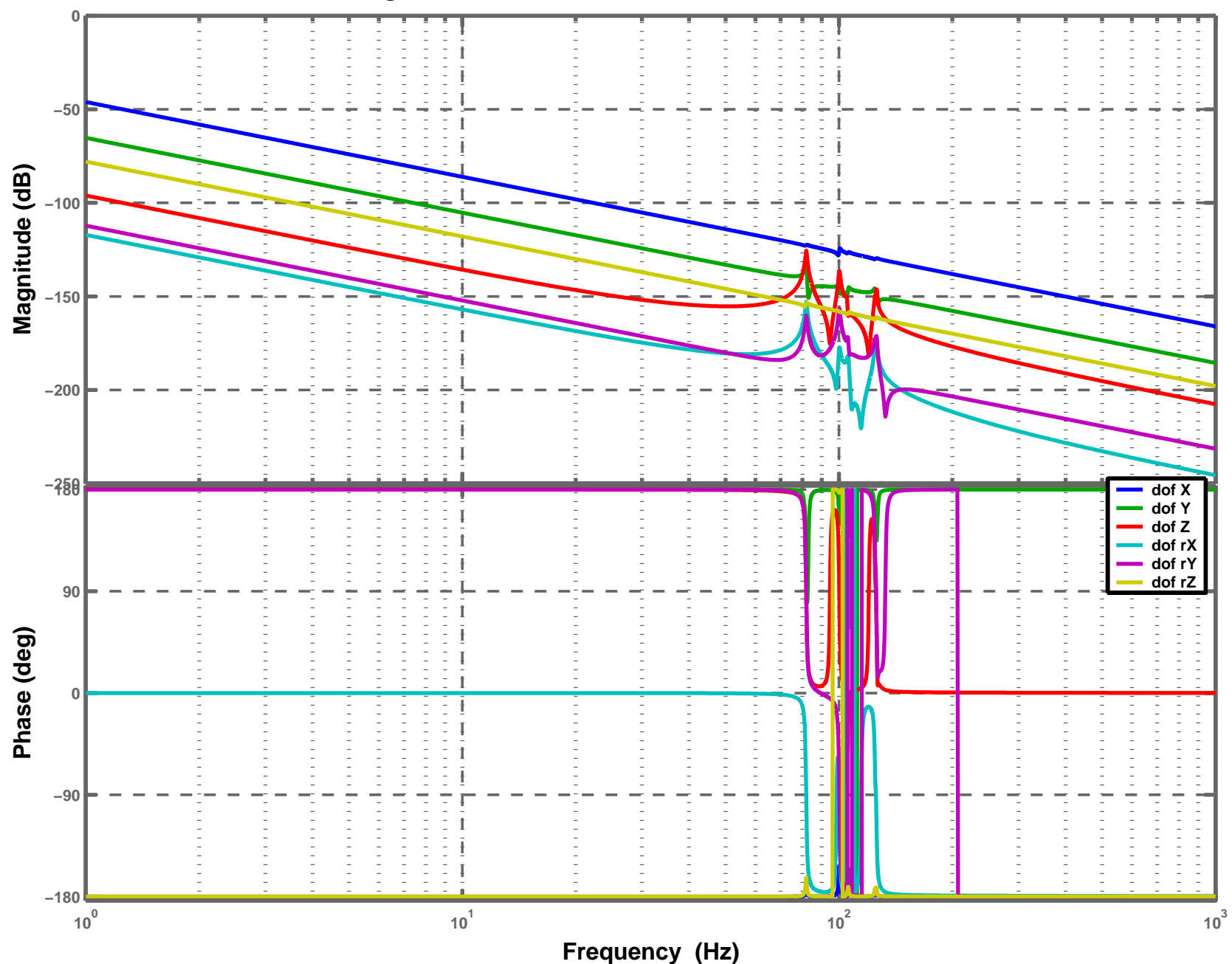
Stage2 + Quad D040519-04, Actuation: H3, Sensor: V1



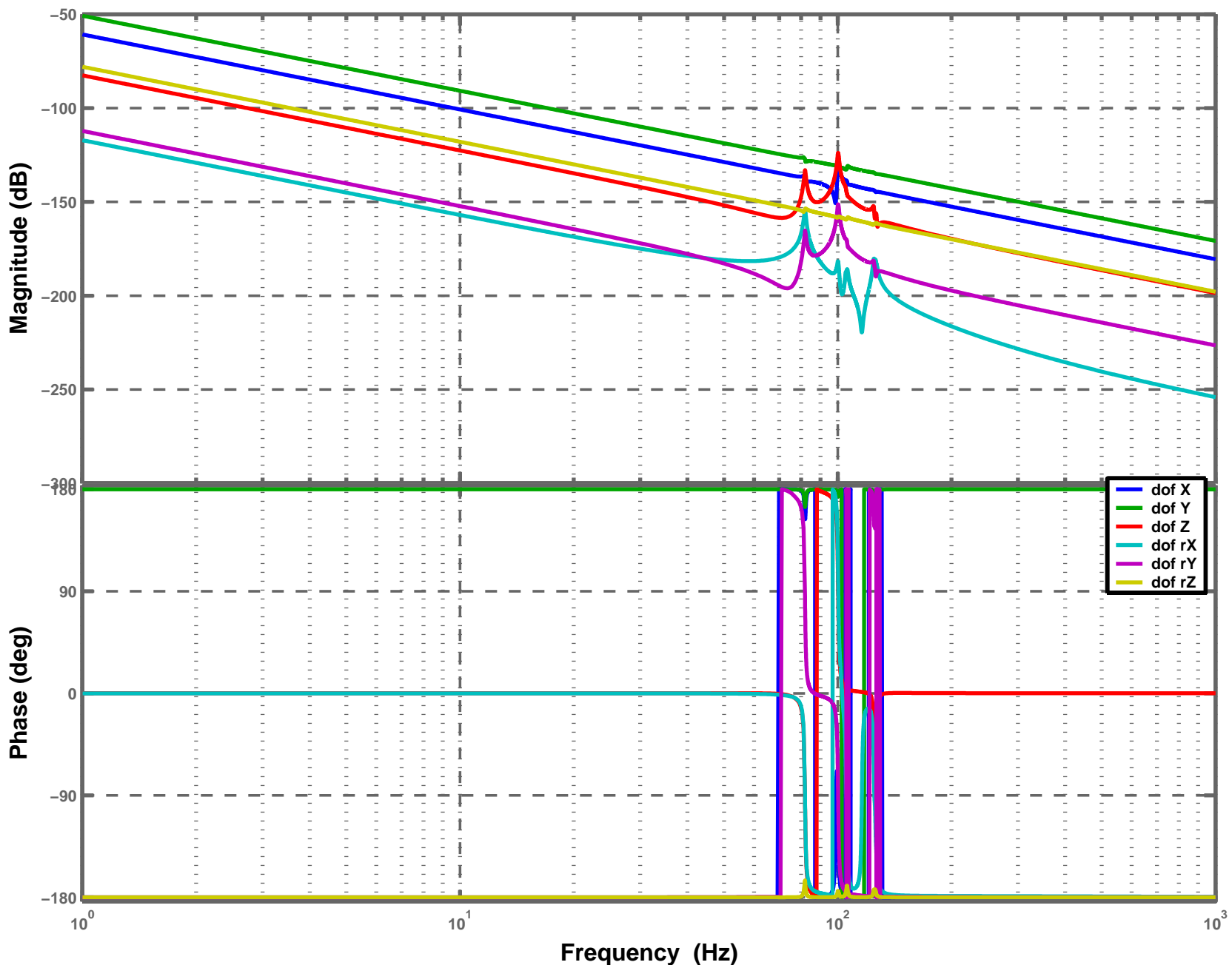
Stage2 + Quad D040519-04, Actuation: H3, Sensor: V2



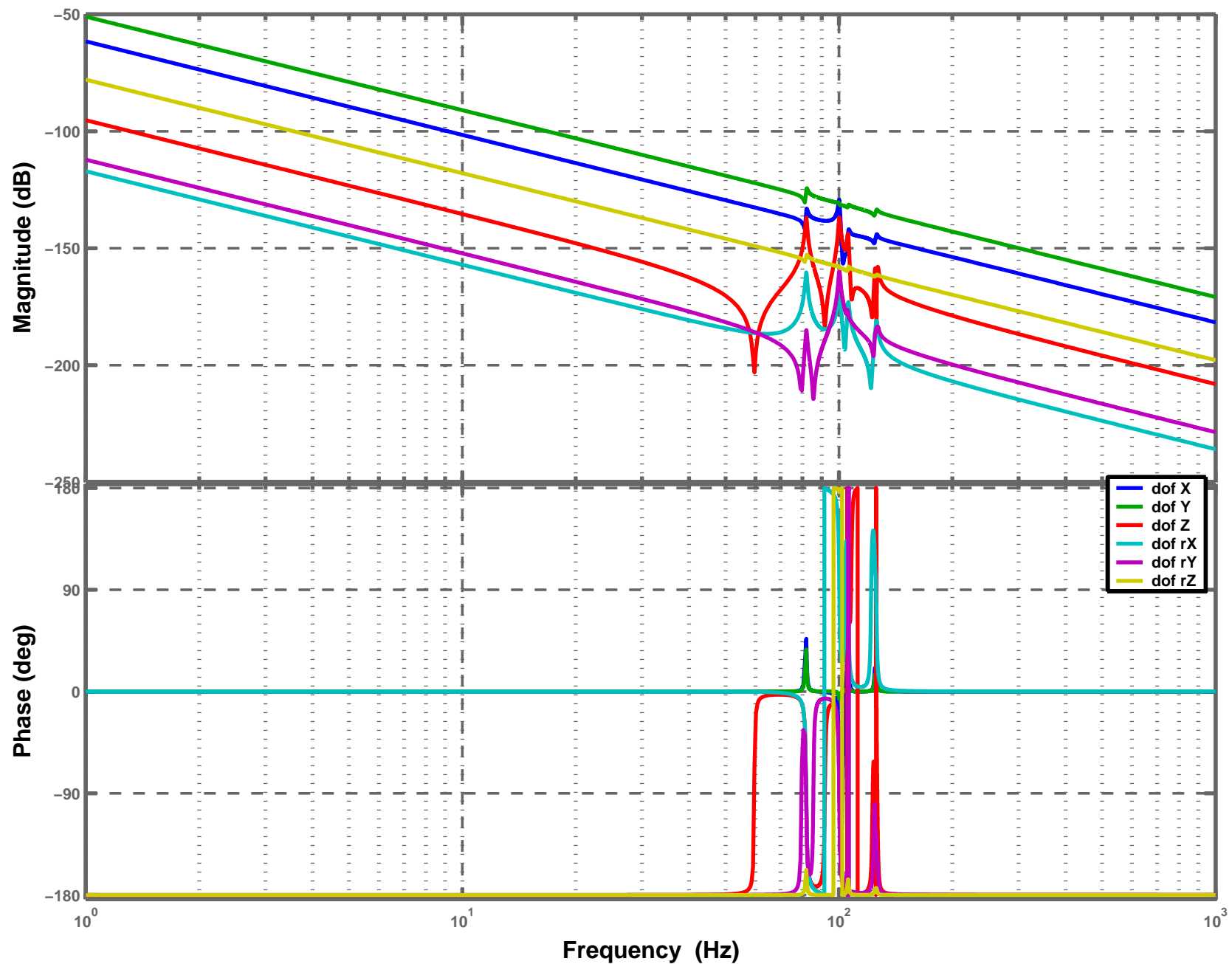
Stage2 + Quad D040519-04, Actuation: H3, Sensor: V3



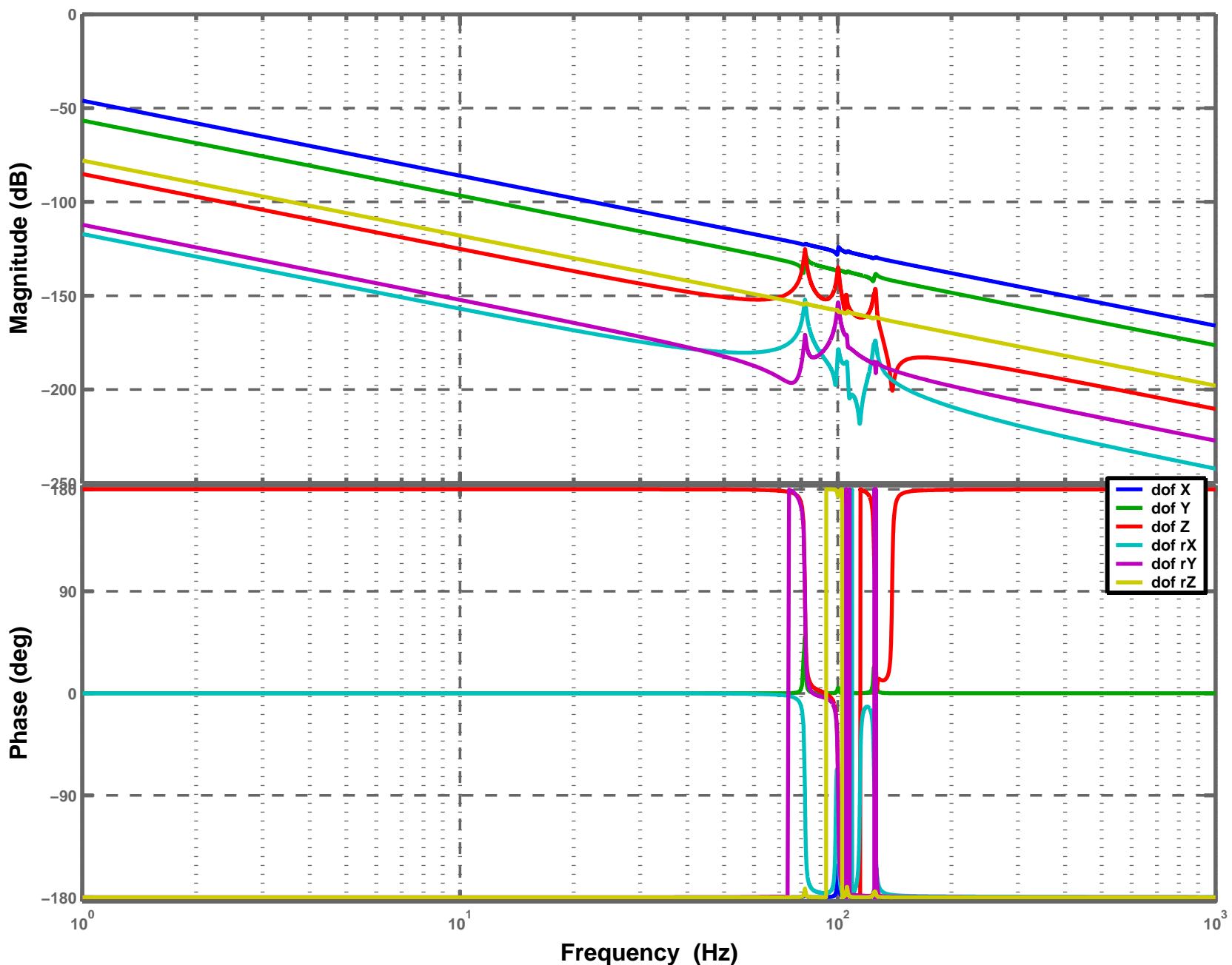
Stage2 + Quad D040519-04, Actuation: H3, Sensor: H1



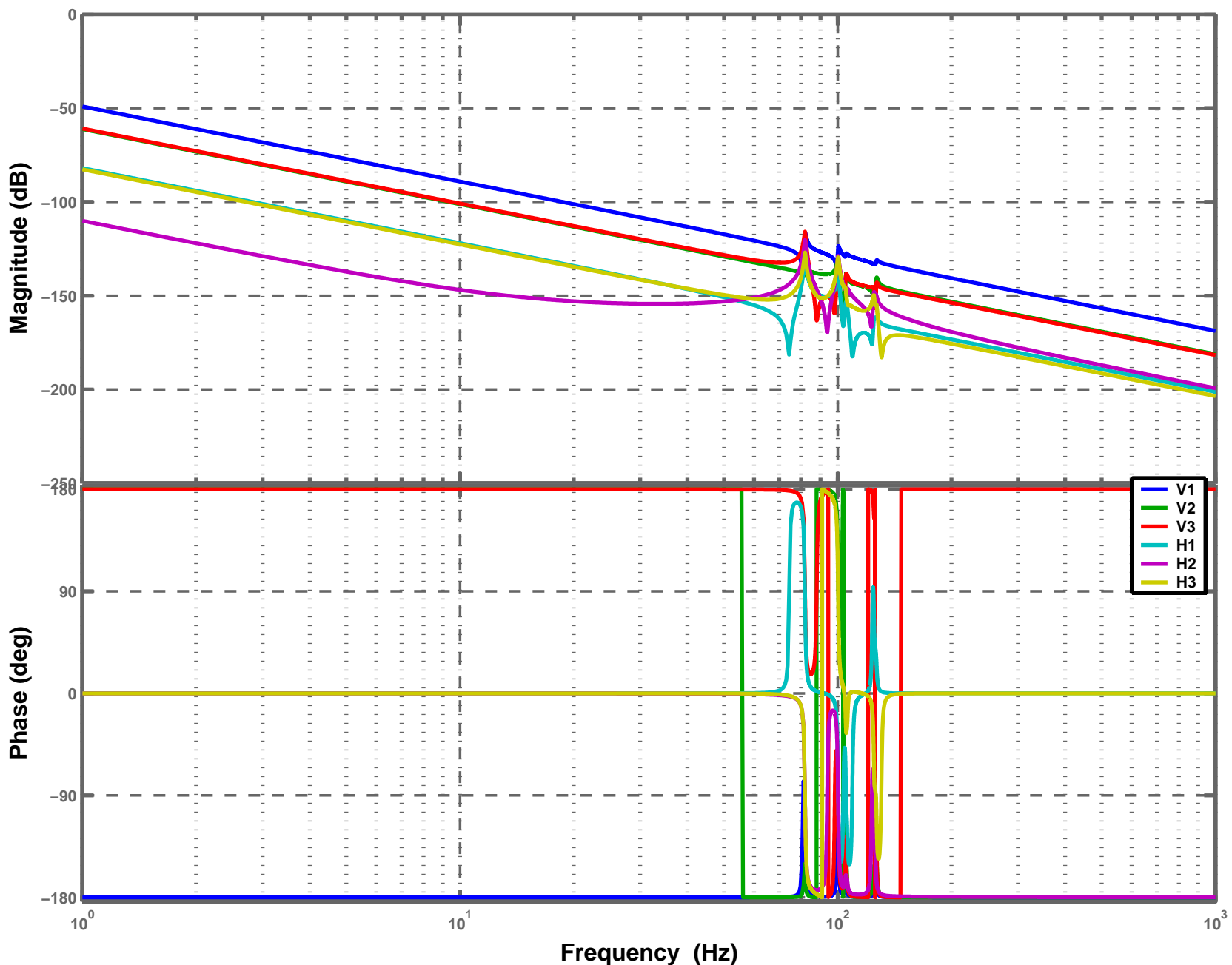
Stage2 + Quad D040519-04, Actuation: H3, Sensor: H2



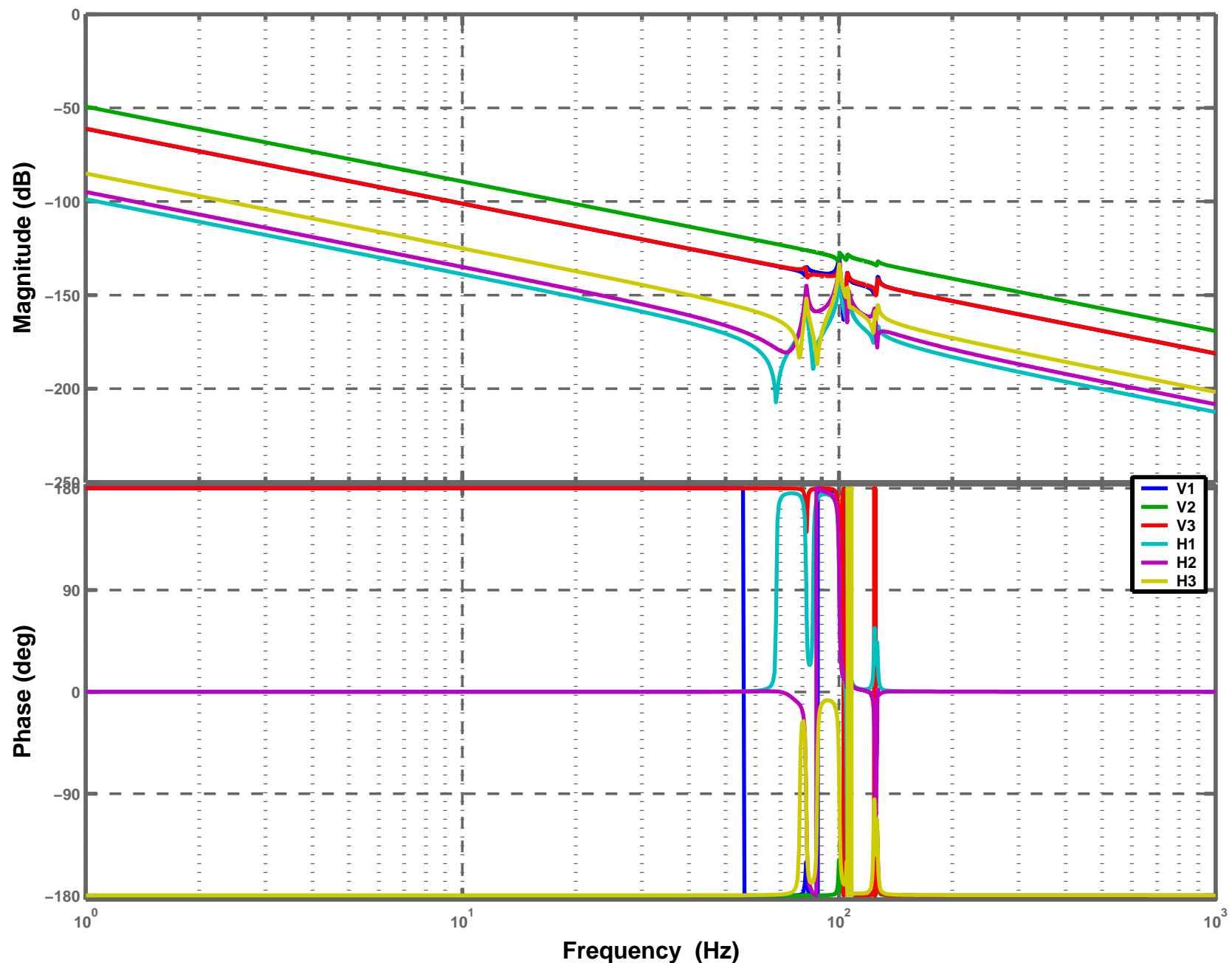
Stage2 + Quad D040519-04, Actuation: H3, Sensor: H3



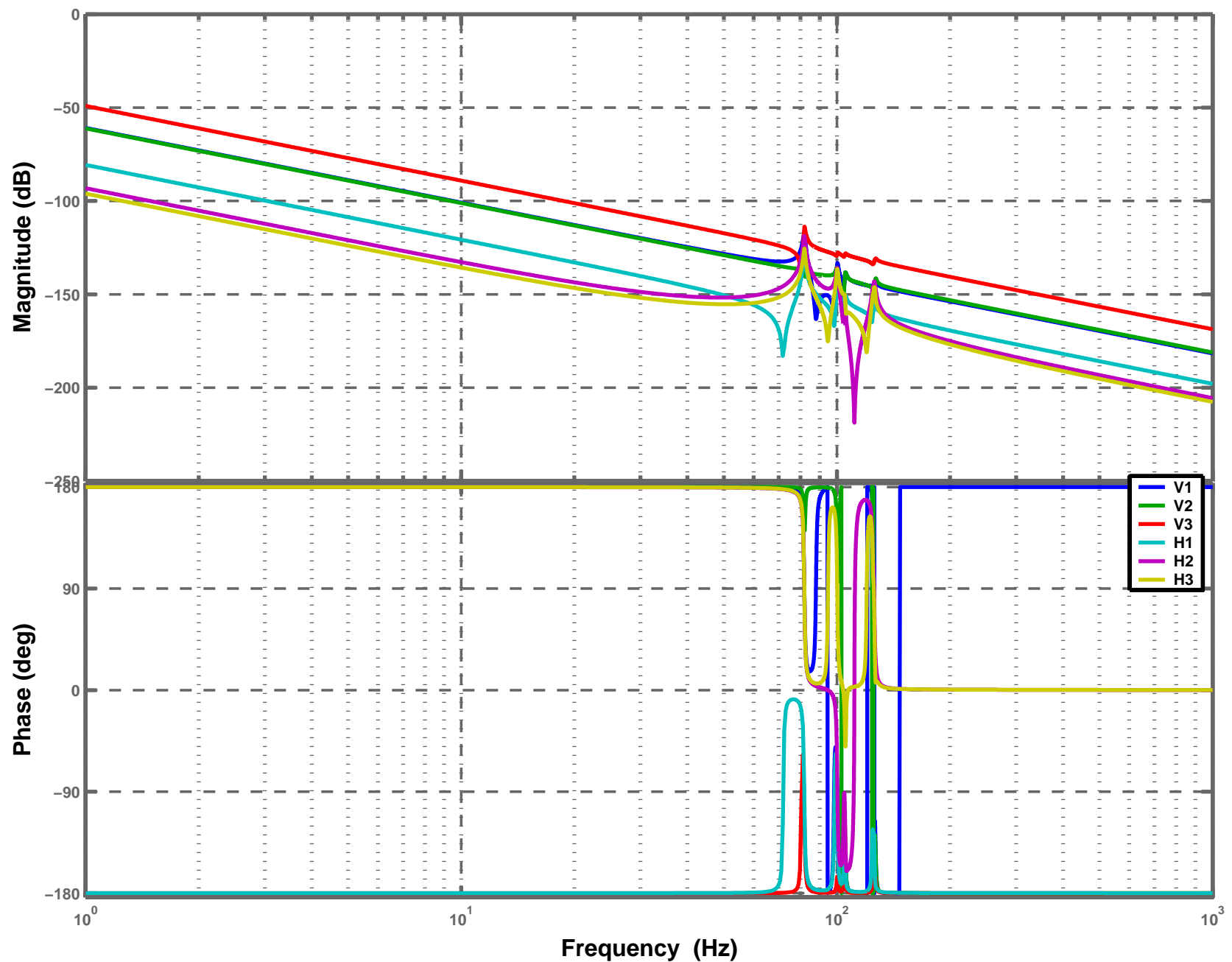
Stage2 + Quad D040519–04, Actuation: V1



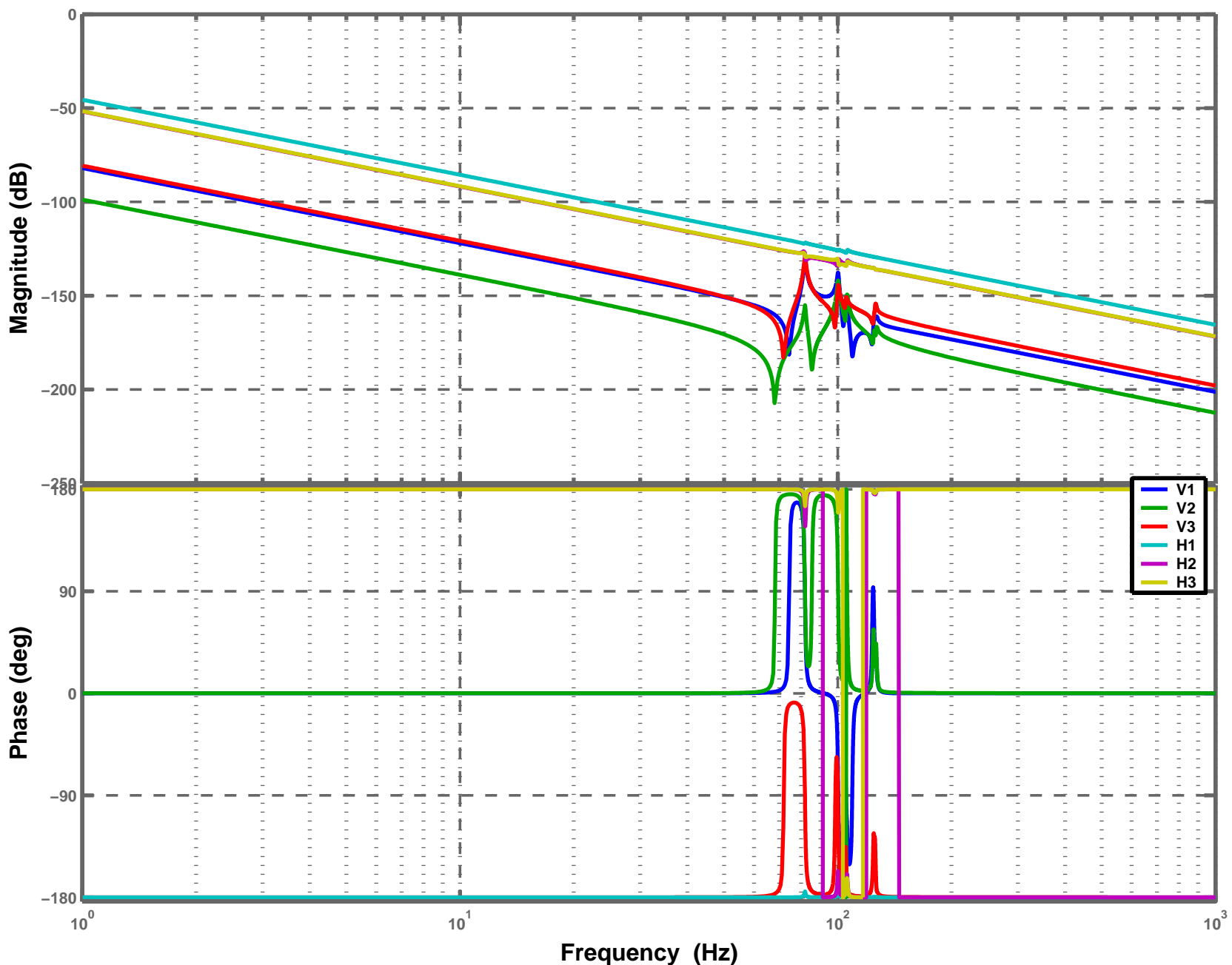
Stage2 + Quad D040519–04, Actuation: V2



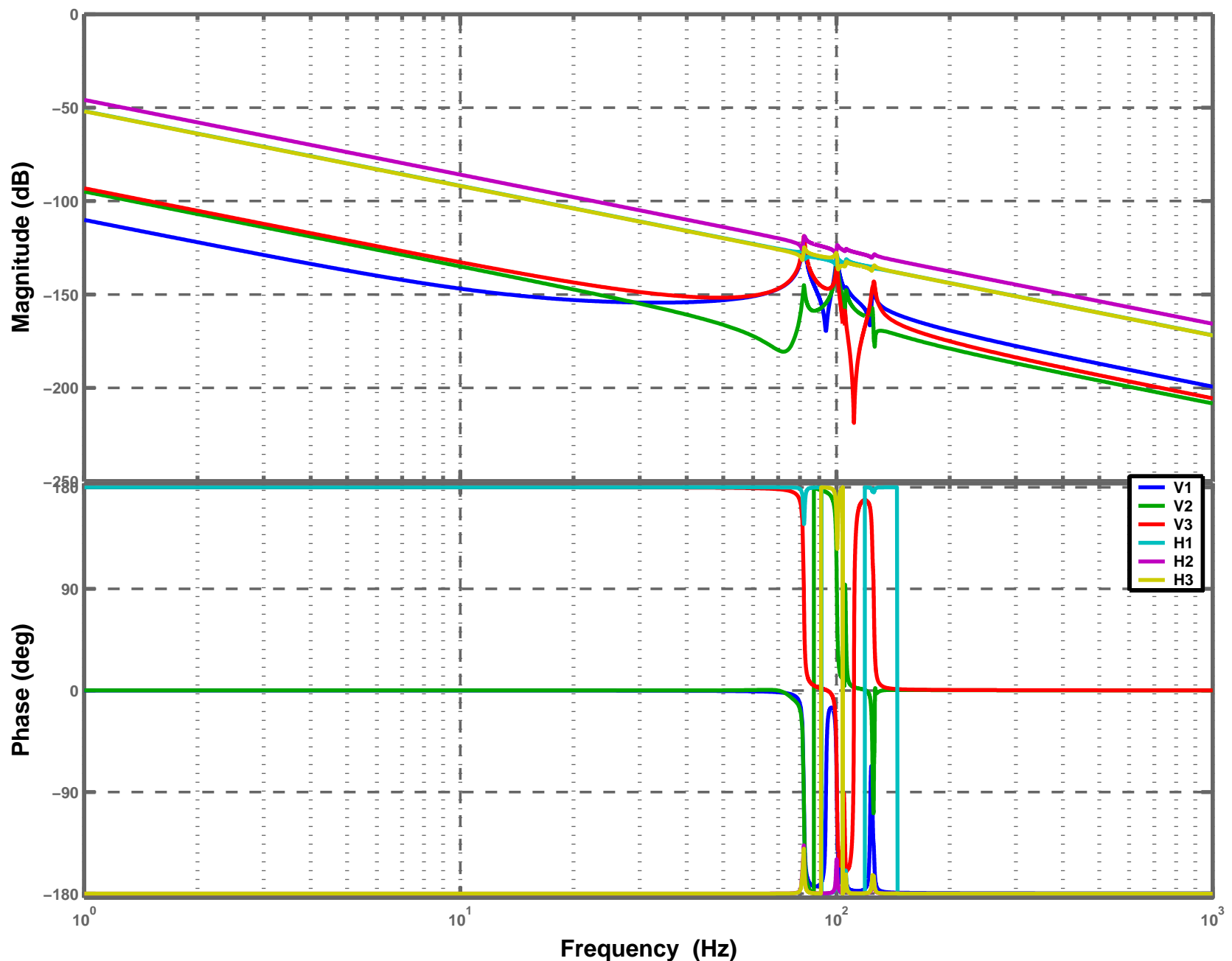
Stage2 + Quad D040519–04, Actuation: V3



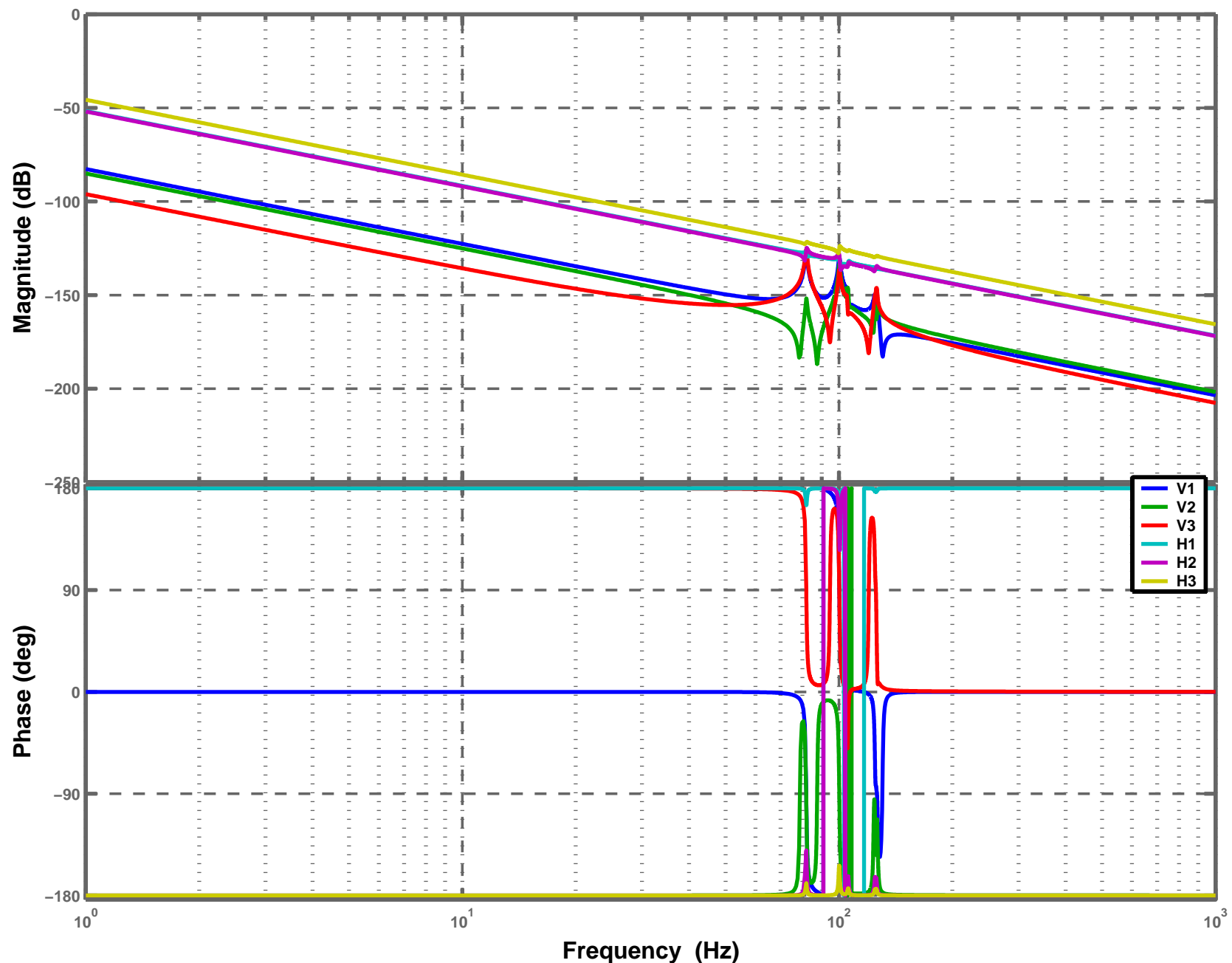
Stage2 + Quad D040519–04, Actuation: H1



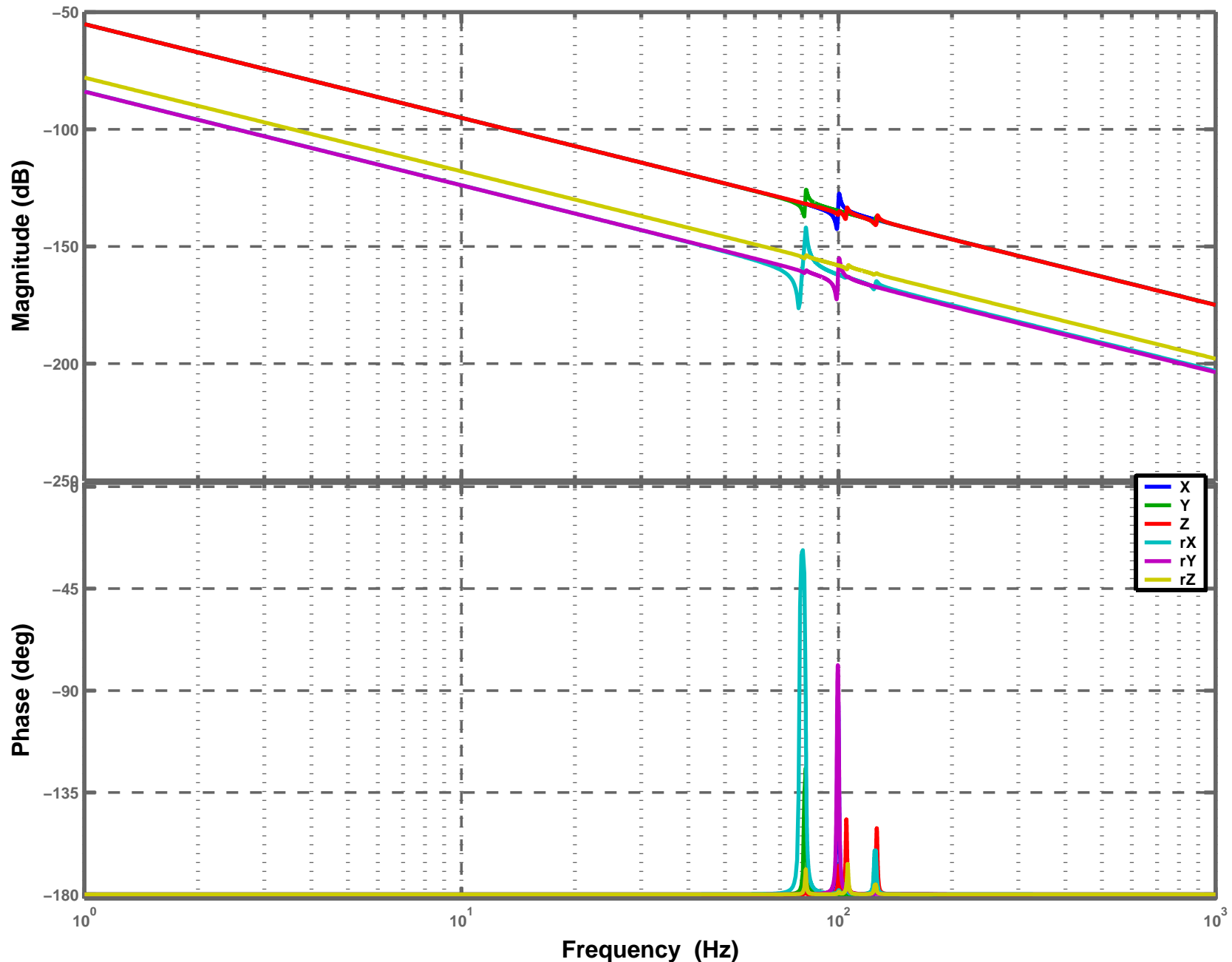
Stage2 + Quad D040519–04, Actuation: H2



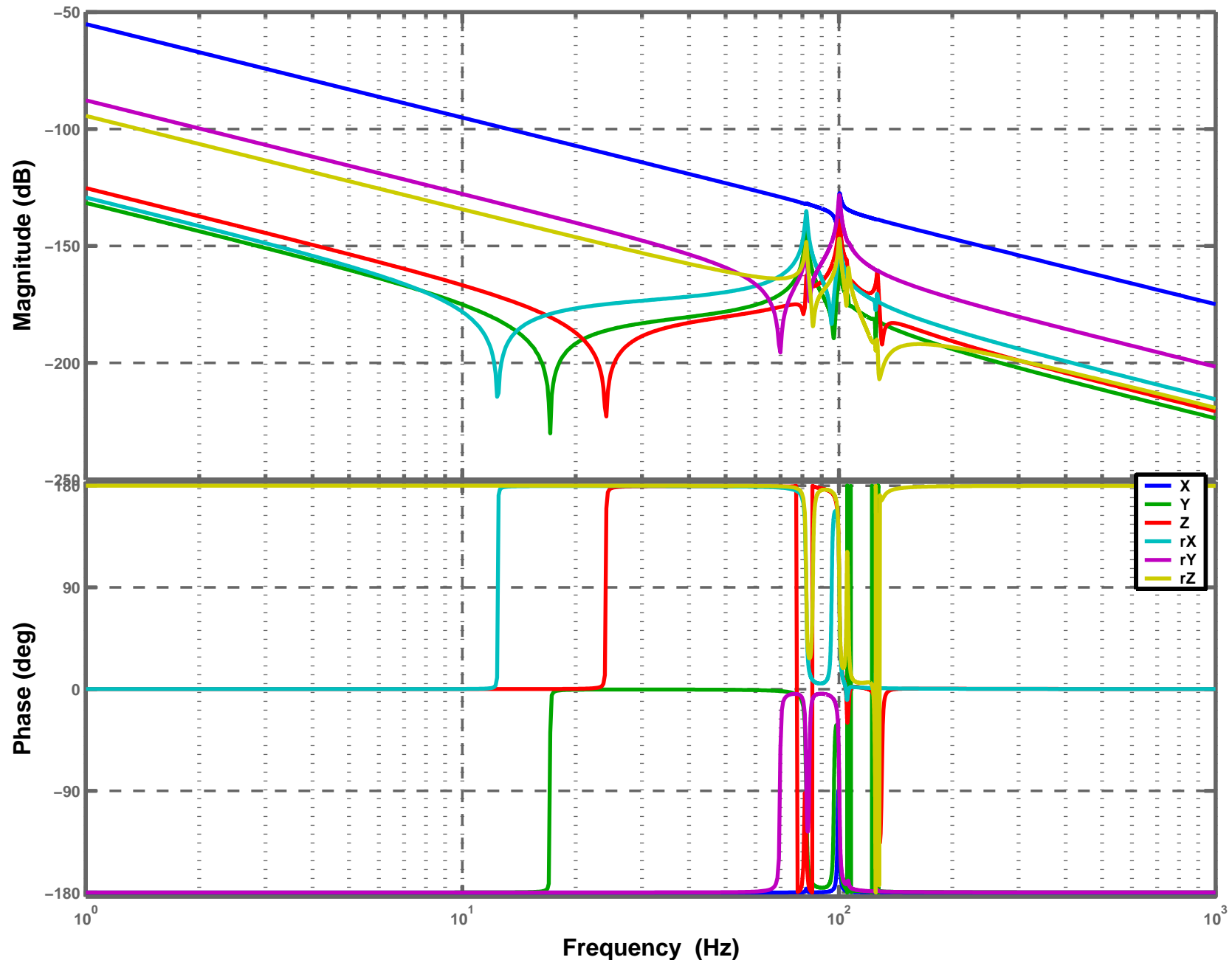
Stage2 + Quad D040519–04, Actuation: H3



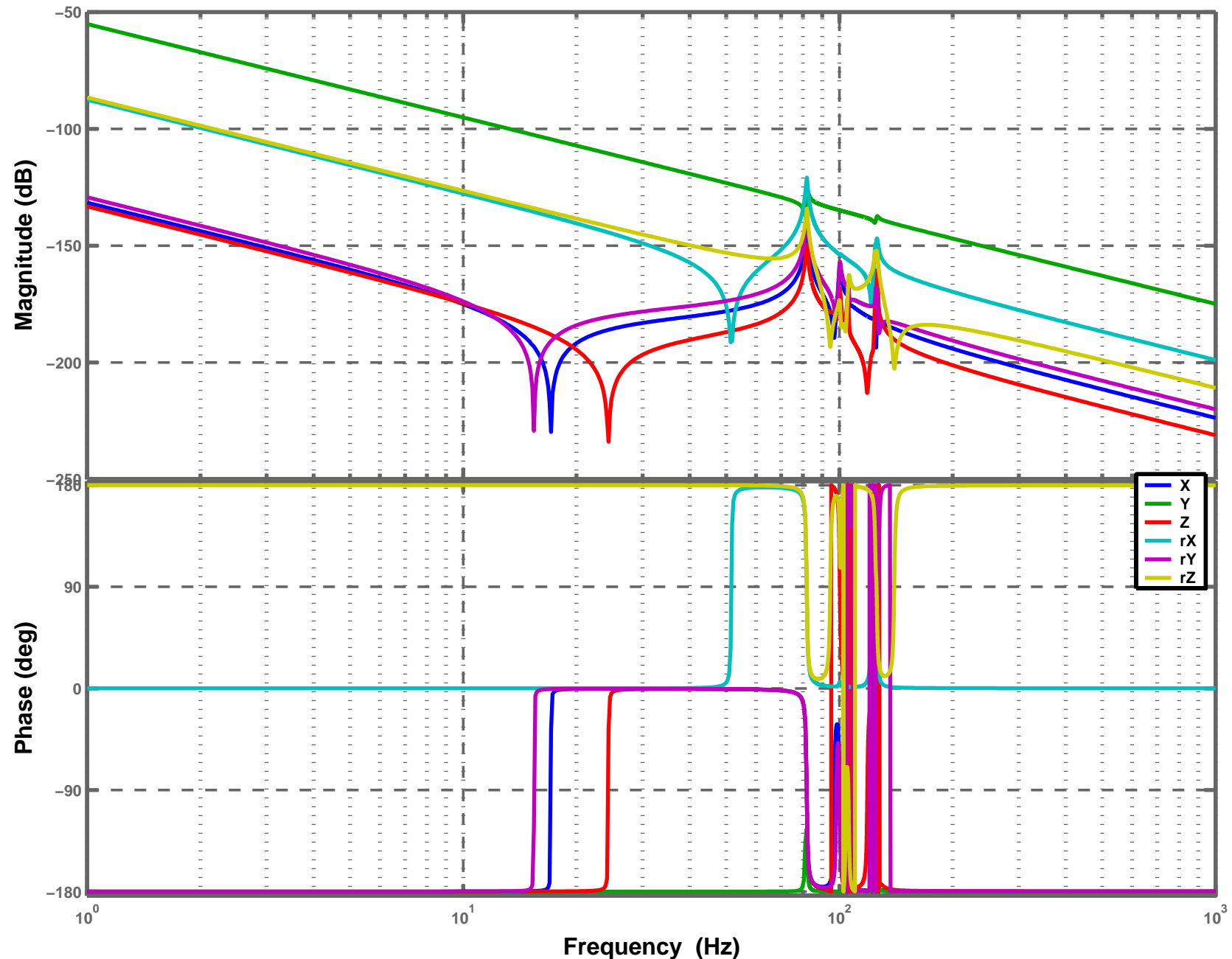
Stage2 + Quad D040519-04, Rigid Body Modal (Cartesian) Actuation: Diagonal Response



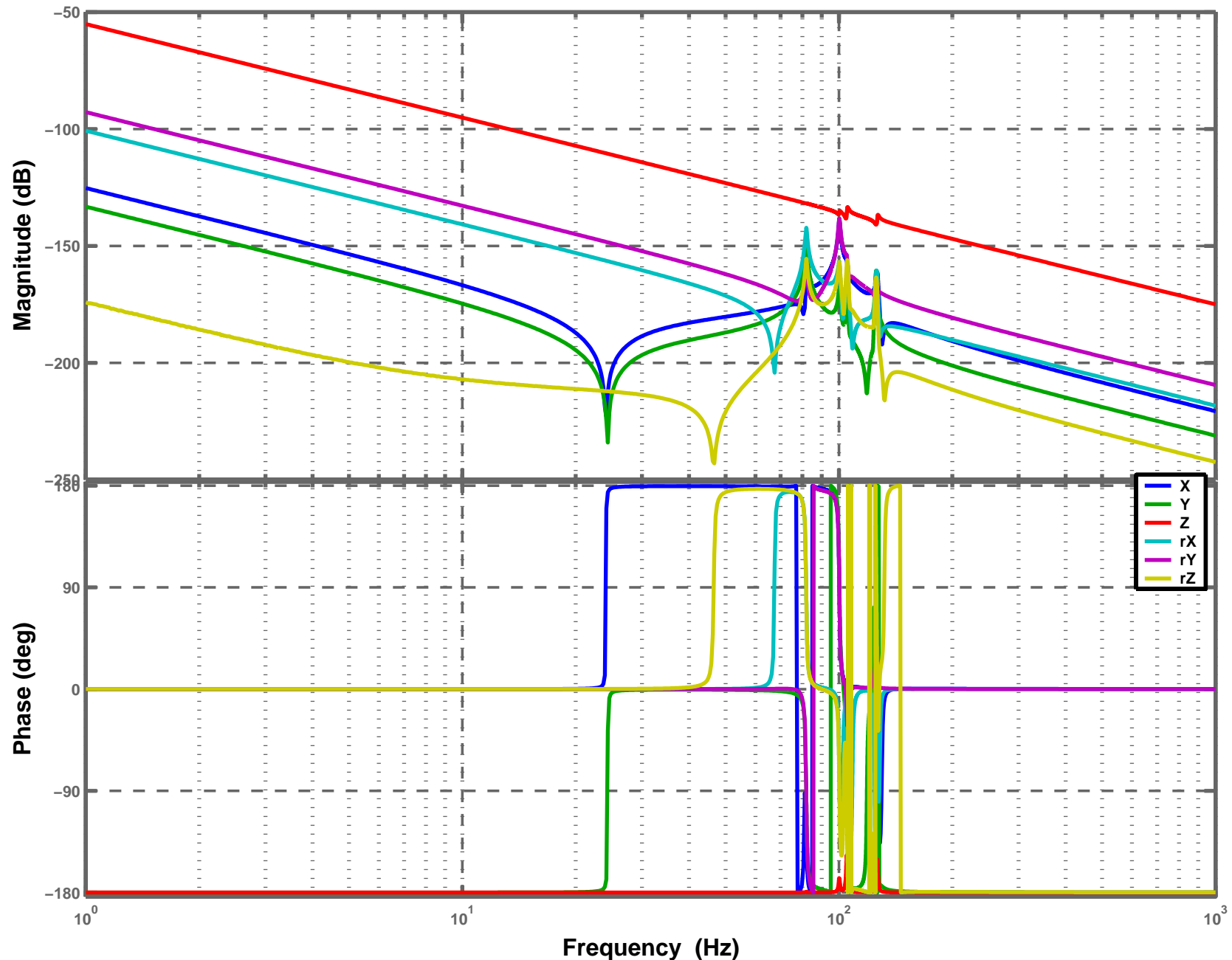
Stage2 + Quad D040519-04, Rigid Body Modal (Cartesian) Actuation: X



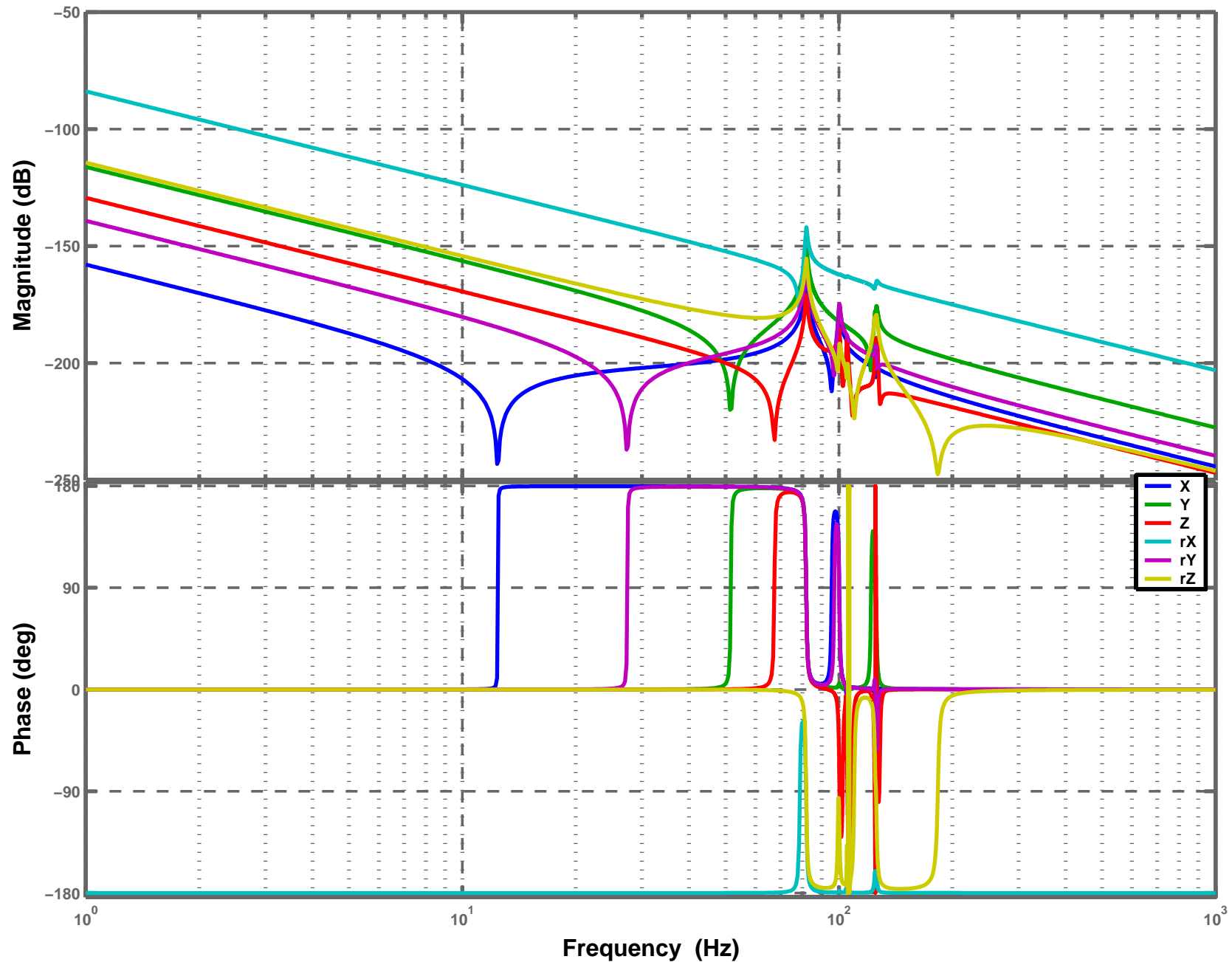
Stage2 + Quad D040519-04, Rigid Body Modal (Cartesian) Actuation: Y



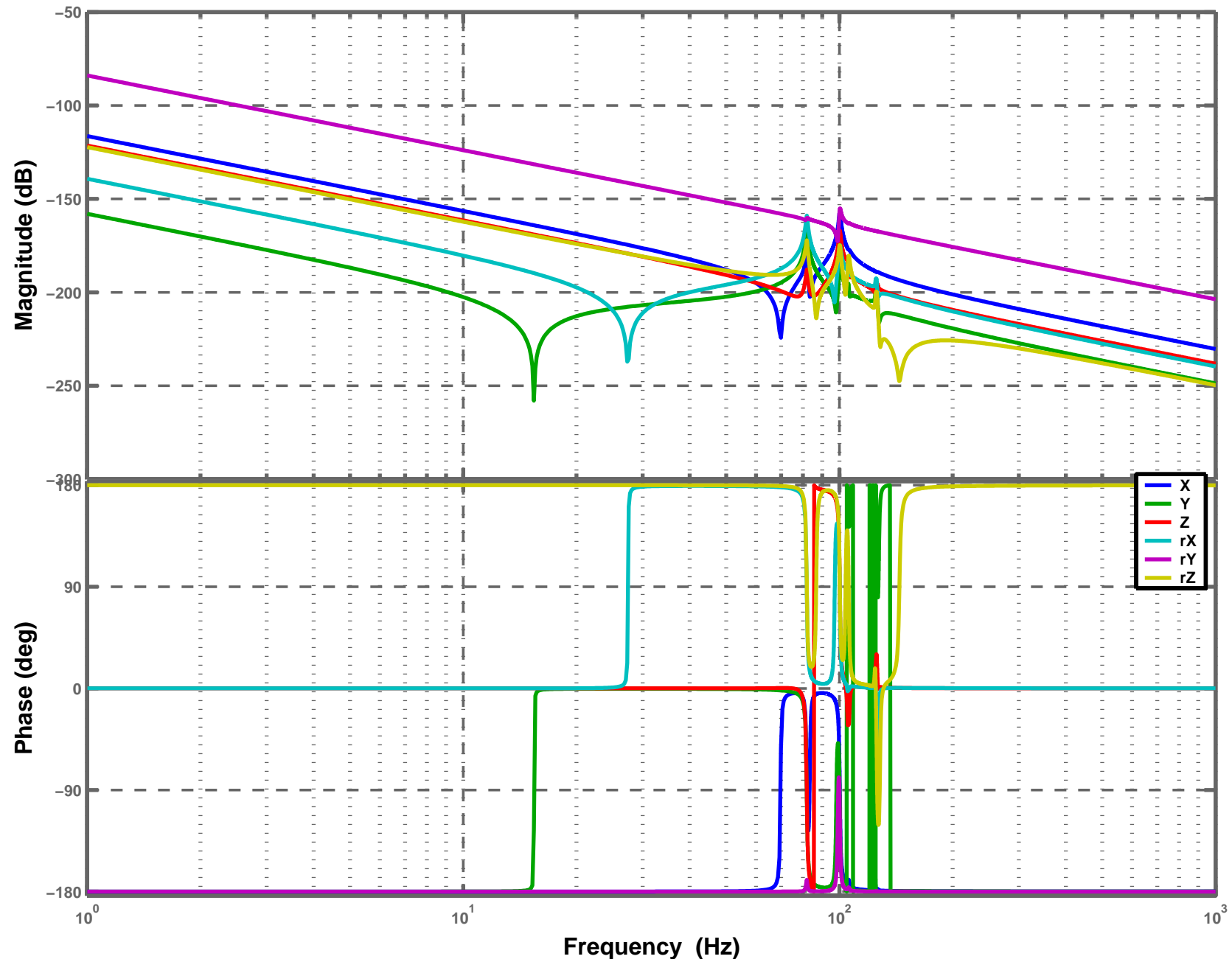
Stage2 + Quad D040519-04, Rigid Body Modal (Cartesian) Actuation: Z



Stage2 + Quad D040519-04, Rigid Body Modal (Cartesian) Actuation: rX



Stage2 + Quad D040519-04, Rigid Body Modal (Cartesian) Actuation: rY



Stage2 + Quad D040519-04, Rigid Body Modal (Cartesian) Actuation: rZ

